LEHRSTUHL FÜR METALLURGIE
MONTANUNIVERSITÄT

Influence of bottom purging on the metallurgical results and the BOF process

Master Thesis

composed by

Thomas Kollmann

attended by

Univ.-Prof. Dipl.-Ing. Dr. techn. Johannes Schenk

Leoben, January 2010

MONTAN UNIVERSITÄT

Lehrstuhl für Metallurgie – Montanuniversität Leoben
Franz-Josef-Straße 18 – 8700 Leoben, Österreich

Kurzfassung

Steigende Produktanforderungen und schwankende Einsatzstoffqualitäten verlangen eine wirtschaftlich optimierte und flexible LD-Prozessführung. Durch die Installation von zusätzlichen bodenspülenden Elementen (CIP-System) kann der rein sauerstoffaufblasend betriebene LD-Konverter (ursprünglicher LD-Prozess) aus metallurgischer und prozesstechnischer Sicht deutlich verbessert und optimiert werden. Das CIP-System (Converter Inertgas Purging) umfasst zwölf moderne, getrennt regelbare MHP24-Spüler (Mult-Hole-Plug) in elliptischer Bodenanordnung.

Die Diplomarbeit bewertet die metallurgischen Vorteile des Bodenspülens mit einem parallel betriebenen Sauerstoffaufblaskonverter (232 t Abstichgewicht). Dabei werden die damit verbundenen Prozessänderungen in Schlacken- und Frischprozessführung diskutiert. Konverterpflegephilisophien und deren Auswirkungen auf die Verfügbarkeit und Wirkung der Spülelemente werden ebenso betrachtet, wie der Einfluss von Ausfallzeiten und Spülgasänderungen auf die erreichbaren metallurgischen Ergebnisse.

Abstract

Higher sophisticated products and unsteady charge materials require an economically optimized BOF-Process operation. Installing a CIP-System (Converter-Inertgas-Purging) enhances the performance of the top blowing BOF-Process (original LD-Process) from the metallurgical and procedural point of view. The CIP-System consists of twelve independent and separate controllable MHP24 plugs (Multi-Hole-Plugs) in ecliptic bottom arrangement.

This thesis evaluates the advantages of inertgas bottom purging in direct comparison to a top blowing vessel (232 t tapping weight). Process adjustments (e.g. slag, fluxes, blowing and purging pattern) are discussed. Maintenance philosophies and their influence on the availability of the bottom purging are considered as well as down-times and total gas amounts on the metallurgical results.

Affidavit

I declare in lieu of oath, that I wrote this thesis and performed the associated research myself, using only literature cited in this volume.

.....

Thomas KOLLMANN

Leoben, January 2010

Acknowledgement

RHI

Dr.-Ing. Jürgen Cappel

Dipl.-Ing. Christoph Jandl

Dipl.-Ing. Hans-Jörg Junger

Dipl.-HTL-Ing. Bernhard Knabl

Dipl.-Ing. Karl-Michael Zettl

Ing. Heinz Kammerhofer

Hans-Peter Kainz

Alois Märzendorfer

Surendra Mishra

Mike Skaltsas

Mike Pellegrino

University of Leoben / Chair of Metallurgy

Univ.-Prof. Dipl.-Ing. Dr. techn. Johannes Schenk

Mag. Yuriy Lytvynyuk

TBR

Ing. Christian Schober

FC-Technik

Dipl.-Ing. Christoph Vetterli

Table of Contents

Used Symbols

[ ] dissolved in liquid metal

{ } gas phase

( ) slag

<> refractory lining

Acronymes

BF	Blast Furnace
BOF	Basic Oxygen Furnace
BOS	Basic Oxygen Steelmaking
CC	Continuous Casting
CIP	Converter Inert Gas Purging
EAF	Electric Arc Furnace
HC	High Carbon
HM	Hot Metal
LCAK	Low Carbon Aluminium Killed
LD	Linz-Donawitz
LTS	Ladle Treatment Station
MC	Medium Carbon
MHP	Multi Hole Plug
OBM	Oxygen Bottom Maxhütte
RE	Richardson-Ellingham
RH-OB	Ruhrstahl-Hereaus Oxygen Blowing

SM	Siemens Martin
ULC	Ultra Low Carbon
WOBS	BOF Dust Briquettes

List of figures

List of tables

1 BOF-Development

1.1 Overview of different BOF characteristics

Different kinds of oxygen steelmaking processes have been developed in the last century depending on the raw material situation and the energy availability. A historical overview is given in **Figure 1-1** [1], [2].

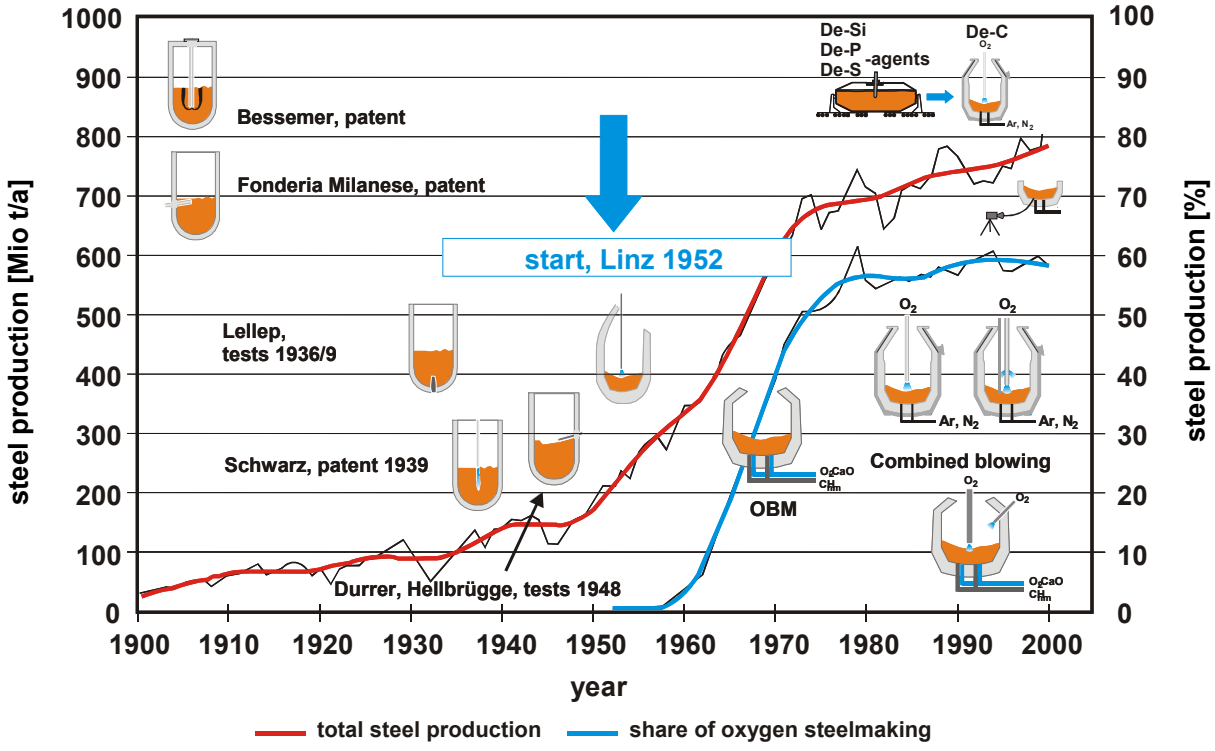

Figure 1-1: Oxygen steelmaking overview [3].

With a share of 30 percent electric and 70 percent basic oxygen steel, the Basic Oxygen Steelmaking (BOS) and the Electric Arc Furnace (EAF) are the most important steelmaking processes worldwide today. The manufacture base for the BOS is the Basic Oxygen Furnace (BOF), also called LD-Converter. A typical BOF shop (**Figure 1-2**) consists of two converter in parallel operation with a maximum capacity of 400 tons per vessel. Each converter (**Figure 1-3**) is tiltable and operates with a oxygen top blowing lance and an optional purging plug system, off-gas- and sublance-measurement system. Furthermore the hopper system for the flux charging is above and the ladle / pot transfer car beneath the vessel.

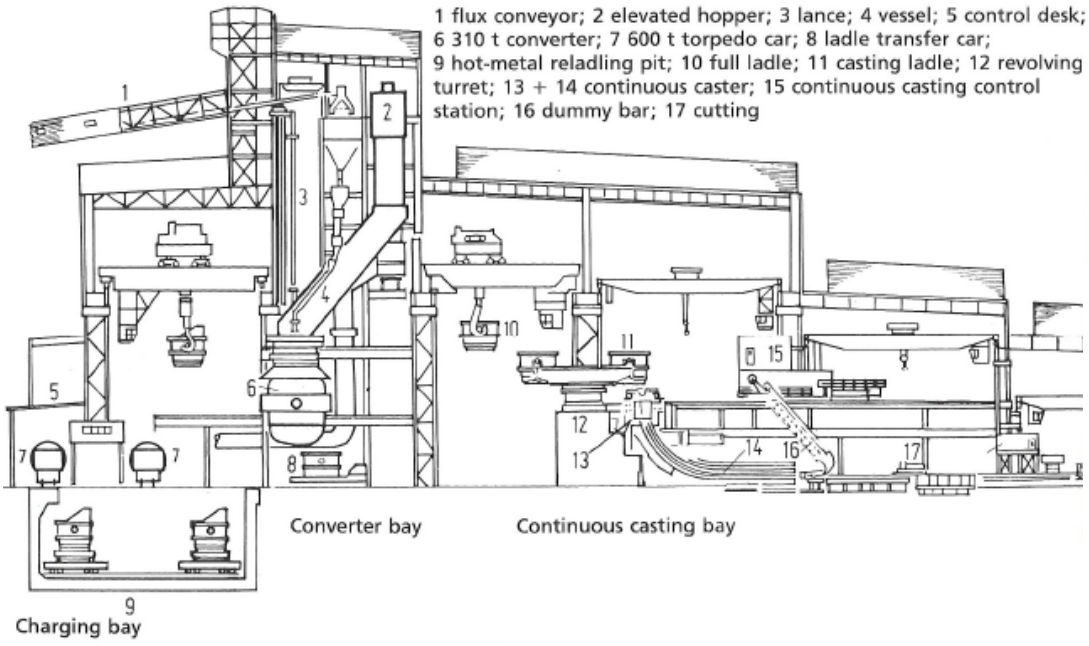

Figure 1-2: Section of a basic oxygen steelmaking plant with a CC [11].

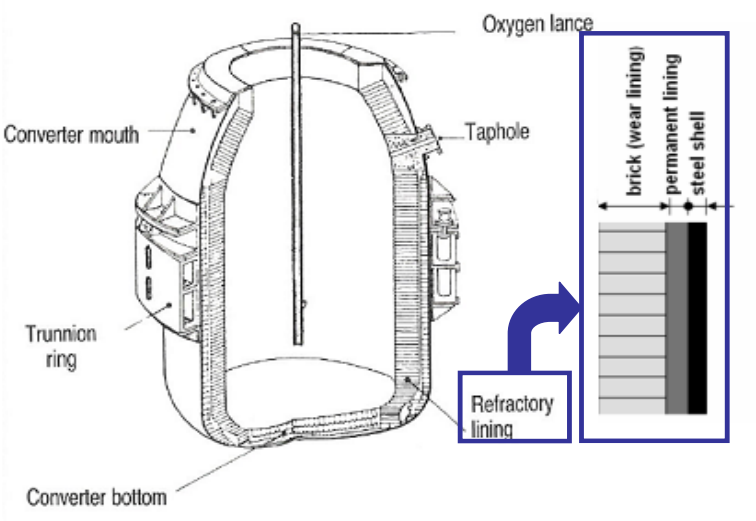

Figure 1-3: BOF design [11].

The BOS procedures can be divided into three main groups: the oxygen top blowing (LD, LD/AC), oxygen bottom blowing (OBM) and the combined blowing process. The strengths and weaknesses of each process is summarized in **Figure 1-4** with special focus on the combined blowing process, which is the currently implemented state of technique in Europe [1],[2],[4].

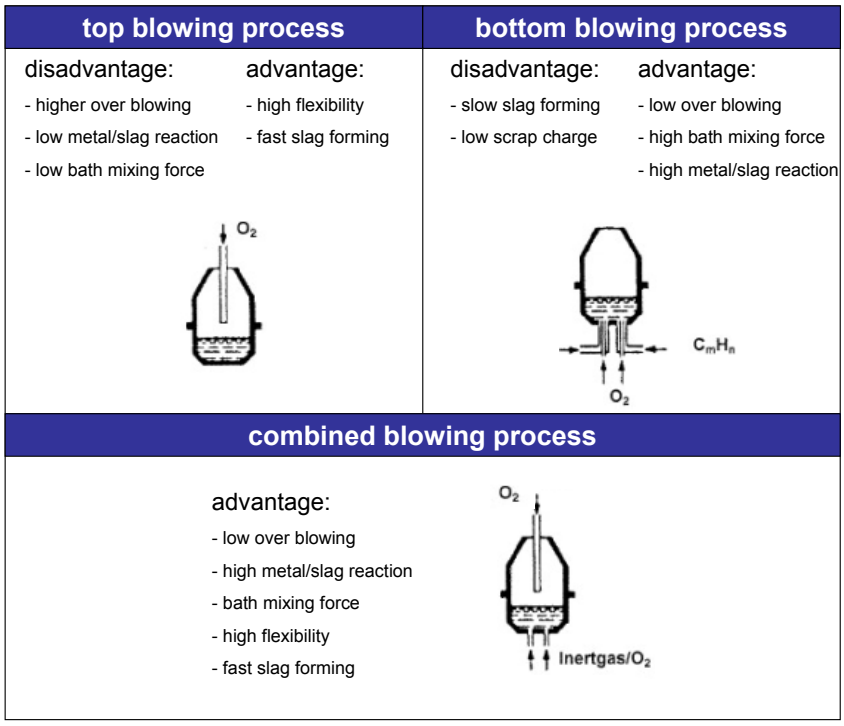

Figure 1-4: Various converter steelmaking procedures [4].

1.1.1 Oxygen top blowing process

In the original LD process oxygen is blown onto the liquid metal bath from the top by a oxygen lance. This process has been developed and installed in industrial scale the first time in Linz/Austria 1952. Characteristic for an oxygen top blown process is a low bath agitation, reduced metal/slag reaction and furthermore a high over oxidation potential of heats. That causes slopping, iron losses and high dissolved oxygen levels at tapping and hence an increase of de-oxidation-agents such as aluminium, FeSi or manganese at secondary metallurgy ladles. The essential benefits of a top blown converter are the slag formation and process flexibility [1],[4].

1.1.2 Oxygen bottom blowing process (OBM)

Pure oxygen is blown into the liquid metal through the bottom using tuyeres (**Figure 1-5**). These tuyeres are individually cooled. Hydrocarbons and fine lime in combination with oxygen may also be used as injection medium. An endothermic hydrocarbon decomposition in the melt causes a cooling and a characteristic mushroom forming around the tuyeres (wear rate of the tuyeres is decreasing). Good bath agitation, shortest reaction ways and tap to tap times are significant for the bottom blowing procedure. Weaknesses can be described with considerable wear rates at tuyere surrounding bottom areas, limited tuyere lifetimes and the lower scrap melting potential [1],[4].

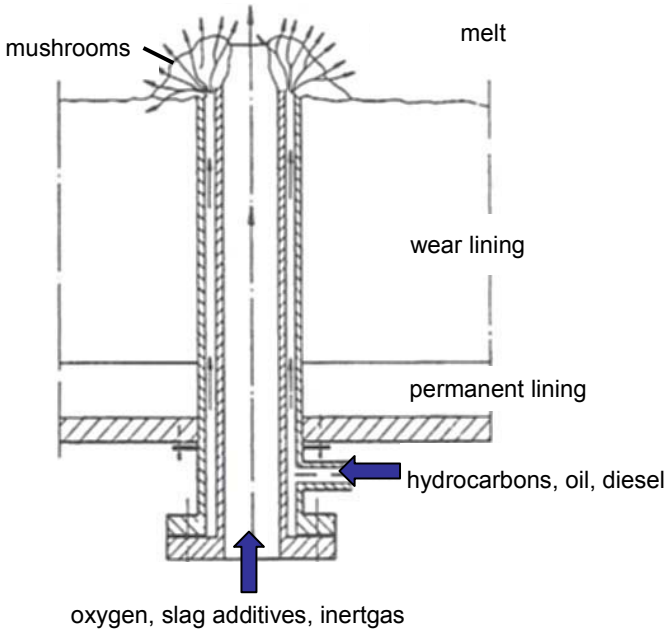

Figure 1-5: OBM tuyere [10].

1.1.3 Combined blowing process

As the name implies the process combines the advantages of the other two established procedures and can be understood as a further development of the original LD process. It is the most implemented oxygen steelmaking practice worldwide and the converter is operated with a top blown oxygen lance and bottom purging elements, through which oxygen, hydrocarbons or inert gases such as nitrogen or argon are injected. The combined blowing process can be divided into three main groups:

- Oxygen top blowing with bottom purging (inertgas)
- Oxygen top blowing with bottom blowing (oxygen, hydrocarbons)
- Oxygen top blowing with bottom blowing and purging

An overview and the particularly corresponding brief description as well is listed in **Figure 1-6**.

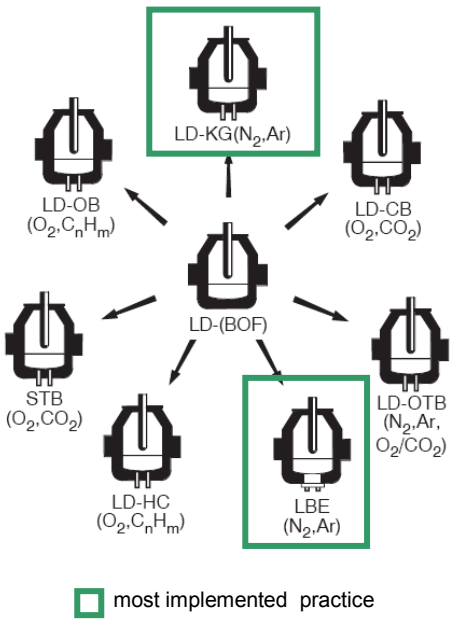

Figure 1-6: Different modes of bottom purging and blowing gases [5].

Improved slag formation, bath agitation, melt/slag reactions and an enhanced refining flexibility are the essential benefits compared to the original LD process [1],[4],[5].

2 BOF-Process

The primary aim of the BOF process is the oxidation of undesired elements ([P], [S], [Mn],[C], [Si]) of the HM to lowest levels and the adjustment of reproducible temperature, carbon and oxygen contents at the end of blow. The BOF is a more efficient decarburisation and dephosphorisation than desulphurisation application. This is caused by the oxidizing atmosphere during the refining, where oxygen is blown through the top blown lance onto the steel bath and a lot of heat energy generated.

The refining requires 15 to 20 minutes in average. For an economically operated BOF process a permanent optimization between lance height, oxygen flow, slag practice and bottom purging due to the required steel quality and charging agents (HM, scrap, flux addition analysis) is indispensable (**Figure 2-1**). Calculation models such as heat or slag balances and sub-lance samples close to the end of blow, act as serious optimization references [2], [6], [7].

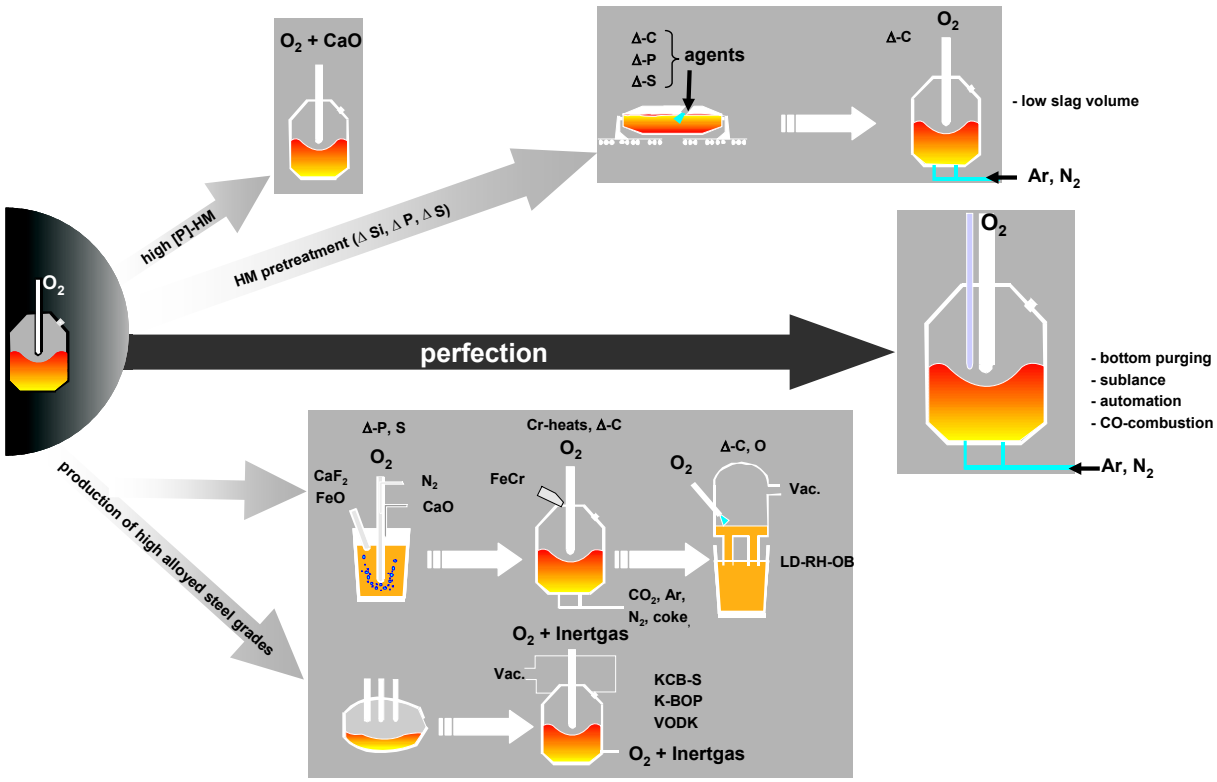

Figure 2-1: Course of BOF perfection [2].

2.1 BOF-Steps / Metallurgy

After charging of scrap, hot metal and fluxes (lime, dololime, etc.) the converter is prepared for the refining. The refining is divided into the soft and hard blowing mode. At first a water cooled oxygen lance is retracted into the converter and chemical pure oxygen is blown with supersonic speed onto the liquid hot metal. The oxygen lance is situated approximately 2.5 meters above the metal bath level and due to the kinetic energy of the oxygen stream the bath begins to circulate. The first element oxidation takes place at the hot spot of the oxygen stream, where iron, carbon and other hot metal elements are oxidized and hence a lot of heat energy is released. This process phase is called soft blowing and the defined aim is decelerated by forming a quick, reactive slag with low viscosity. The first formed slag consists of (FeO), (SiO_2) and (MnO) and has an acidic analysis. During the blowing process, the solid charged lime dissolves in slag and increases the slag basicity and minimizes the chemical reaction potential between the refractory lining and the slag. Afterwards the lance is lowered continuously with a lance height endposition adjustment of 0.5 to 1.0 meter above the liquid metal bath. The period of the main decarburisation (hard blowing mode) starts and

a so called foamy slag is formed caused by the sprayed liquid metal drops and hence the {CO} formation in slag. This foamy multi phase actually consists of molten slag, undissolved fluxes and liquid metal and is characterized by a huge surface and short reaction ways between the phases.

After half of the blowing time the maximum of the decarburisation rate is attained and the oxygen stream is still working as a pumping unit to continue the foamy consistence of the slag. This period is associated with the highest slag level in the converter and a slag volume, which is doubled compared to the starting slag weight. The logical result is an enhancement of the oxidation of [Fe] from the melt into the slag in comparison to the reduction of (FeO) by [C].

At the third fourth of the blowing time the slag volume decreases again as a result of the heterogeneous di-calciumsilicate formation in slag. Close to the end of blowing the decarburisation rate moves to lowest levels and the undiminished oxygen offer entails a higher iron oxidation. If the carbon content, element levels and the steel bath temperature meets the defined steel requirements (taking of sub-lance samples) the oxygen is turned off and the oxygen lance is withdrawn. The converter is tilted to the tapping position and the liquid steel is poured through the tap hole into a ladle. A carry over of slag should be avoided otherwise the steel purity is reduced. Hence the metallurgical work (treatment time, flux agents consumption, etc.) at the secondary metallurgy is considerable higher and more cost intensive. To minimize this carry over slag stopping systems such as pneumatic slag stoppers, dart systems or slide gates in use. After the steel tapping is finished the converter is tilted into the deslaging position and the remaining slag is poured over the converter mouth into a slag pot. Afterwards it is possible to maintain the vessel (gunning, etc.), which is optional and dependent on the converter wear profile. Finally the converter sequence is completed and the converter is prepared again for charging (30 min < tap to tap time < 60 min). The whole procedure is shown in **Figure 2-2** [8],[9],[10],[11].

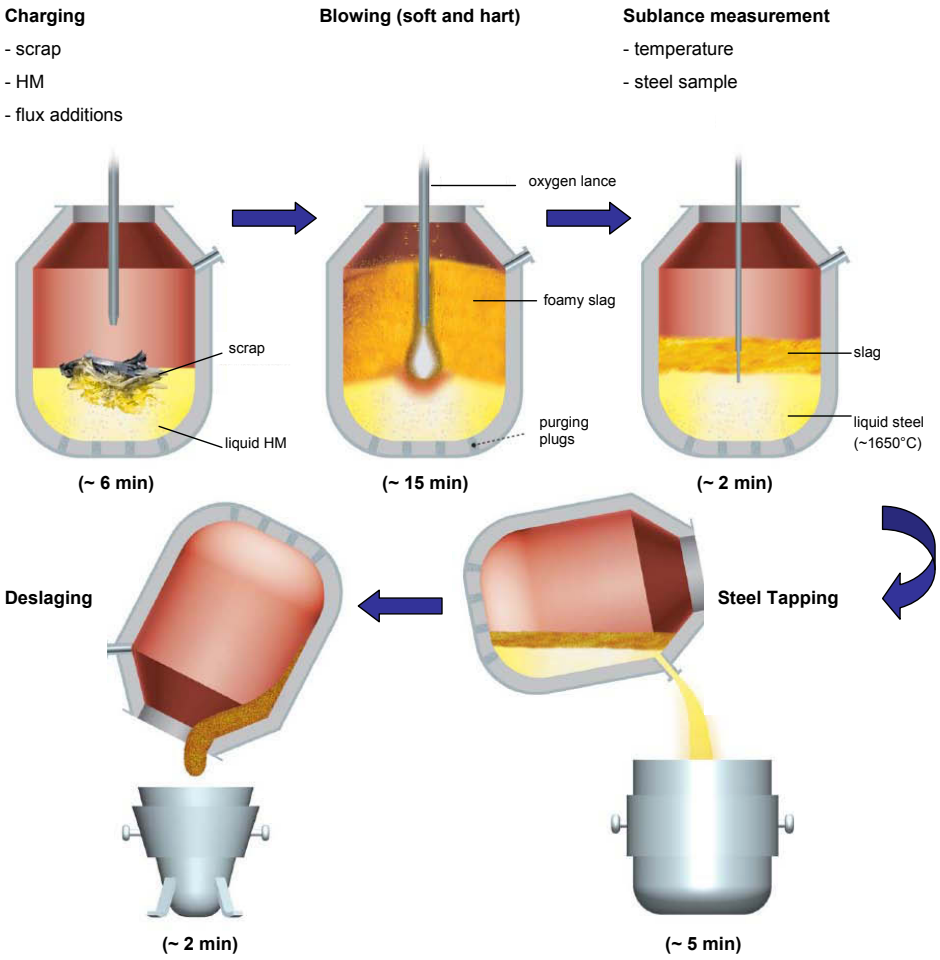

Figure 2-2: BOF-Process-Steps [8].

2.2 Behaviour / Oxidation of Elements

Reaction areas are:

- Hot spot, i.e. interface melt / oxygen stream
- Liquid metal bath
- Converter atmosphere
- Interface melt / slag
- Interface liquid iron drop / slag

- Interface melt / refractory lining

The main oxidation of the hot metal elements takes place both in the hot spot at the interface between liquid hot metal and oxygen stream and at the interface of hot metal and slag.

The behavior of elements during the refining is summarized in **Figure 2-3** and discussed in detail below [6],[11],[12].

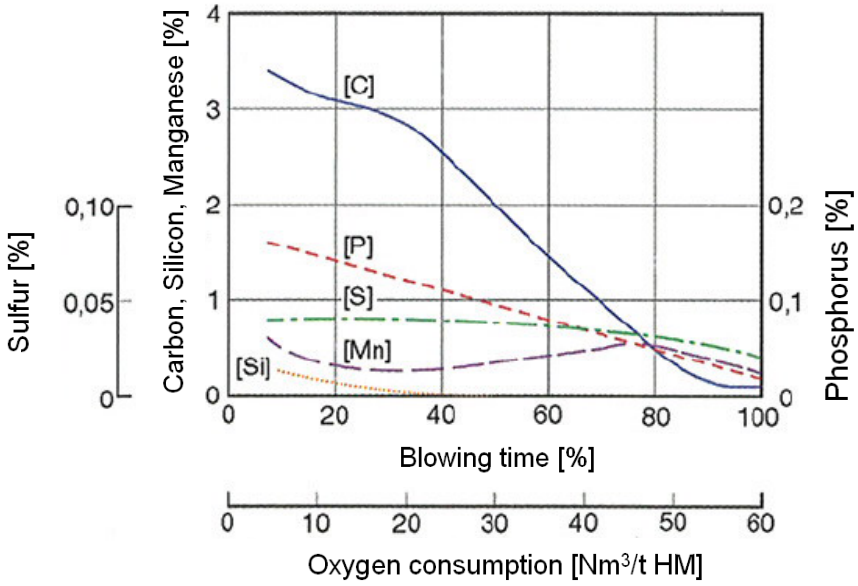

Figure 2-3: Behaviour of elements during refining [6].

2.2.1 Silicon

The element silicon shows a very high affinity to oxygen. That is why - besides iron, carbon and manganese – it is oxidized first. As a result it is one of the main components of the primary formed slag. In course of the refining the silicon is oxidized very quickly and already lowered after 25 percent of blowing time to the tapping level in steel bath (0.000x %). The oxidation of silicon is an exothermic reaction and the created heat energy is used for scrap melting.

Table 2-1 shows the most important chemical reactions.

Table 2-1: Silicon Oxidation [10].

Reaction Areas	Chemical Reaction
Interface melt / slag	$[Si] + 2(MnO) \rightarrow (SiO_2) + 2[Mn]$ $[Si] + 2(FeO) \rightarrow (SiO_2) + 2[Fe]$
Hot Spot	$[Si] + \{O_2\} \rightarrow (SiO_2)$
Liquid metal bath	$[Si] + 2[O] \rightarrow (SiO_2)$

Scrap and lime inputs are influenced by the silicon level in the HM. To realize the aimed slag basicity, more lime is charged, when the silicon content of the HM is higher (**Figure 2-4**). Furthermore the slag volume is rising simultaneously and as a consequence slopping becomes more likely. If the silicon level of the HM is lower, the scrap rate has to be reduced due to the decreased energy input [9], [10], [14].

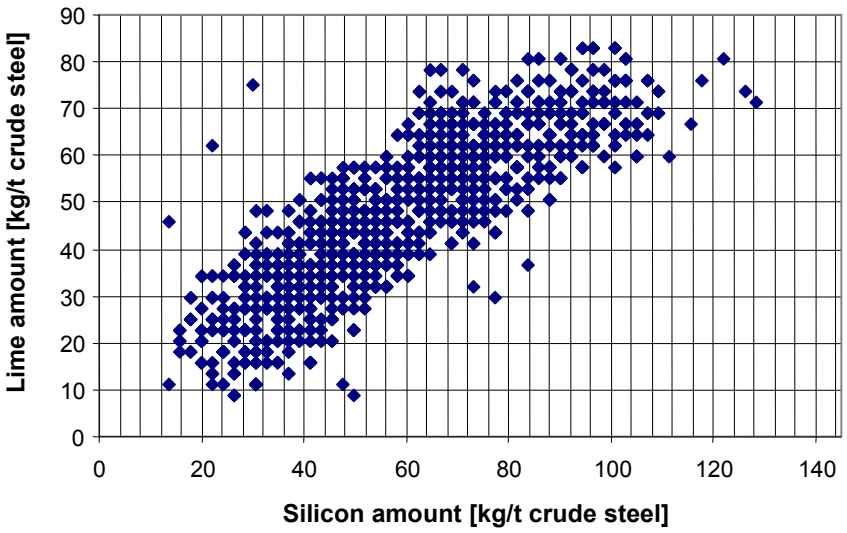

Figure 2-4: Charged lime dependent on [Si] in HM [13].

2.2.2 Manganese

At start of blowing the element manganese is oxidized at the same time as silicon and iron at the hot spot. After 40 percent of blowing time, especially when the silicon oxidation is finished, the reduction of the (MnO) in slag with the dissolved carbon in liquid metal begins (metal bath temperature increases continuously). The chemical reactions are listed in detail in **Table 2-2**.

Table 2-2: Manganese Oxidation [10].

Reaction Areas	Chemical Reaction
Interface melt / slag	[C] + (MnO) $\rightarrow$ [Mn] + {CO}
Hot Spot	[Mn] + ½{O_2} $\rightarrow$ (MnO)
Liquid metal bath	[Mn]+ [O] $\rightarrow$ (MnO)

That is why the [Mn] content is increasing again and showing the characteristic increase after 50% of blowing time (**Figure 2-5**). Close to the end of blowing where the decarburisation rate decreases significantly and deepest carbon levels are attained, the manganese is oxidized again. Thereby the [Mn] level drops to 0.2% [9], [10], [16].

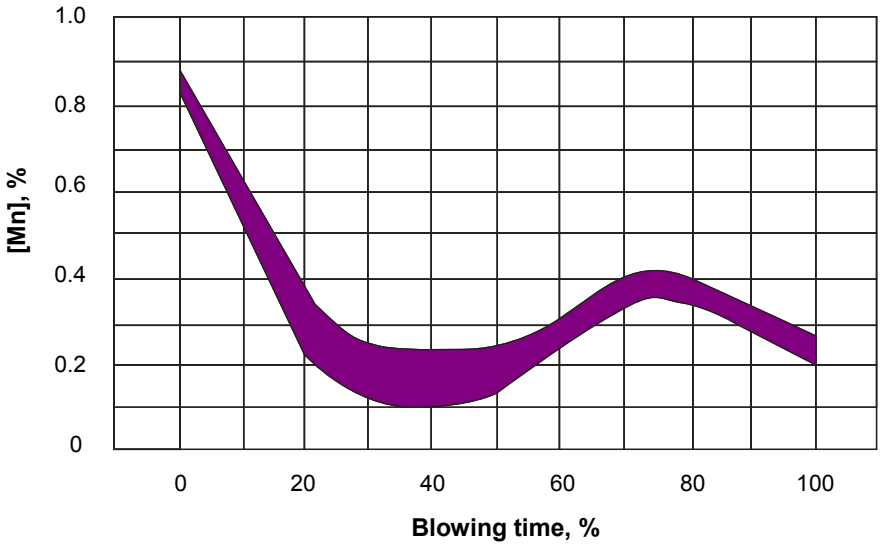

Figure 2-5: Manganese-Oxidation-Course [16].

Conditions for lowest Manganese levels in steel bath are [10]:

- Lowest [C] in steel bath
- Lowest [Mn] in charged HM
- High slag volume
- Low temperature and slag basicity (B ~ 3)

2.2.3 Carbon

At the initial stage of the refining the decarburisation occurs in a dispersion (formed slag, liquid metal, gas and unsolved charged additions) at the hot spot (**Table 2-3**). In course of soft blowing (lance height 2.5 metres above the steel bath) the formation of a quick and reactive slag is aimed. The decarburisation velocity at the blowing start is significantly low due to the higher oxidation rate of silicon and manganese. After 25% of blowing time the oxygen lance is continuously lowered and the period of the main decarburisation begins. This phase is called hard blowing. Through the sprayed liquid iron droplets the slag forms a foamy slag. Two third of the decarburisation reactions take place in the slag and the rest of the carbon oxidizes at the hot spot.

Table 2-3: Carbon Oxidation [10].

Reaction Areas	Chemical Reaction
Interface melt / slag	[C] + (FeO) $\rightarrow$ [Fe] + {CO}
Hot Spot	[C] + ½{O_2} $\rightarrow$ {CO}
Liquid metal bath	[C] + [O] $\rightarrow$ {CO}

The reaction product {CO} from the hot spot area leaves the converter through a channel formed around the oxygen lance (**Figure 2-6**). {CO} from the interface reaction of the melt and slag forms the bubbles in the slag. With advanced refining (close to the end of bow) the carbon level in the steel bath and the decarburisation rate decreases to lowest levels.

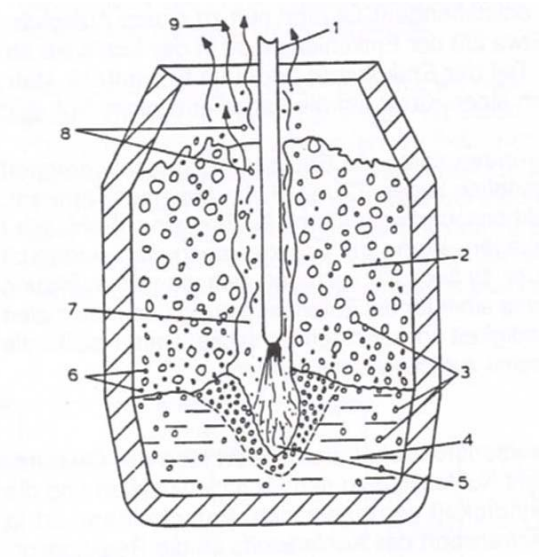

1.oxygen lance; 2. foamy slag; 3. {CO} bubbles; 4. liquid metal bath; 5. hot spot

6. liquid iron drops; 7. lance canal; 8. sprayed liquid iron drops ; 9. brown smoke

Figure 2-6: Hard blowing [10].

Figure 2-7 shows the course of slag volume, gas and emulsion refining during the BOF process in detail. Gas refining describes the direct carbon oxidation via the oxygen stream at the hot spot and emulsion refining the reaction over the slag-liquid iron-gas emulsion. The transition from the soft into the hard blowing mode means a higher share of emulsion reaction and a decreasing of the direct carbon oxidation [9], [10], [17].

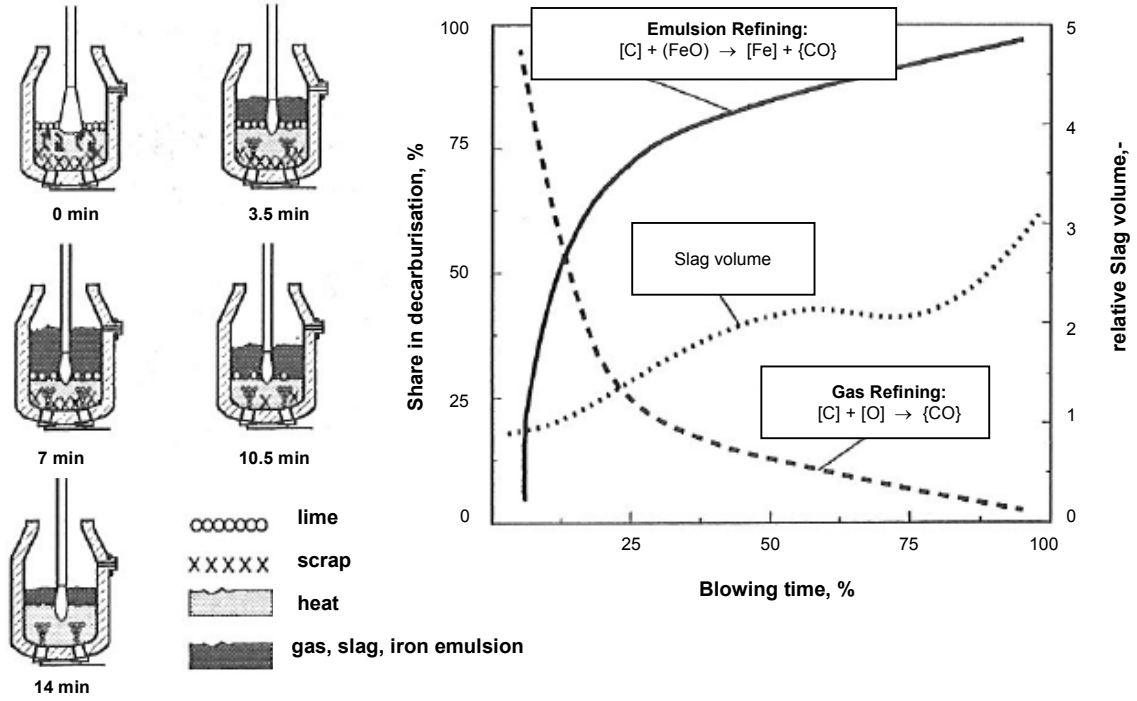

Figure 2-7: Course of carbon oxidation [9].

2.2.4 Phosphorus

The refining is focused on decarburisation and dephosphorisation. An efficient dephosphorisation is necessary, because phosphorus shows a tendency to segregation during solidification. The dephosphorisation occurs at the interface between slag and melt using the charged lime (**Table 2-4**).

Table 2-4: Phosphorus Oxidation [10].

Reaction Areas	Chemical Reaction
Interface melt / slag	$2[P] + 5[O] + (CaO) \rightarrow (CaO \cdot P_2O_5)$

For attaining lowest [P] levels at tapping it is essential that a quick and (FeO) rich slag is formed (**Figure 2-8**). (FeO) is acting as flux for lime dissolution and promotes the dephosphorisation. The charging of dust briquettes enforces the dephosphorisation effect too, because the melt temperature is decreasing.

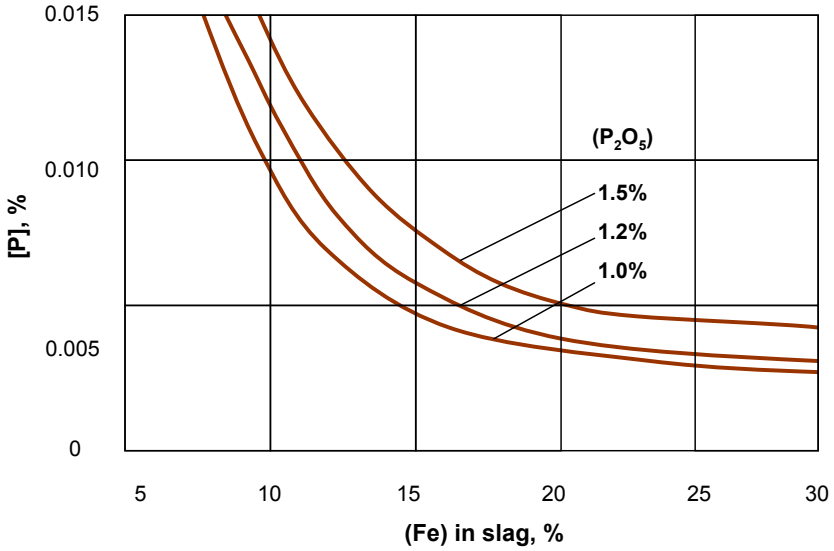

Figure 2-8: [P] dependent on (Fe) content in slag [10].

Simultaneously to the manganese increase there is also a decrease in the phosphorus content of the melt (**Figure 2-9**). After 50% of blowing time the (P_2O_5) is thermodynamically unstable causing a reduction from slag.

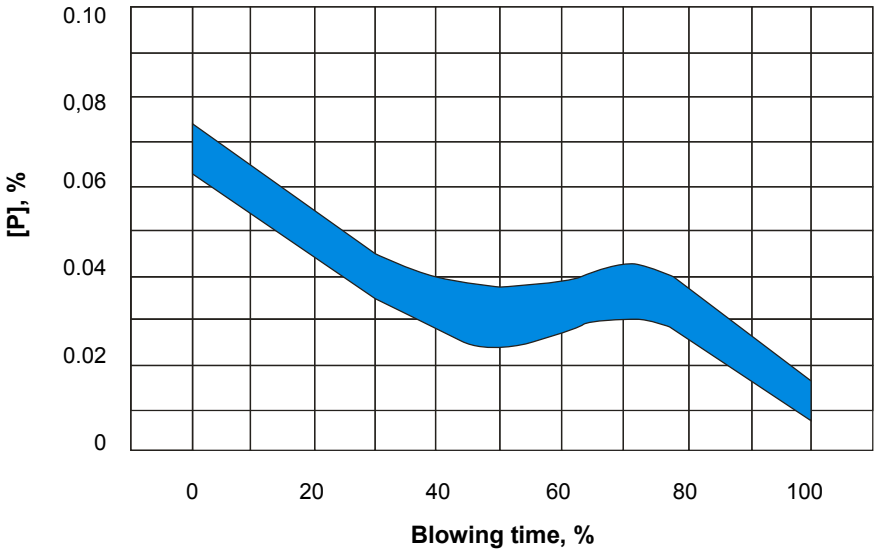

Figure 2-9: Course of phosphorus during refining [16].

The phosphorus distribution at tapping is determined by the dissolved manganese level in the bath and the tapping temperature (**Figure 2-10**). This is the reason for the final dropping of the [P] content close to end of blow [9], [16], [18].

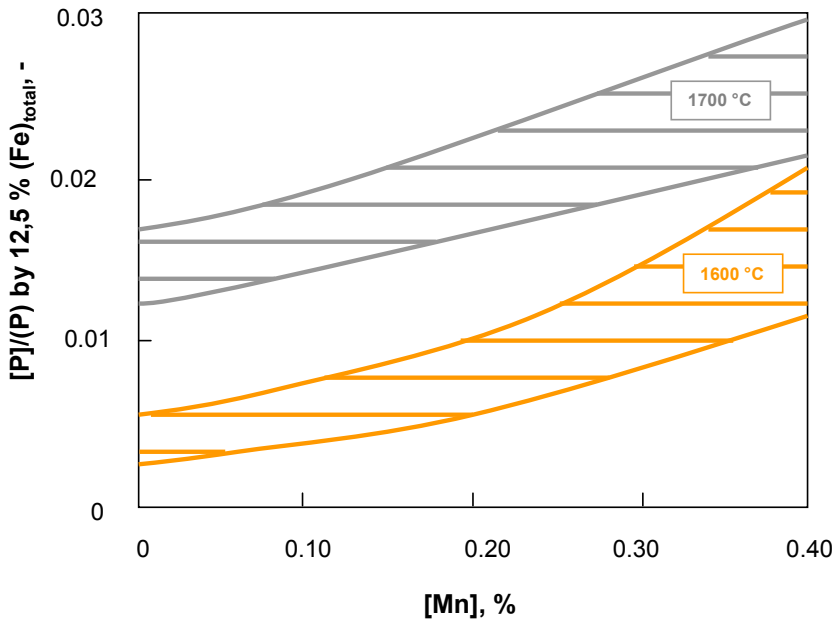

Figure 2-10: Phosphorus distribution in according to [Mn] level [9].

Conditions for attaining lowest phosphorus levels in steel bath [10]:

- Low refining temperature
- High slag basicity
- (FeO) rich slag (high activity of (FeO) in slag)
- Good bath agitation (bottom purging)
- Lowest [P] in charged hot metal

Reduced tapping temperatures lead to lower [P] levels in liquid steel baths.

2.2.5 Sulphur

During the refining process the desulphurisation takes place at the interface between slag and liquid metal (**Table 2-5**).

Table 2-5: Sulphur Oxidation [10].

Reaction Areas	Chemical Reaction
Interface melt / slag	[S] + (CaO) $\rightarrow$ (CaS) + [O]

A reducing atmosphere and high temperature support an efficient desulphurisation, but the BOF process works with oxidized conditions. That is why the desulphurisation procedure is done prior the BOF process in torpedo or HM ladles via injection of lime, lime carbide or manganese [9], [10], [16].

Table 2-6 shows a typical chemical HM-analysis and a liquid tapped steel analysis is given in **Table 2-7**. The common tapping temperature is in the range between 1650 and 1680° C and depends on the availability of a ladle furnace in the secondary metallurgy.

Table 2-6: HM analysis [15].

Element	Level [%]	
	Lower Limit	Upper Limit
Fe	95	
C	4.2	4.6
Si	0.25	0.80
Mn	0.20	0.60
P	0.070	0.13
S	0.010	0.035

Table 2-7: Steel analysis after tapping [15].

Element	Level [%]	
	Lower Limit	Upper Limit
Fe	99	
C	0.015	0.04
Si	< 0.01	
Mn	0.08	0.40
P	0.005	0.02
S	0.005	0.02
N	0.002	0.004

2.3 BOF-Slag

For realizing an efficient and economical operated converter it is necessary to aim a very quick slag formation with a high steel bath reaction potential and low viscosity. These conditions support the dephosporisation, desulphurisation and decaborisation during the refining. The principal assignment of the BOF slag can be divided into two essential parts – the metallurgical and the maintenance part. The most important points are summarized below.

- Removal of undesirable iron elements from the liquid metal bath during the refining

  → Dephosphorisation

  → Desulphurisation
- Protection against heat loss and atmosphere reactions ([N] problem)
- Utilization for converter maintenance, especially wear stabilization (e.g. slag splashing, slag washing,..)

The slag practise, in detail the flux amount, interval and sequence is adapted to the produced steel grades and maintenance practise[20], [21].

Table 2-8 shows a typical slag analysis for a German steel plant. The average slag basicity $\left(\frac{CaO}{SiO_2}\right)$ is in the range of approximately three.

Table 2-8: Slag analysis [15].

Element	FeO	SiO_2	MnO	CaO	MgO	TiO_2	Na_2O
content [%]	18 - 30	10 - 15	~7	~45	~5	~1.2	~0.04

2.3.1 Slag formation

During refining the slag composition is changed subject to HM analysis, scrap amount/analysis, flux analysis, refractory wear, blowing (oxygen lance) and slag practise. Due to the HM and scrap analysis with special focus on the silicon content there are two significant ways for the converter slag formation: the lime ferrite and lime silicon way. For a serious interpretation of both ways, the ternary system CaO-FeO-SiO_2 (**Figure 2-11**) acts as primary reference.

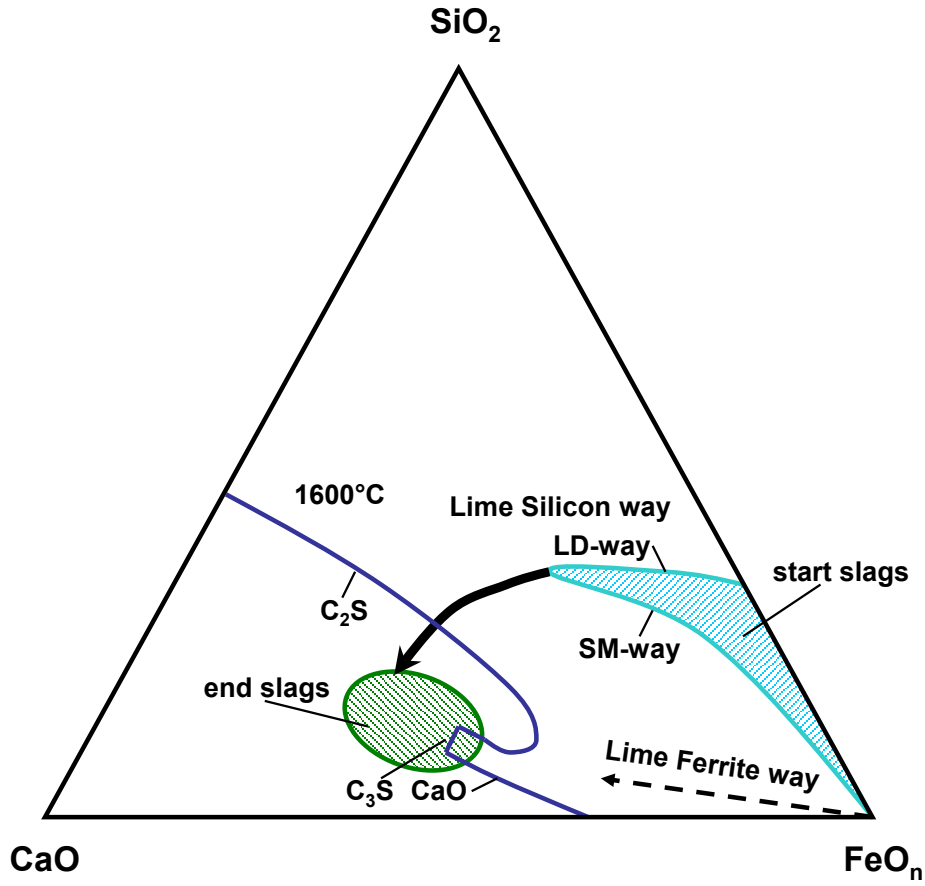

Figure 2-11: Slag ways fort the BOF process [22].

2.3.1.1 Lime Silicon path

The Richard-Ellingham diagram shows the free reaction enthalpy of different stabile oxides depend on temperature and hence the oxygen affinity of elements. Iron, carbon, silicon and

manganese are oxidized first, the starting point of this slag path is at the line FeO-SiO_2. The primary slag formation consists of fayalite ($2FeO.SiO_2$) and olivine. Consequently the charged lime is dissolved by the primary slag forming a CaO containing slag with low melting temperature. That means a quicker dissolution of lime and further a modification of the chemical slag configuration to the area of CaO at the ternary system. Therefore it comes to a formation of di-calcium-silicate ($2CaO.SiO_2$) and to a reduction of (FeO) in the slag via the dissolved carbon in the liquid metal bath. Thus the formed slag moves to the di-calcium-silicate area consisting heterogeneous consistency, less reaction potential and rising slag viscosity. The modification of the slag properties can be explained by the development of a blocking layer, which surrounds solid lime particles and hence avoids the lime dissolution. After the oxygen lance practise changes from the soft into the hard blowing pattern the slag gets foamy. At the end of blow the slag way drifts to the (FeO) side at the ternary system. This is a result of the removal of the decarborisation rate, lowest [C] levels and hence higher [Fe] oxidation via the oxygen stream [10], [21].

2.3.1.2 Lime Ferrite path

To meet the defined requirements of low BOF slag volume philosophies and higher yields, modern steel plants especially in Japan are still operating with lower silicon and phosphorus levels ([Si] < 0.2 %) in the charged hot metal. This can be explained by the HM treatment, where besides the regularly desulphurisation in Europe, a desiliconsation and dephosphorisation is done. In comparison with the classic lime silicon way the (FeO) content in slag at blowing start is much higher and hence the potential or rather condition for lime dissolution is improved. It is an effect of the formation of a lower melting eutectic (CaO) slag at the beginning, caused by the oxidized iron, which is acting as a lime flux. The run through the area of dilime silicate is partially avoided and the sector of lime saturation is aimed directly. The blocking layer surrounded solid lime particles at the dilime silica area have a negative influence on the dephosphorisation effect. Due to the higher iron oxidation and reduced (SiO_2) levels in slag the formation of the blocking layer can be mostly avoided. In association with better conditions for the lime dissolution in the slag the chemical reaction between slag and the refractory lining can be dropped considerably [10], [21].

2.3.2 Preconditions for realization of a (MgO) over saturated slag

The BOF lining is made of basic materials (magnesia) causing especially at start of blowing an enormous chemical reaction potential between refractory lining and acidic slag. For a low wear rate at the initial stage of slag formation it is necessary to charge or rather offer a MgO carrier in form of additions (for example dolomite) and avoid the <MgO> dissolution from the lining. Rising (MgO) levels in the slag involve increased viscosities and lower metallurgical slag activities. The primary purpose of a (MgO) oversaturated BOF end slag can be answered with the converter maintenance after tapping (slag splashing, slag washing, etc.). This type of slag consistence is needed to achieve an adherence effect on lining to stabilize the wear at pre-wear areas such as charge pad with the strong scrap impact (**Figure 2-12**). The (MgO) saturation in the slag is limited by the sequence and amount of lime addition and hence the slag basicity [21], [26], [27].

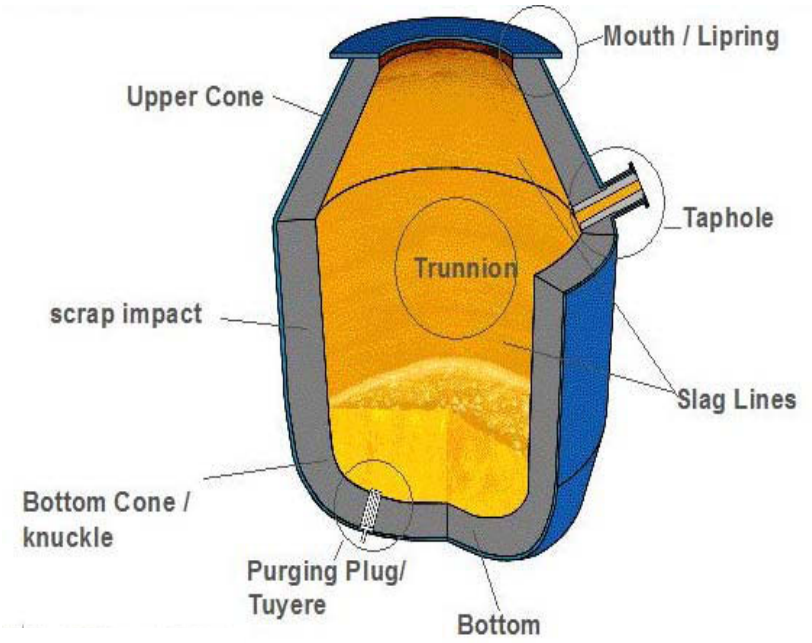

Figure 2-12: BOF pre-wear zones [19]

2.3.2.1 Influence of lime on the (MgO) solubility in slag

The (MgO) solubility in BOF slags is demonstrated in **Figure 2-13**. It shows a considerable solubility at blowing start and a falling ability with advanced refining time and increased slag basicity (**Figure 2-14**). The solubility depends on the lime addition sequence, amount and furthermore on the lime dissolution rate, which is influenced by bottom purging and the oxygen lance practise. Based on the slag way theory the silicon content in the charged hot metal is also a significant lime parameter (focus on the area of di-calcium-silicate).

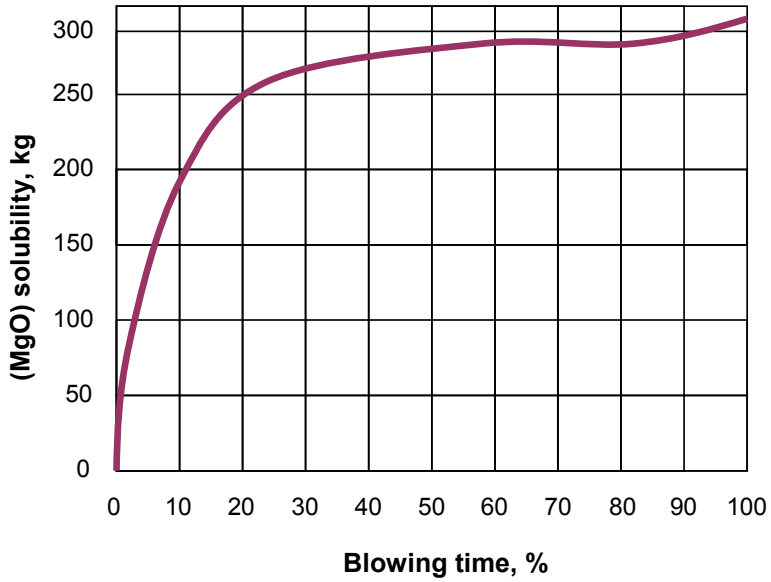

Figure 2-13: MgO solubility during refining time [20].

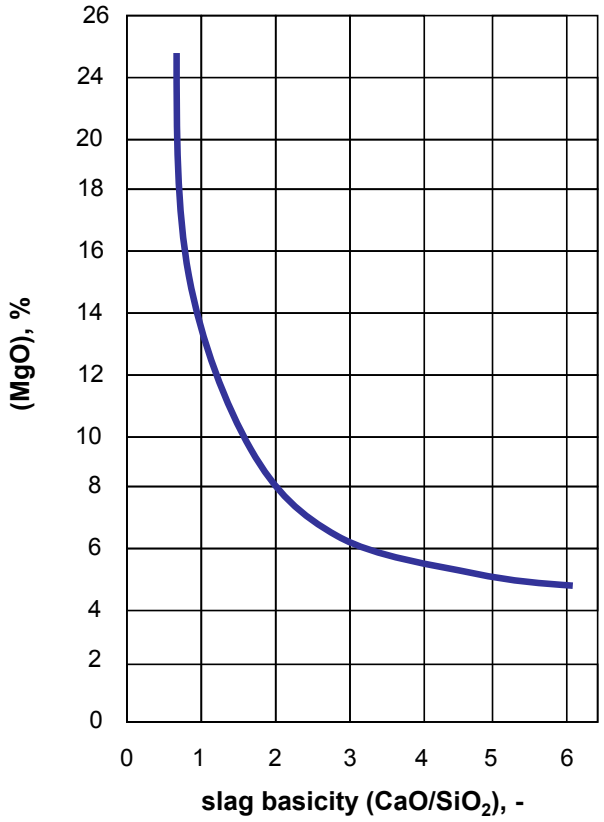

Figure 2-14: MgO level in slag depend on basicity [24].

MgO and CaO are showing very low interdependence dissolutions. The (MgO) saturation in slag is reached first, before the slag is saturated with lime. This fact is described with different driving forces or rather their distances to the saturation. In common dololime (40% MgO and 60% CaO) is charged first followed by lime. The sequence has to be observed, because just on this way a significant increasing of the (MgO) level in the first formed slag is realized. Hence a reduction of the wear in the slag zone to a minimum is possible. By deliberate later charging of lime the already dissolved (MgO) has an essential influence on the di-calcium-silicate (C_2S) area. The di-calcium-silicate area or rather the nose is pushed back (blocking layer partially avoided) and so better conditions for the lime dissolution are created. The effect is demonstrated in **Figure 2-15** with the main focus on the 10% MnO and MgO line, where no lime saturation area is existent any more. This configuration is characterized with a very high share of slag heterogeneity [23], [24], [25], [26].

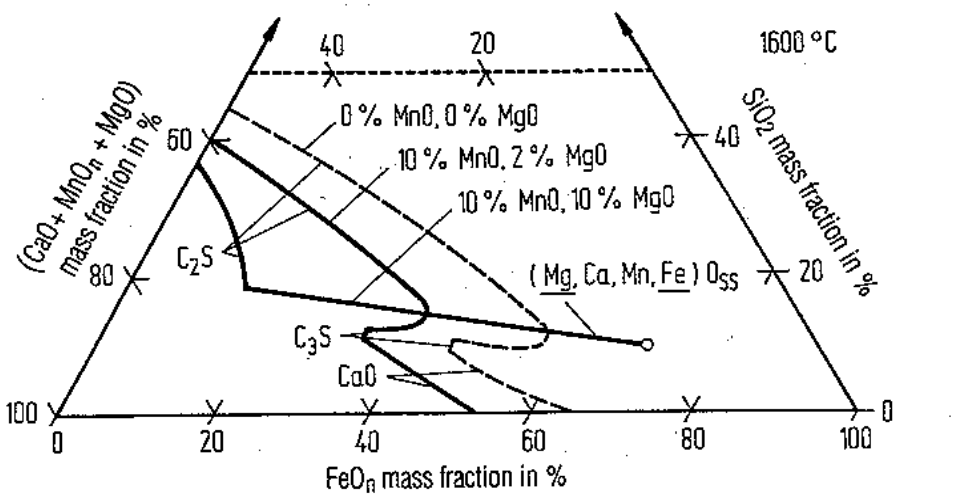

Figure 2-15: Influence of MgO level on C_2S area [10].

2.3.2.2 Influence of the (MgO) level on the (P)/[P] distribution

Increased (MgO) l evels i n s lag c ause a hi gher s lag v iscosity w ith l ower l ime di ssolution potential. A t this the s lag reactivity and the dephosphorisation effect in th e BOF are decreasing significantly (**Figure 2-16**) [45].

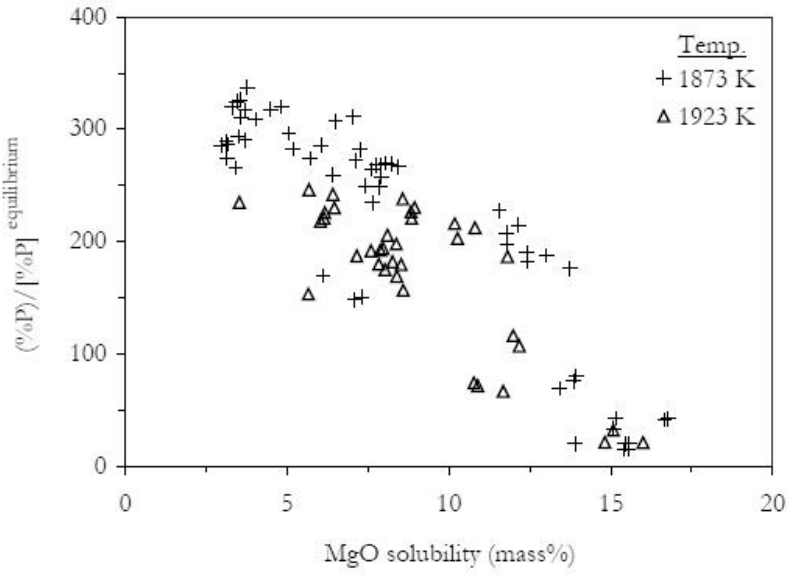

Figure 2-16: Variation of phosphorus partition ratio with (MgO) concentration [45].

3 Bottom purging

The fundamental reasons for implementing a bottom purging system are on the one hand to improve metallurgical results and on the other hand to guarantee a high quality economical oxygen steel production at lowest costs (**Figure 3-1**).

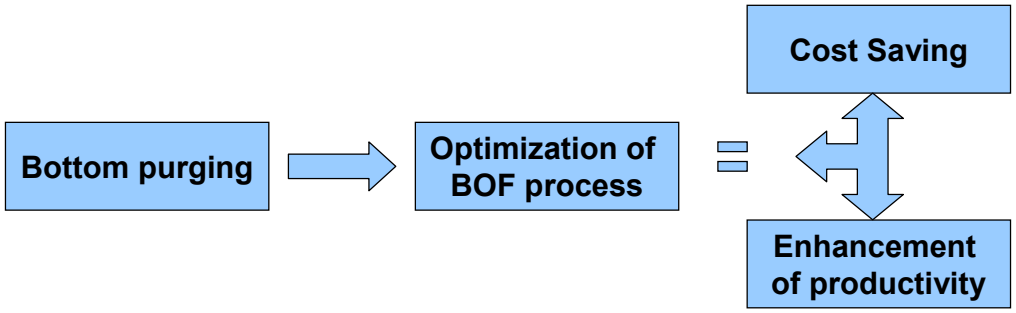

Figure 3-1: BOF-Purging-Matrix.

The most important benefits are summarized below [28], [29], [30].

- High quality and economical steel production

→ shortening of the tap to tap time

→ reducing of the re blow rate numbers

→ lower (FeO), [P] levels and [Mn] oxidation

- Realizing of lower [C]x[O] products / p_{CO} values

→ less de-oxidation alloys (e.g.: Al) are needed

→ releaving of the RH-operation (saving costs)

- Improved steel bath homogenization/agitation and temperature distribution

→ shorter and quicker reaction ways between slag and steel bath (better conditions for scrap/ flux addition melting, higher scrap / hot metal ratio)

→ improved process control (higher accuracy for tapping temperature and element levels)

→ improved steel and flux addition yields (less slag volume and slopping material)

3.1 Metallurgical benefits

Purging patterns, especially number of plugs, flow rates and the kind and quality of purging gases have a remarkable influence on the BOF metallurgy. Those parameters must be strictly coordinated otherwise the process is getting beyond control and aimed metallurgical results cannot be achieved [31], [32].

3.1.1 Carbon/Oxgen

As a result of bottom purging the kinetics for decarburisation are improved and thus lower carbon levels at the end of blow without steel bath over oxidation are realized. The indicator for an efficient purging performance is the [C]x[O] product, which is compared to a top blown operated converter much lower and in average in the range between 20 and 25×10^{-4}. Due to

the refining process there are non-equilibrium conditions in liquid steel bath existent - also between slag and liquid steel bath [34].

An investigation for adjusting the carbon [wt%] and oxygen [ppm] equilibrium was published by Vacher and Hamilton. The [C]x[O] product is estimated using defined parameters (p_{CO}=1.0 bar; steel bath temperature=1600°C) at 0.0025 and the completely equilibrium diagram with the corresponding equations is shown in **Figure 3-2**.

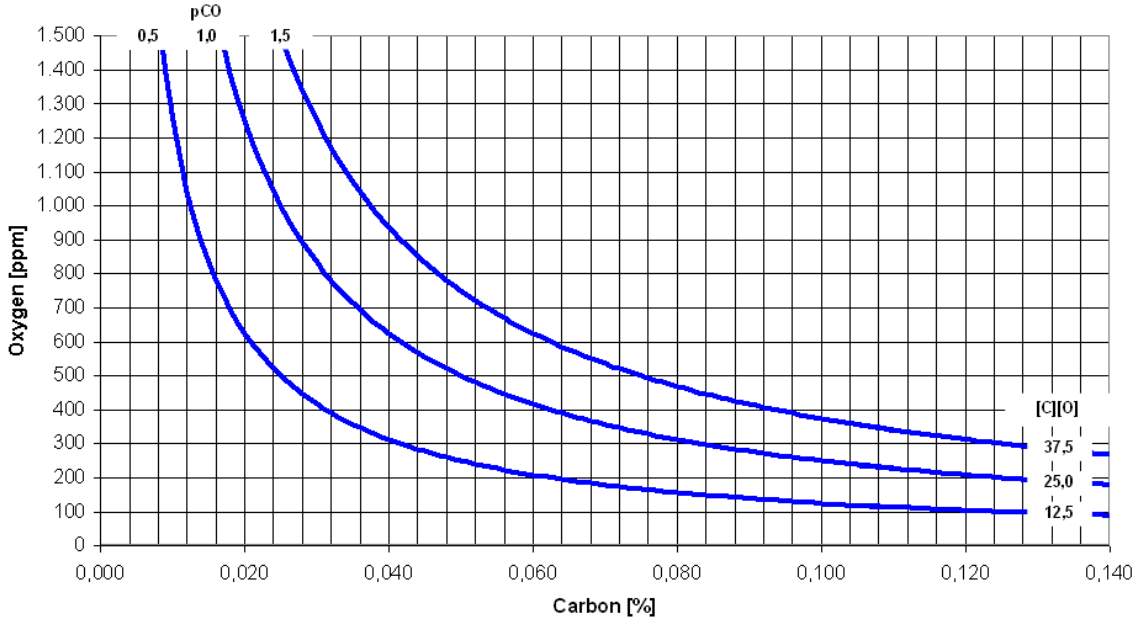

Figure 3-2: Vacher-Hamilton-Diagram [13].

With an appropriate bottom purging program the reactions can be driven closer to the equilibrium at the end of blow and hence the decarburisation effect is strengthened. The duration of post stirring intensifies that effect additionally. For aiming lowest carbon levels, the carbon content of the refractory lining is also a significant parameter.

In reference to a top blown operated converter dissolved [O] contents at equal [C] levels at tapping are lower resulting in a minimization of the de-oxidation-agent consumption in the ladle (**Figure 3-3**). There is also the chance to release or save the expensive RH treatment caused by lowest refined carbon levels at tapping (= cost saving). The RH treatment is a

vacuum procedure at the secondary metallurgy and is utilized for liquid steel decarburisation to lowest levels, alloying and the steel bath removal ([H], [O] reduction).

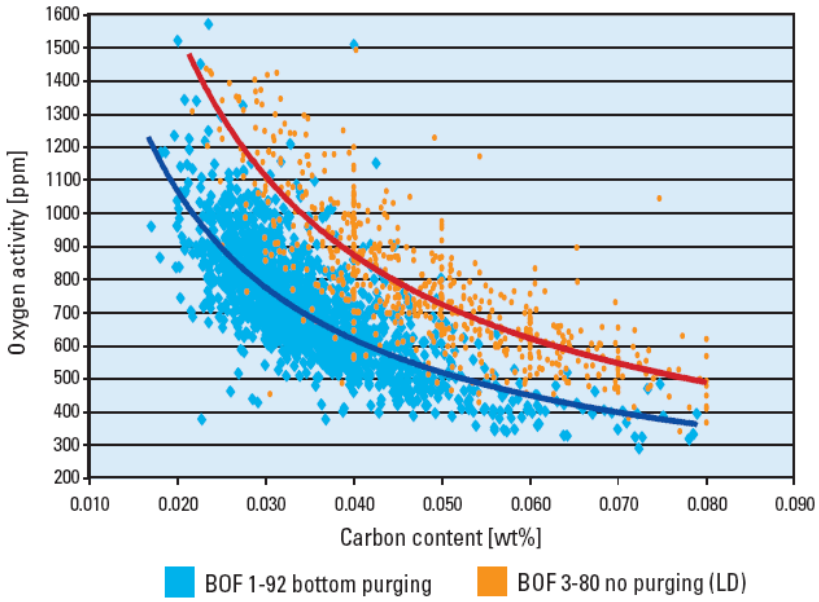

Figure 3-3: Comparison between BOF with bottom and without bottom purging [34].

3.1.2 Iron yield

Bottom purging, hot metal composition ([Si] content), the slag practise and blowing programs influence the (FeO) level in the slag und hence the chemical reaction potential between slag and lining and the effect of post stirring. A BOF with bottom purging system is characterized with lower iron contents in slag and also lower slag volumes in comparison to a top blown converter (LD) (**Figure 3-4**). Furthermore the (FeO) level in slag at tapping is dependent on the dissolved carbon in steel bath [36].

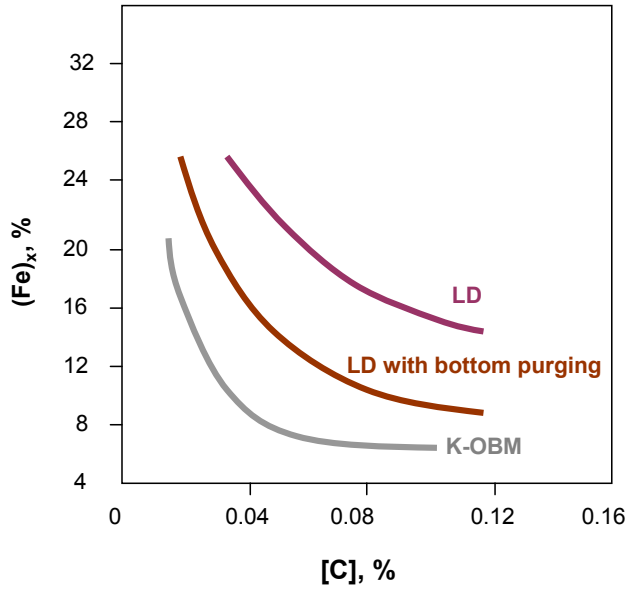

Figure 3-4: $(Fe)_x$ level in slag due to different BOF characteristics [19].

3.1.3 Manganese

The manganese yields at equal carbon levels at tapping are higher due to a conventional LD process. In this connection less Fe Mn agents are needed for the secondary metallurgy alloying depending on the steel grades. Thereby the adjustments of manganese levels are better controllable. At this the OBM process shows higher manganese yields in comparison to the LD process with bottom purging system (**Figure 3-5**) [30].

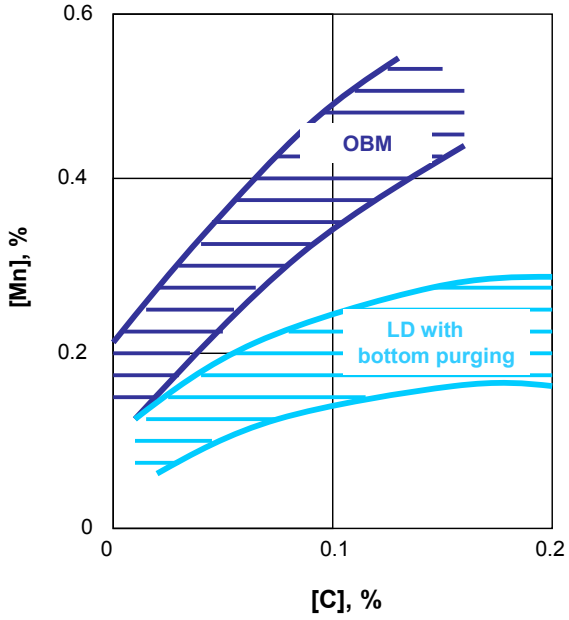

Figure 3-5: [Mn] / [C] level [10].

3.1.4 Phosphorus

Bottom purging is characterized through a better intake capacity of (P_2O_5) in slag and a quicker lime dissolution. The phosphorus distribution due to the steel bath temperature is demonstrated in (**Figure 3-6**).

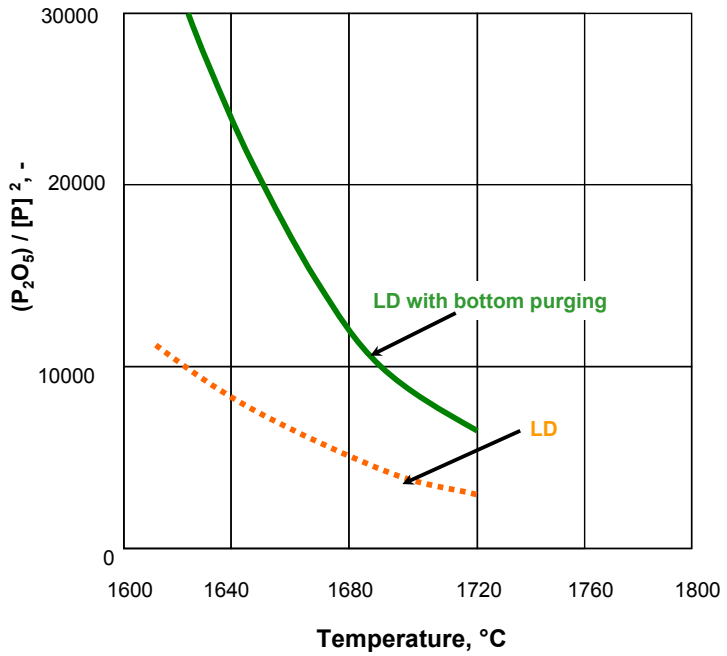

Figure 3-6: Phosphorus distribution [10].

According to the sprayed liquid iron drops during the refining process, especially during the hard blowing phase, the temperature of the formed slag is higher than the melting bath. This results in weaker conditions for dephosphorisation. Through purging the slag temperature is lowered considerably caused by the excellent bath agitation and the better temperature equilibration between slag and steel bath [28], [30].

3.1.5 Influence of post stirring

The main purpose of post stirring is on the one hand the realization of lowest carbon and phosphor levels at tapping and on the other hand the quick and precise adjustment of the tapping temperature (cooling effect). Purging time and intensity are the two decisive parameters for the achievement of certain element levels. Post stirring enhances the decarburisation effect significantly by leading the dissolved carbon and oxygen in steel bath closer to the equilibrium (**Figure 3-7**) [30], [33].

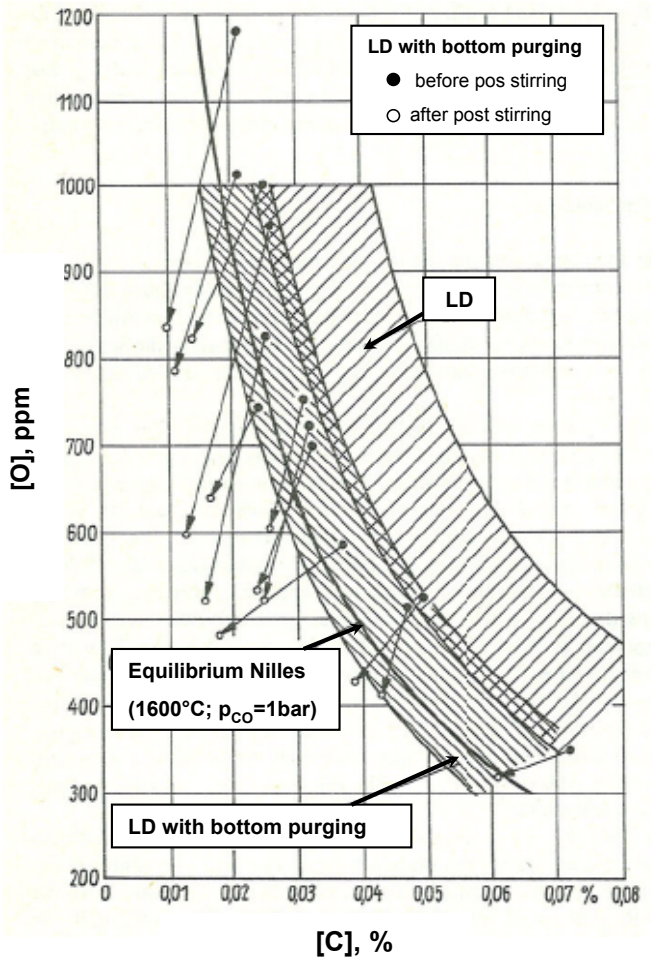

Figure 3-7: [C] and oxygen activity before and after post stirring [30].

Implementing an appropriate purging program with three minutes post stirring an additional carbon reduction of 50% and resulting carbon contents of 0.010% are absolutely achievable. The post stirring also influences phosphor, manganese and sulphur levels. The sulphur distribution (S) / [S] is improved and higher sulphur reductions up to 20% are finally achieved. The same effect is clearly visible at the phosphor and manganese distribution (**Figure 3-8**).

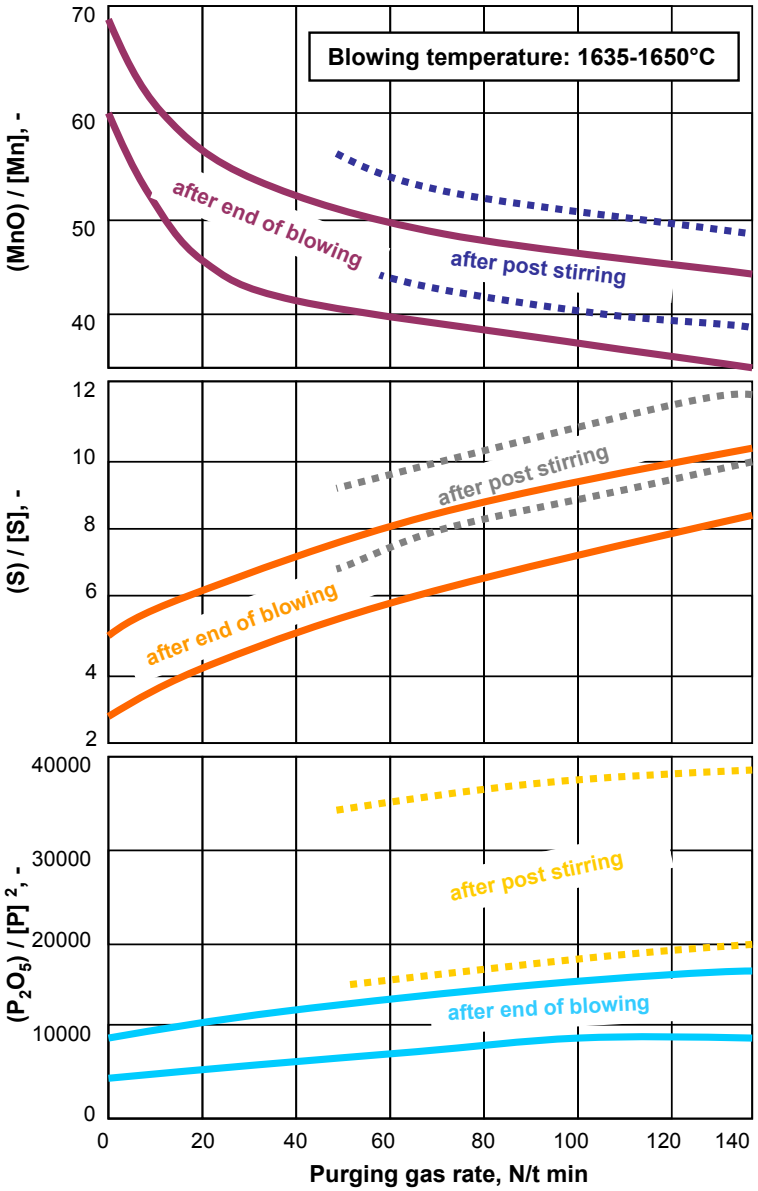

Figure 3-8: Manganese, Sulphur and Phosphorus distribution depending on post stirring [28].

Post stirring causes cooling of the liquid steel bath enhanced by additional charging of LD-slag. That means an enhancement of the phosphor distribution at factor three and a decreasing of the phosphor level at tapping to 0.005% (**Figure 3-9**).

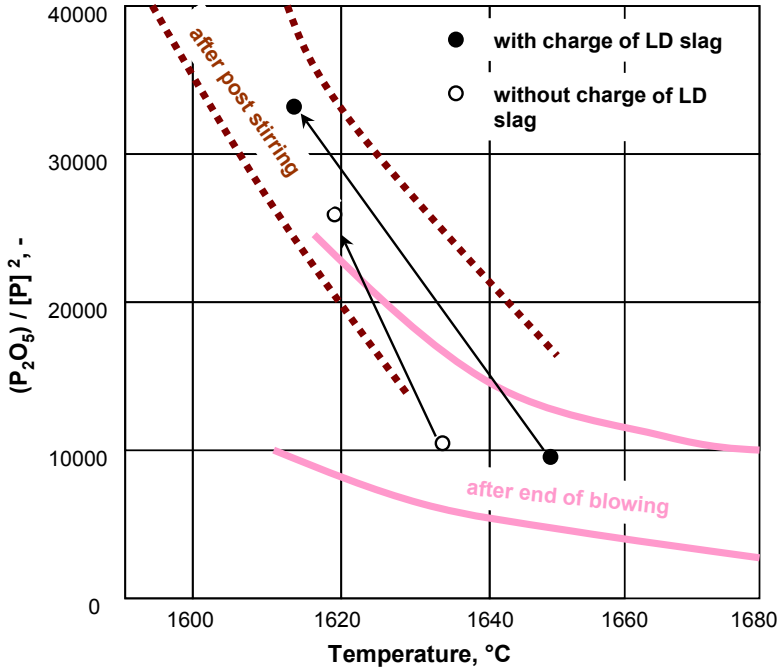

Figure 3-9: Influence of extra charging of LD slag on phosphor post stirring effect [28].

3.1.6 Influence of purging plug arrangement and number of plugs

The purging system influences the equilibrium conditions in the steel bath during the refining process and thereby the metallurgical results. Bottom purging permits to get closer to or rather approach the equilibrium at the end of blowing. The effect of decarburisation and dephosphorisation is considerably improved. **Figure 3-10** shows the consequence of various plug arrangements and numbers on the equilibrium approaching (defined by the purging parameter Rp) [37], [38].

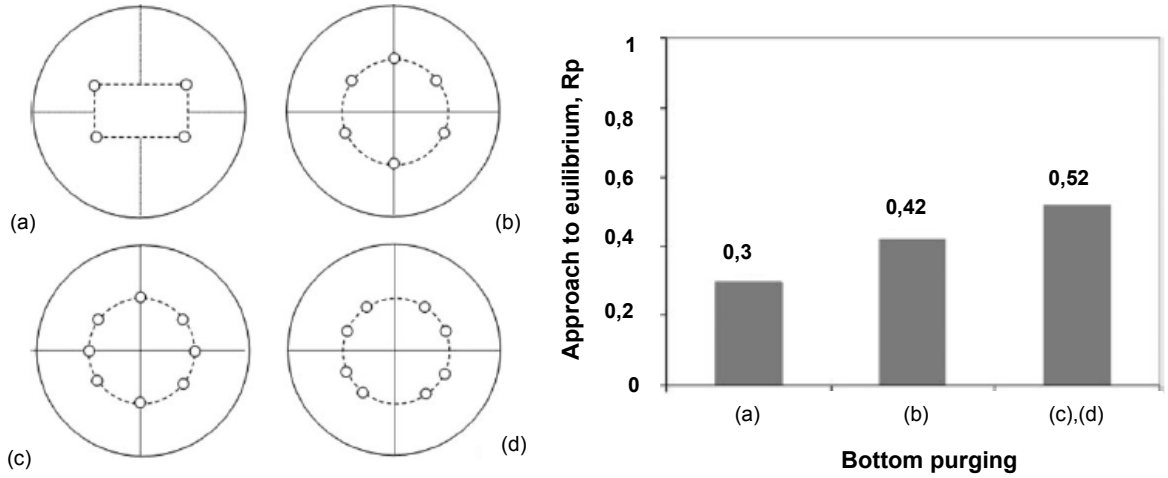

Figure 3-10: Plug arrangement and numbers / approaching equilibrium [37].

For effectiveness of the purging the parameter Rp has been established. Rp describes the ratio of the condition $_{actual}$ to the condition $_{equilibrium}$. If the equilibrium is attained the parameter Rp is one. An increasing of the number of plugs means enhanced bath agitations and hence higher values of Rp closer to one.

The influence of the purging plug arrangement (circle, elliptical, rectangular) by different circle diameters, number of plugs and angles is discussed according to **Figure 3-11** and **Table 3-1**.

The relative mixing time (**1**) is defined as [37]:

$$t^{r}_{mix} = \frac{t_{mix}}{t_{mix,top\ blowing}} \qquad (\mathbf{1})$$

t^{r}_{mix} ..... relative mixing time [ ]

t_{mix} ..... mixing time for a top blown converter with bottom purging system [minutes]

$t_{mix,\ top\ blowing}$ ..... mixing time for top blown converter [minutes]

The indicator for bath agitation or mixing is the relative mixing time. A reduced mixing time means an improved bath mixing / kinetic and hence an acceleration of the chemical reactions (shortening of reaction ways). A further parameter for the description of the bath kinetic is the mixing energy. The mixing energy involves the lance height, geometry, blowing practise, the bath level of the liquid metal and for the top blown converter with bottom purging system the purging flow rates as well. The equations of Nakanishi for the top and combined blown converter are listed below [35].

Equation (**2**) for the top blown converter [35]:

$$\varepsilon_T = 0.0453 * Q_T * D * U^2 * \cos^2 \Theta * N_n{}^{-0.833} / W / X \qquad (\mathbf{2})$$

ε_T..... kinetic energy dissipated from top blow [J/min]

Q_T..... blow rate of oxygen [Nm^3/min]

D..... diameter of the lance nozzle [m]

U.....linear speed of gas in the outlet of the lance nozzle [m/s]

N_n.....amount of lance nozzles [ ]

W.....weight of the HM [tons]

X..... height of the lance [meters]

Θ.....blowing angel [°]

Equation (**3**) for the top blown converter with bottom purging system [35]:

$$\varepsilon_{TB} = \varepsilon_T + (28.5 * Q_B * T * N_i{}^{-0.833} / W) * \lg\left(1 + \frac{H}{148}\right) \qquad (\mathbf{3})$$

ε_{TB}.....kinetic energy dissipated from the top blown converter with bottom purging system [J/min]

ε_T.....kinetic energy dissipated from the top blown converter with bottom purging system [J/min]

Q_B.....blowing rate of the gas in bottom purging [Nm^3/min]

N_i.....amount of the bottom nozzles [ ]

H..... depth of the metal bath [cm]

Due to **Figure 3-11** and **Table 3-1** various plug arrangements lead to approximately same relative mixing times. By flow rate increasing, the mixing time is dropped and the bottom purging effect is strengthened.

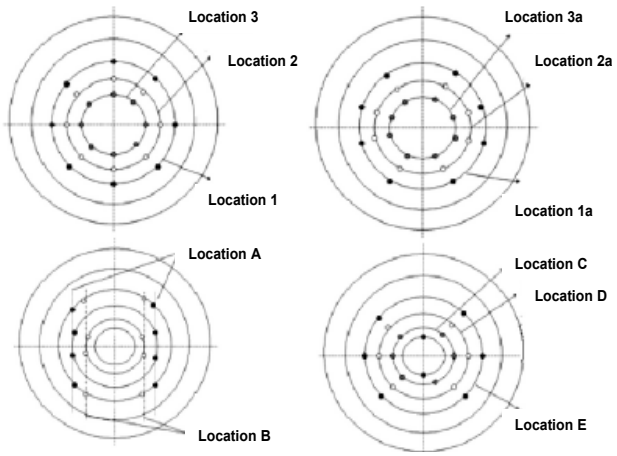

Figure 3-11: Various bottom plug arrangement [38].

Table 3-1: Relative mixing time depend on various plug arrangement [38].

Sl. No.	Bottom tuyere configuration	Relative mixing time at bottom flow rate 1.44 % of top flow rate	Relative mixing time at bottom flow rate 2.88 % of top flow rate
1.	Location 1	0.66	0.65
2.	Location 1a	0.61	0.38
3.	Location 2	0.48	0.35
4.	Location 2a	0.36	0.27
5.	Location 3	0.45	0.39
6.	Location 3a	0.51	0.31
7.	Location A	0.49	0.45
8.	Location B	0.46	0.33
9.	Location C	0.51	0.47
10	Location D	0.64	0.49

Key for a successful operating bottom purging system are primary the purging pattern, number of plugs, wear rates and the availability of each plug. The purging plug arrangement is almost irrelevant and just a design element and finally chosen by the customer.

3.1.7 Influence of purging intensity

The level of purging intensity plays a decisive role for attaining lowest [C]x[O] products and iron losses in steel bath. **Figure 3-12** shows the set flow rates dependent on the obtained [C]x[O] products close to the end of blow by implementing different kinds of purging models.

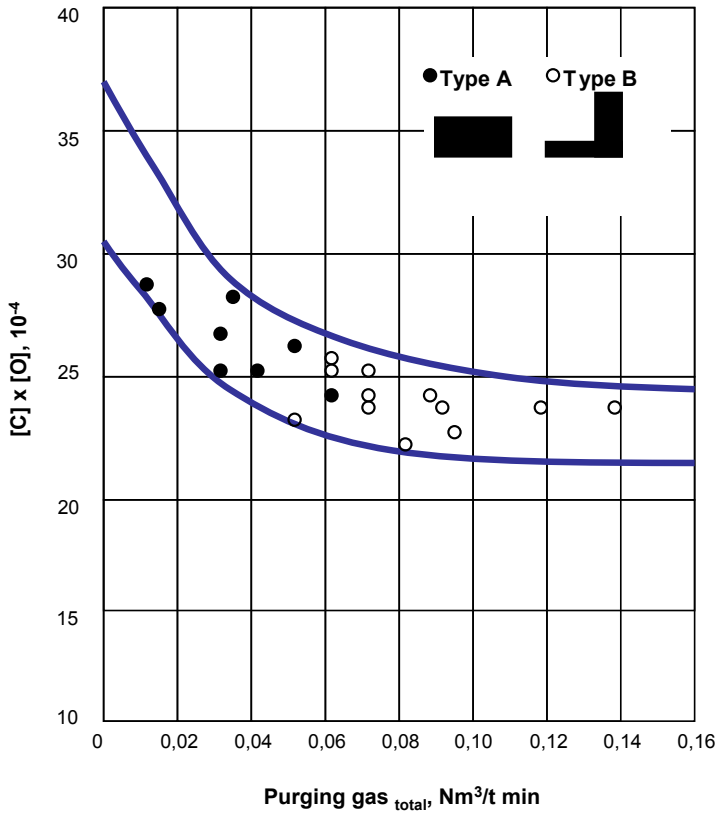

Figure 3-12: Influence of purging intensity on [C]x[O] product close to the end of blow [36].

Investigated purging pattern:

- Type A: constant purging intensity during the whole refining
- Type B: lowest flow rates at refining start; considerable increasing close to the end of blow (during hard blowing)

A minimum level of purging leads to a considerable decreasing of the [C]x[O] product, especially below a set flow rate of 0.06 [Nm^3 / t min]. Furthermore it is visible that purging model type A is connected with higher [C]x[O] product values and lower flow rates in comparison to type B. Low flow rates at refining start (gas and plug wear saving) and higher flow rates (intensifying of steel bath agitations) close to the end of blow should be aimed finally. At this [C]x[O] product levels in the area between 18 and $20*10^{-4}$ are achievable. Actual flowrates and sequences are not given in the literature source.

3.2 Operating benefits

A top blowing process with bottom purging system is also reflected in less turbulent refining and therefore reduced slopping with the consequence of higher yields. Furthermore the total oxygen consumption is approximately 2% and the tapping temperature in average 10° C lower compared to the conventional LD process. It is definitely a result of the better bath agitation and homogenisation conditions of the steel bath. The charged lime amount is reduced about 10 to 15% in comparison to a top blowing operated converter [30].

3.3 Types of inert gases

Argon and Nitrogen are used as "inert" bottom purging gases. "Inert" means unreactive and hence no reaction with other dissolved elements at highest temperatures in steel bath takes place. The type of the inert gas depends on the critical Nitrogen level in steel grades. The [N] content is influenced by [9], [39]:

- Switching point Nitrogen to Argon and purging intensity
- [N] content in scrap
- $\{N_2\}$ content in oxygen of the lance (purity of oxygen)
- $\{N_2\}$ in atmosphere

3.3.1 Ideal switching point from argon to nitrogen

Nitrogen levels at tapping are flexibly adjusted during the refining process by shifting the point of switching from Nitrogen to Argon and the particularly purging flow rates. **Figure 3-13** shows the influence of the switching point. This diagram is valid for lower Nitrogen flow rates at refining start and a significant increasing of the Argon purging intensities after switching. Thereby it should be mentioned that for realized lowest [C]x[O] products an intensive purging at the last third of refining is adequate.

It is visible that until 25% of the refining process gas type and purging intensity does not have any influence on the Nitrogen level in steel bath. A purging with Argon at this refining phase is not cost effective and without purpose. Argon is at factor four more expensive than Nitrogen. For aiming lowest Nitrogen levels it is necessary to switch from Nitrogen to Argon between 25 and 50 of blowing time. A retarded switching especially over 50% of refining causes very high [N] levels at tapping – higher purging intensities enforce that effect, too. Post stirring with Argon is reflected in practicable unchanged [N] contents, while the use of Nitrogen enhances the [N] values at 20 to 40% (**Figure 3-14**).

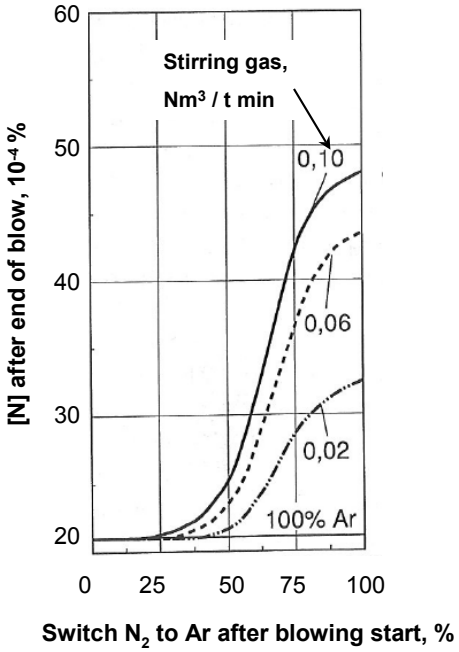

Figure 3-13: Influence of switching point from Nitrogen to Argon on [N] level [9].

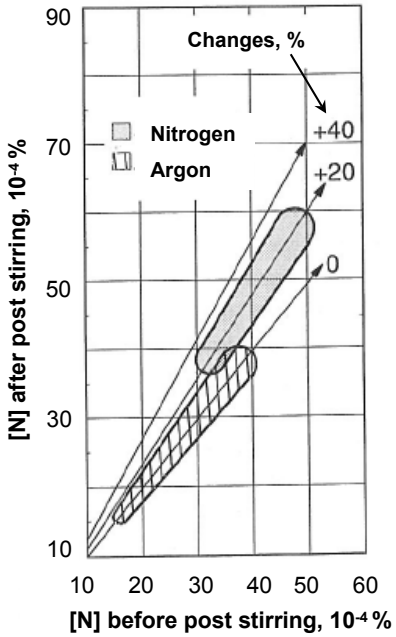

Figure 3-14: Influence of post stirring on [N] level [9].

4 Different methods for converter maintenance / wear stabilization

The converter wear rate influences the metallurgical results and the converter availability and hence the steel plant productivity. A maximum of refractory lining lifetime and a minimum of repair time is aimed. The concept or design of a converter lining is determined by three main groups of wear mechanisms: thermal, mechanical and chemical. The wear triangle (**Figure 4-1**) gives a general overview about these mechanisms. Pre-wear areas are tap pad, converter mouth, charge pad and trunnion area. With an appropriate converter maintenance the wear rate is stabilized. Furthermore, a premature relining is avoided (saving costs). In the following some maintenance strategies are discussed in detail [40], [41].

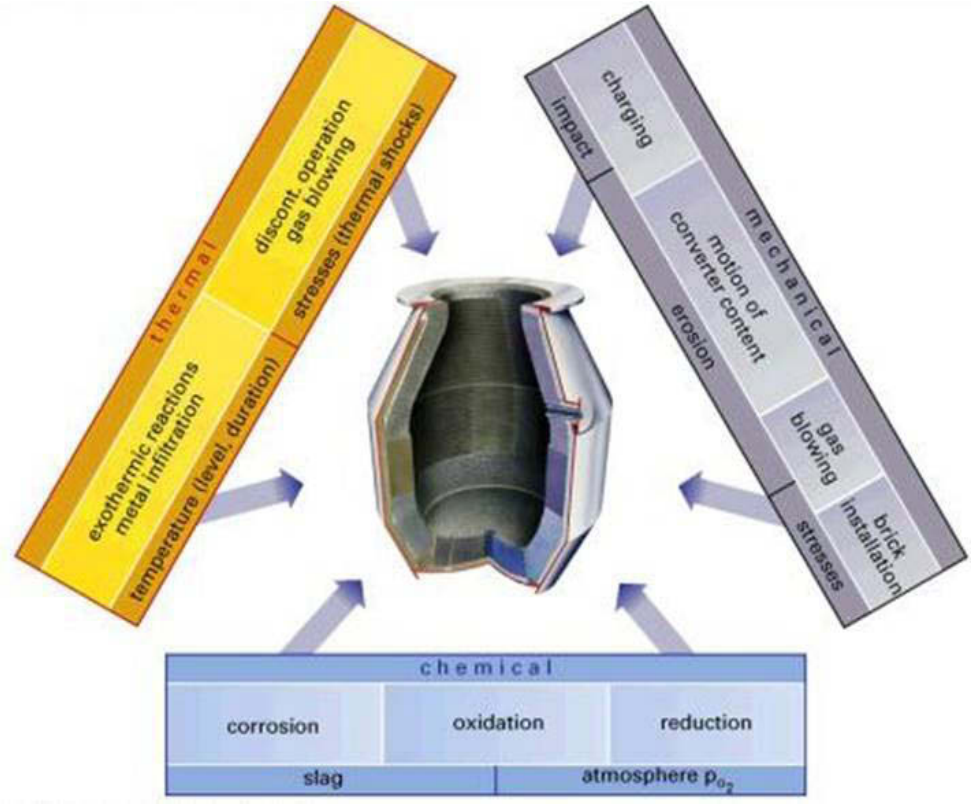

Figure 4-1: Wear mechanism triangle [40].

4.1 Slag splashing

After steel tapping the remaining slag in the converter is splashed with a high pressure nitrogen jet using the blowing lance (**Figure 4-2**). The slag coats the lining, solidifies, creates a solid layer and finally decreases the wear rate and consumption of gunning material. After the slag splashing mode is used successfully the nitrogen flow is stopped, the lance removed and any slag remaining in the converter dumped into the slag pot. For an efficient splashing operation a range of (MgO) in the slag between 8 and 14% is necessary otherwise the slag does not adhere on the lining. Hence limestone, dolomite or other MgO bearing materials must be charged after steel tapping.

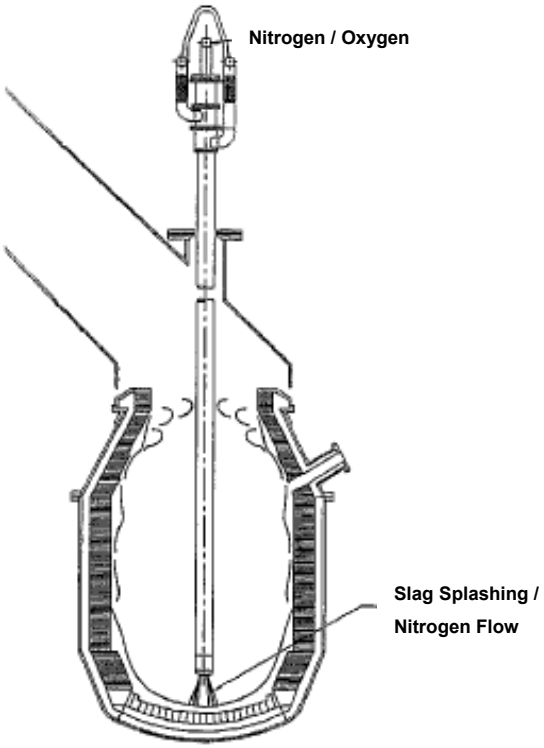

Figure 4-2: Method of slag splashing [43].

This maintenance method was developed in the USA in the 1980´ies. In North America, 50.000 heats on lining are possible, but that requires an excessive slag splashing practise with splashing after every heat. Hence the converter availability is reduced. Slag splashing also causes several other problems such as yield, bottom build up (negative for bottom purging performance), lance and mouth skulling [42], [43].

4.2 Slag washing

After tapping the converter with the remaining slag is rocked back and forth several times. A thin slag layer (max. 5 inch) covers the lining and wear zones such as bottom, tap and charge pad are protected. Afterwards, the rest of the excess slag is dumped into the slag pot and the converter is ready for charging. Due to very thick slag layers the bottom purging

elements may be plugged and in the worst case they never re open (too excessive slag washing - bottom build up). Remedies are:

- The immediate stop of slag washing until the plugs are open
- Bottom burning with the oxygen lance
- Charging of hot metal for dissolution the slag layer solidification at the bottom area.

As mentioned earlier in the slag splashing chapter, a (MgO) range between 6 and 8% in slag is to be aimed [44].

4.3 Hot repair mixes / Self flow mixes

After deslagging the hot repair self flow mix is charged in big bags using the scrap box. Afterwards the converter is tilted to the repairing position and due to the prevalent converter temperature (more than 1300 °C is optimal) the mix liquidises and hence flows directly in the pre wear area. After one minute the mix is completely hardened and 20 minutes later fully sintered. This maintenance method is associated with a maximum of life time and a minimum of repair time. The procedure is shown in **Figure 4-3** in detail.

Figure 4-3: Procedure of hot repair method [44].

4.4 Gunning

Gunning is a common way to repair worn refractory in the most damaged zones with special gunning mixes by using a mechanised gunning manipulator. The target is a decreased and equal wear rate. The latest development of this practise is “Super Gunning”. This improved gunning operation can be performed in continuous BOF operation during the short cycle breaks between tapping an charging. Therefore, a special gunning machine is used and allows higher gunning speed and more precise repair adjustment control. Another advantage is the conservation of the bottom purging elements.

5 Practical Part

The practical part of this thesis acts as instrument for the demonstration of the metallurgical benefits of the CIP (Converter Inertgas Purging) System in comparison to a top blowing converter. Furthermore, it describes the motivation for the CIP installation, the process problems and the parameters of influence on metallurgical results during the first purged BOF campaign as well.

5.1 Target of the CIP Project

After a CIP introduction presentation at the steel plant, a subsequent fact finding and a pre calculation of cost savings, the steel plant management made a decision for a BOF CIP installation. The installation is connected with a change in the BOF process, especially for slag practice (flux addition interval, amount), lance philosophy (height and oxygen consumption) and converter maintenance. Furthermore the [C]x[O] product and the p_{CO} levels as well are indicators for the bottom purging efficiency. At this the steel plant defined an upper and lower limit for the p_{CO} values in the area between 0.9 and 1.3 bar.

5.1.1 Production overview

The investigated steel plant consists of two LD-vessels (#60 and #50 BOF) in parallel operation with a tapping weight of 232 metric tons per vessel. The average produced heat

amount of the steel plant is in the range between 30 and 35 heats per day. One RH degasser and one {Ar}-stirring station are available for secondary metallurgy operations and the caster is a twin strand, vertical bending machine. ULC (51.5%), LC-AK (41.2%) and CRML (6.3%), are produced, which are hot and cold rolled to sheets and coils. The principal customer is the automotive industry. An installation of a CIP-system was done at #60 BOF in July 2008. **Figure 5-1** gives an overview about the current production situation after the CIP installation. It is seen, that #50 BOF (top blowing mode) achieves a lining lifetime of approximately 50.000 heats due to excessive slag splashing. Related to the bottom purging, #60 BOF operates with slag washing, gunning and without slag splashing. The target campaign life is in the range of 3.000 heats.

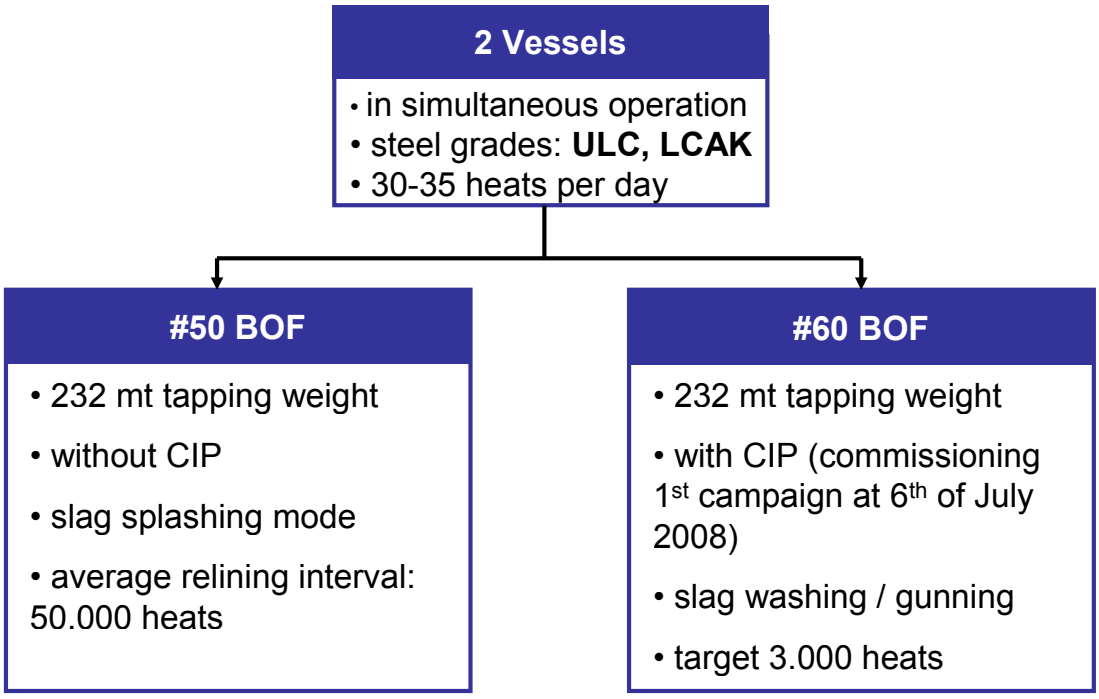

Figure 5-1: Steel plant complex.

5.1.2 Reasons for CIP installation

The LC-AK grades are produced via the RH degasser route. This practise is introduced to gain the metallurgical benefits of a low oxygen content of the melt. The LC-AK grades are tapped at higher [C], but lower [O] levels at the vessel and the main/final decarburisation and degassing is carried out using the RH degasser. Furthermore the scrap sourcing near the

investigated steel plant is much more expensive than the production of HM. Therefore it is beneficial to operate with a higher HM ratio with lower scrap rates and to utilize the chemical superheat of the HM to serve the RH route. The result is a significant conversion cost difference between the RH- and the LTS-route of almost 4.99 U$/t liquid steel.

Bottom purging reduces the [O] content of the steel and [C] levels (in the area of 300 ppm). This can be achieved already during the top blowing converter with CIP without using the RH degassing technology.

Claimed benefits of CIP in general are:

- Lower [O], less (FeO) in the slag, lower [P] and higher [Mn] levels
- Lower consumption of oxygen due to more efficient refining; lower CO_2 levels in offgas
- Lower Aluminium deoxidation costs for CC heats
- Improved yield (flux addition saving)
- Enhancement of the refining and productivity (decreased tap to tap times)
- Improved [P] control
- Reducing of the reblow rates
- Improved scrap melting due to better mixing
- Improved temperature control due to better mixing
- Possible change in the hot metal/scrap ratio
- Quick operation practise caused by the elimination of slag splashing, when bottom purging is working

The disadvantage of bottom purging is that slag splashing cannot be used, because the slag layer is blocking the plugs. That is why heats on one lining will be reduced significantly from 50.000 to 3.000 heats per campaign.

The cost savings from the preliminary benefit calculation are given in **Table 5-1**. The calculation is based on internal unit costs, consumption figures and yields.

Table 5-1: Preliminary benefit calculation.

Changes in the metallurgical process	**Economic Result**		
Result for Si-Reduction in HM (- 0.10% in HM)	=	2.24	US$/t
Result for Change in REF Cost (Campaign life = 3000 heats)	=	-0.65	US$/t
Results for Production loss during relining (- 13 heats)	=	-0.44	US$/t
Results for MgO Reduction in BOF slag (7% in final slag)	=	0.77	US$/t
Results for [C]x[O] Reduction (0.025% C; 0.050% [O])	=	0.22	US$/t
Result for (Fe) Reduction (25% to 20%)	=	0.09	US$/t
Result for lower Slopping (- no values kg/t)	=	/	US$/t
Results for lower Temperature Losses (- no values °C)	=	/	US$/t
Results for lower Utilisation of Vac Treatment (-28.72% LCAK Grades)	=	1.43	US$/t
Cost Change for Introduction of BOF Bottom Purging	**=**	**3.66**	**US$/t**

It shows a major saving potential coming from a silicon content reduction at the BF which results in huge savings of fuels in the Hot Metal Production at the BF and additionally in reasonable savings of fluxes and slag volume (Fe-yield) in steelmaking at the BOF. In steelmaking itself the major saving potentials are related to avoid the RH-OB route for LCAK steel grades and flux and slag volume reduction (Fe-yield increase) by the modification of the slag chemistry.

On the increasing side of the cost balance higher refractory cost and production losses during the relining period have to be taken into account. The production losses have to be mentioned although a BOF cycle speed-up can be expected and a shortening of the lining time will be organized. Both factors can compensate for most of the expected production losses. However there are still factors which can hardly be influenced like breakdown frequency of the vessel, the caster and taphole changes. But those negative impacts can be minimised by pushing single vessel operation as a standard.

In conclusion, although a change in the hot metal quality is not included in the first step of the optimisation conversion, the bottom purging technology theoretically creates cost savings of 1.43 U$ compared to the top blowing operation (without looking at the effect of the silicon reduction at the BF operations).

5.1.3 CIP preparation phase

RHI together with its partners FC-Technik and TBR supplies a complete system engineering including rotary joint and pipe/hose installation through the water cooled trunnion (**Figure 5-2**).

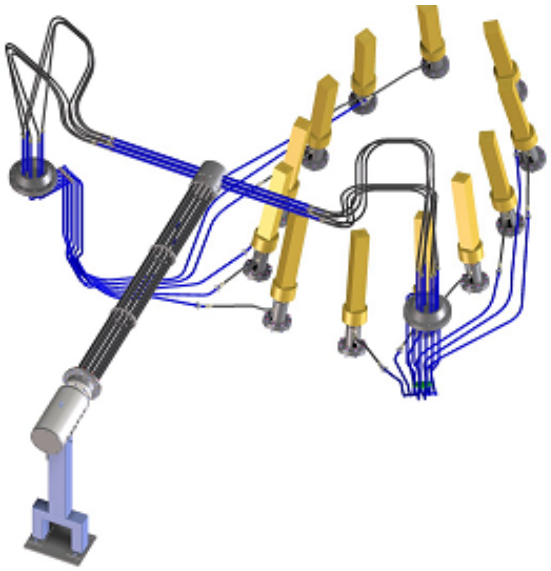

Figure 5-2: Purging plug installation

A valve stand with 12 independently controllable lines – with option to operate with {Ar} or {N_2} (dependend on critical [N] steel grades) is implemented as well (**Figure 5-3**).

Figure 5-3: Valve/Gas station.

For a serious automation and purging plug control during the refining especially in different process steps, supervision screens are installed at the BOF pulpit (**Figure 5-4**).

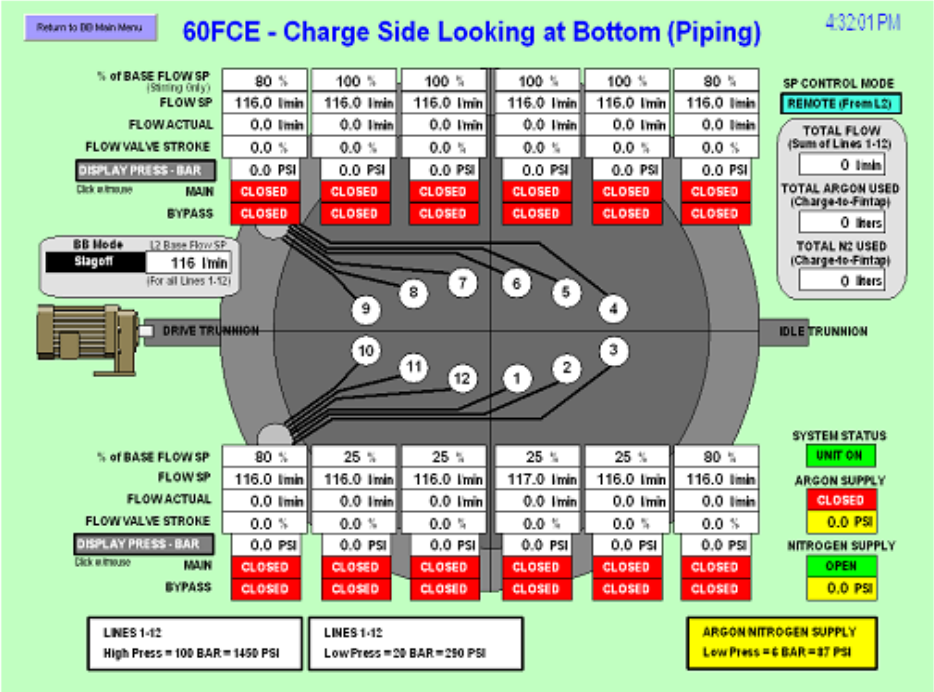

Figure 5-4: BOF pulpit operation screen.

The CIP system at #60 BOF consists of twelve Multihole Plugs (MHP), in elliptical uniform arrangement (**Figure 5-5**).

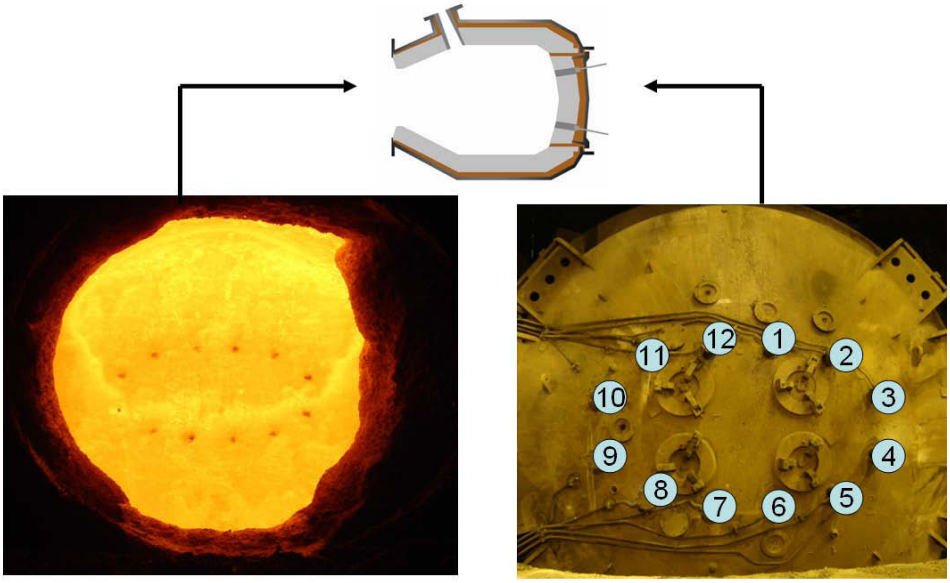

view: into the BOF after tapping **view:** at the BOF backside

Figure 5-5: Purging plug arrangement

Figure 5-6 shows a detailed drawing of a MHP. Flow rate to each plug can be regulated separately and consists of a high quality surrounding Magnesia-Carbon block with 24 pipes (inner diameter of two millimeters).

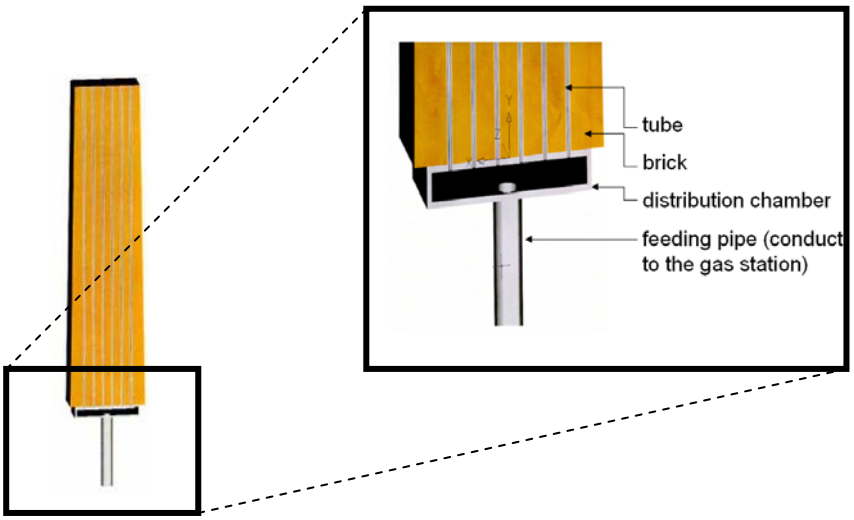

Figure 5-6: Multi Hole Plug (MHP)

The whole installation required two days for preparation, five days for the installation of the pipes and hoses through the trunnion ring and on the vessel and three days for the vessel relining.

5.1.4 Recommendations for the CIP commissioning phase

The BOF process is divided into ten steps with various purging flow rates. During charging, tapping and slag maintenance it is sufficient to operate with suitable high flow rates for keeping the plugs open. Too high set flow rates cause a higher plug wear potential and further a senseless waste of gas (costs ↑). The individual flow rate patterns must be clearly fit to the aimed metallurgical results at tapping and the production situation. **Table 5-2** gives an overview of the reccommended flow rates for the #60 BOF commissioning.

Table 5-2: Reccomended flow rates.

BOF Process Steps	reccommended flow per plug [l/min]
Charging	200
Soft purging	200
Sample taking	200
Hard purging	800
Post stirring	700
Tapping	150
Maintenance	600
Empty	100

5.2 Demonstration of the CIP benefits

The excel data base provided by the investigated steel plant includes heat values of #60 and #50 BOF from the same production period - 6th of July to 25th of September. After 25th of September a turndown of the production level was indispensable caused by the worldwide financial crises. Afterwards the bottom purging at #60 BOF was shut down and the slag splashing mode activated again.

For obtaining serious results it is necessary to verify the data base of plausibility at first. Statistical methods have been utilized and hence heats with non correct values or without analysis have been deleted. That kind of procedure was done for every heat. Seven heats at #60 and 30 heats at #50 BOF have been eliminated and finally the data reduced to 1357 heats at #60 and 804 heats at #50 BOF on trail in simultaneous operation.

5.2.1 [C]x[O] product, p_{CO} values

As mentioned in **Chapter 3.1.1.**, the [C]x[O] products and the p_{CO} levels as well are indicators for the bottom purging efficiency. **Figure 5-7** shows on the one hand the trail of the first 140 purged heats on lining at #60 BOF and on the other hand the effect of a top blowing converter with bottom purging system to a top blowing converter clearly in detail. Caused by the better bath agitations (shorter reaction ways) and hence liquid metal bath conditions closer to the equilibrium, the [C]x[O] products are lowered to a level between 20 and 25. That means a [C]x[O] reduction of approximately ten related to the values before bottom purging installation at #60 and the data of #50 BOF in parallel operation.

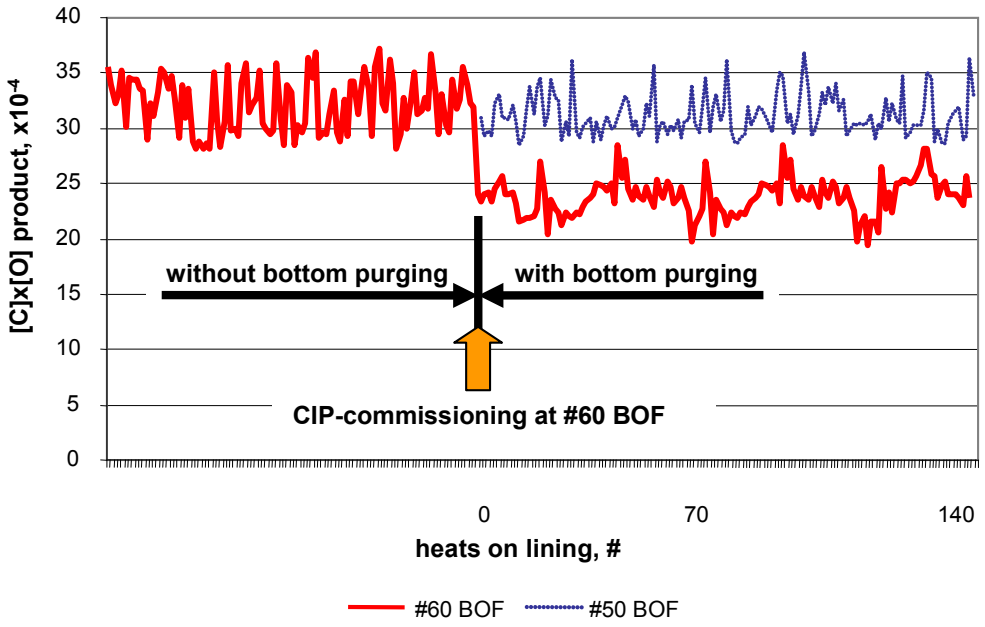

Figure 5-7: Trail of the [C]x[O] product.

Based on the first 534 purged heats, **Figure 5-8** reflects the typical difference in metallurgical results before and after CIP installation according to Vacher Hamilton (**Chapter 3.1.1**). It is visible that aimed [C] levels at tapping can be realized by dropped dissolved [O] contents. As a result, the total oxygen consumption is reduced and hence the danger of heat over oxidation eliminated.

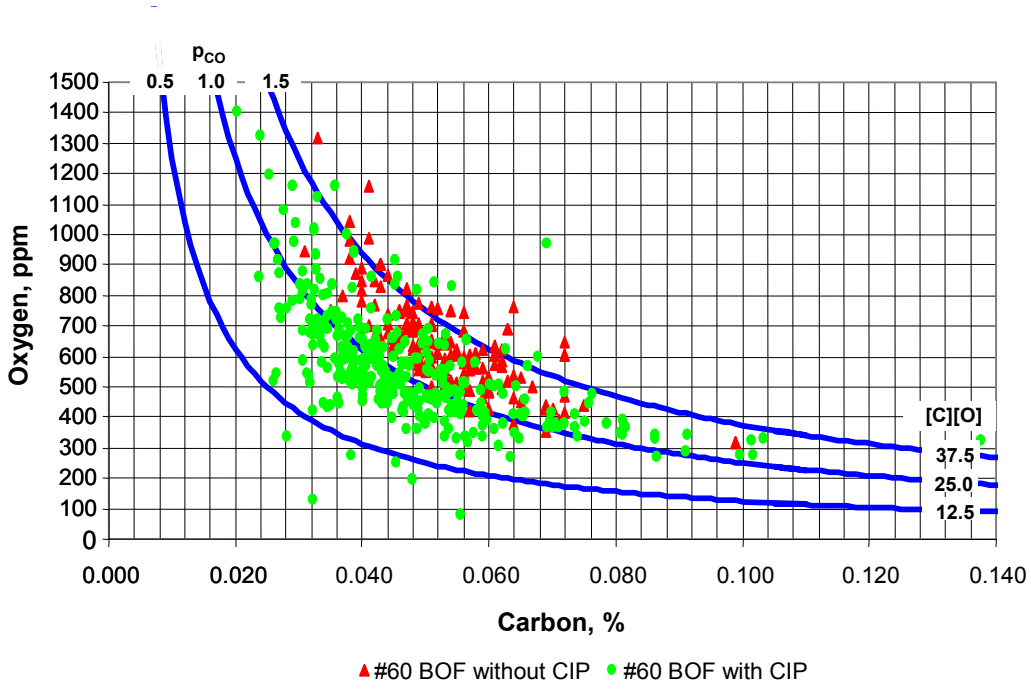

Figure 5-8: [C] and [O] levels according to Vacher/Hamilton diagram.

An implementation of a CIP system leads to a reduction of the [C] levels in average of 0.015% by 200 ppm lower [O] contents in liquid steel bath at tapping.

The improved bath kinetics via bottom purging can be verified by the calculation of the mixing energy. **Figure 5-9** demonstrates the influence of the calculated mixing energy related to the equation of Nakanishi (**Chapter 3.1.6**) on the [C]x[O] product distribution at #50 and #60 BOF at tapping. #50 BOF shows compared to #60 a very high deviation of the [C]x[O] values in the range between 26 to 45. A CIP installation is connected with an increase of the mixing energy and simultaneously a considerable decrease of the [C]x[O] levels and their deviation at tapping. Furthermore, the process is more flexible and the adjustment of aimed [C]x[O] products or p_{CO} levels better controllable.

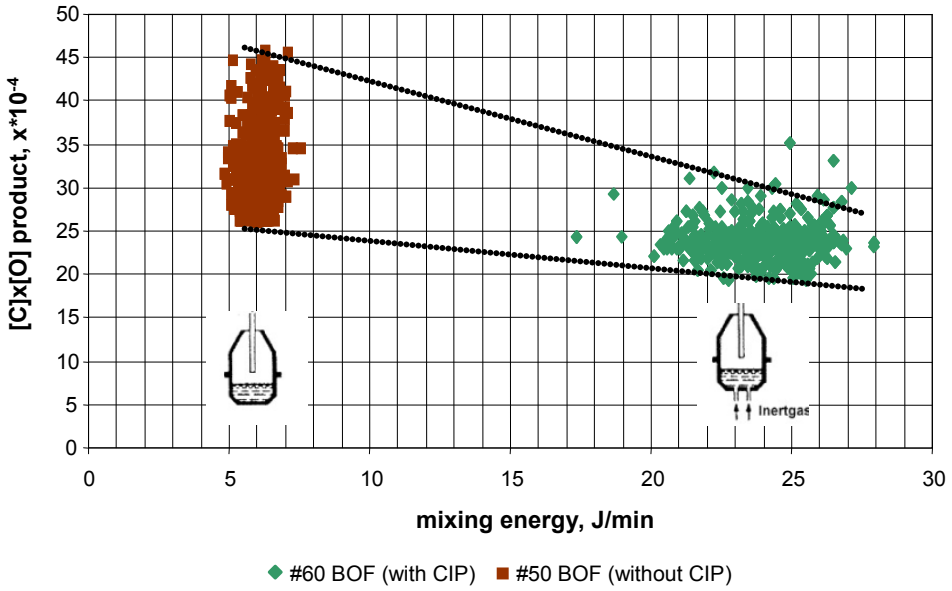

Figure 5-9: [C]x[O] product dependent on the mixing energy.

The effects or rather the parameters of bottom purging due to [C]x[O] products and p_{CO} levels are summarized in **Table 5-3**. Furthermore, a comparison between the obtained results and the theory was done additionally – a correlation is given in all points.

Table 5-3: [C]x[O], p_{CO} summary.

Parameter	Adjustment / Setting	[C]x[O] p_{CO} after End blow	Correlation between theory and evaluation
Purging intensity	↑	↓	YES
Mixing energy	↑	↓	YES
Results			
Difference to #50 BOF (without bottom purging), mean values	[C]x[O] = - 10 [*10-4] p_{co} = - 0.4 [bar]		

5.2.2 Yield

Figure 5-10 specifies the current total flux addition of both vessels in detail. Due to the same produced steel grades the difference between #50 and #60 BOF is significantly. A saving of 8.3 kilogram or rather 0.23 U$ per metric tone (**Figure 5-11**) are achieved by the effect of bottom purging.

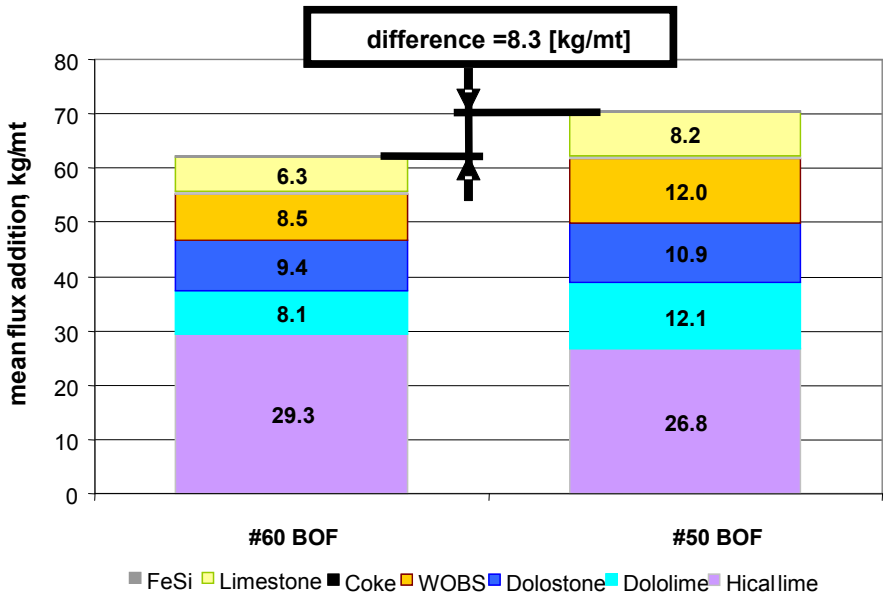

Figure 5-10: Mean charging of flux addition.

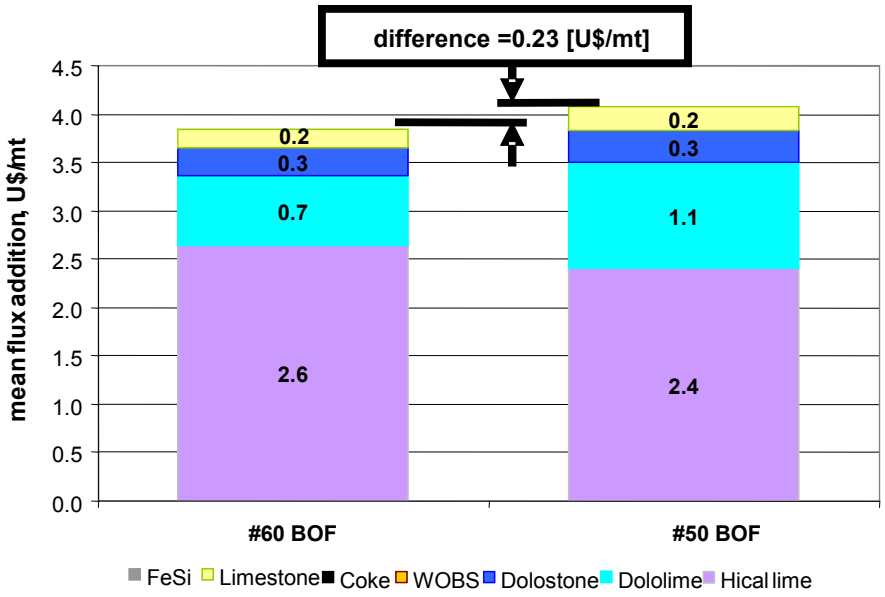

Figure 5-11: Cost saving due to bottom purging.

Based on the improved yield situation and the reduced heat over oxidation at #60 BOF, especially the [Fe]-oxidation after the main decarburisation phase, the slag volume decreases about two tones to 14.000 kilogram per heat. **Figure 5-12** shows that effect and the areas for operation with and without CIP.

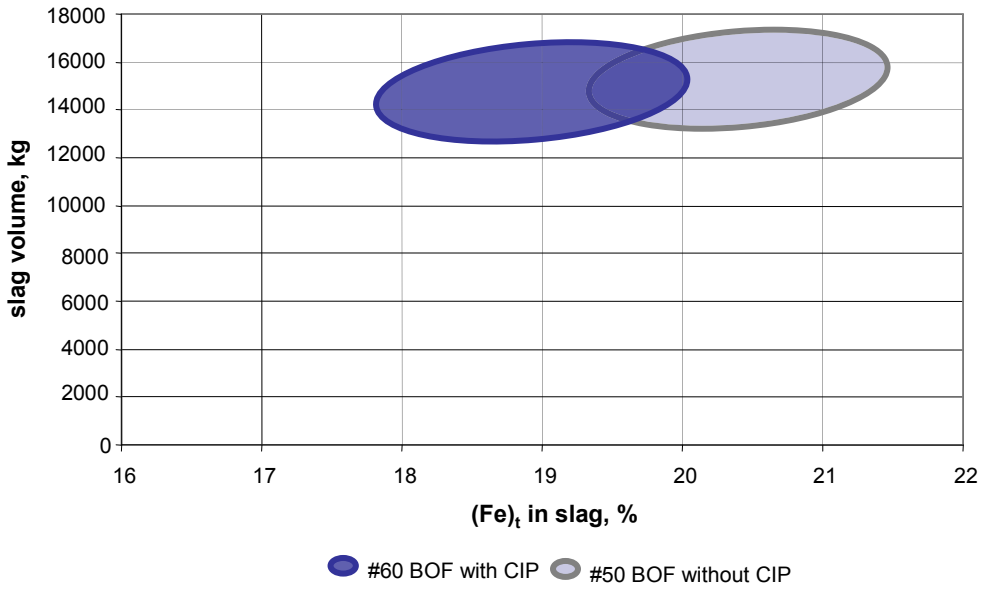

Figure 5-12: $(Fe)_t$ level due to the slag volume.

Hence the obtained $(Fe)_t$ values in slag drop from a level of approximately 19 down to 17% with characteristic lower [O] contents after end of blow in the range between 400 and 700 ppm (**Figure 5-13**).

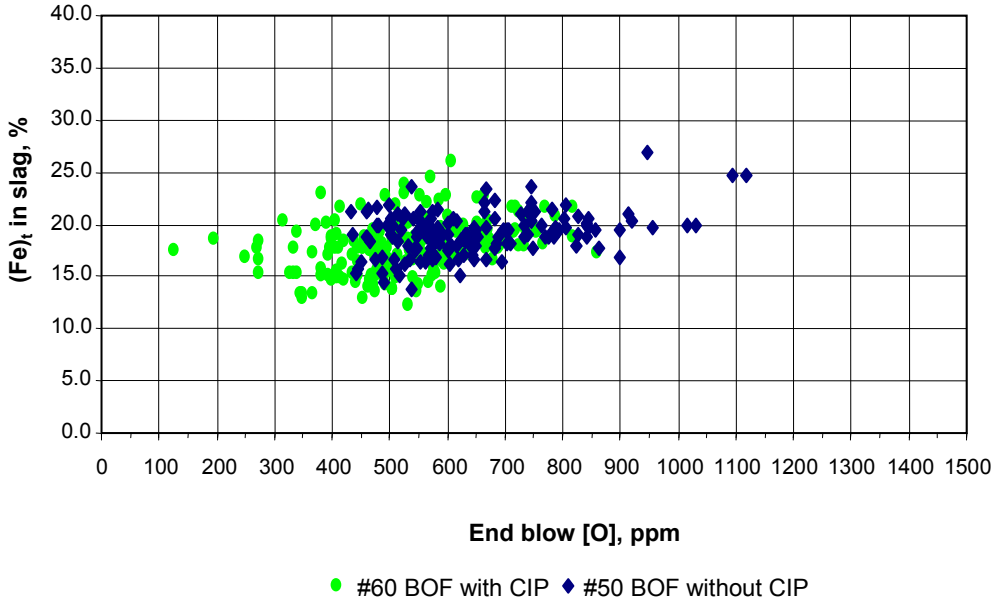

Figure 5-13: (Fe)t level due to end blow [O].

Finally the metallurgical benefits – the influence of the implementation of a CIP system – in comparison to #50 BOF are listed in **Table 5-4**. A conformation between the theory and the evaluation is clearly existent and it supports the motivation for a steel plant to adapt the BOF process with bottom purging system.

Table 5-4: Yield summary.

Parameter	Adjustment / Setting	Slag volume	Flux addition	$(Fe)_t$ in slag	Correlation between theory and evaluation
Purging intensity	↑	↓	↓	↓	YES
Results					
Difference to # 50 BOF (without bottom purging), mean values		- 2 [t]	- 8.3 [kg/mt]	- 2 [%]	

5.2.3 Manganese

Bottom purging leads to an enhanced [Mn] recovery, which means higher [Mn] at lower [O] levels at the end of blow. The characteristic effect for purged heats is demonstrated in **Figure 5-14**.

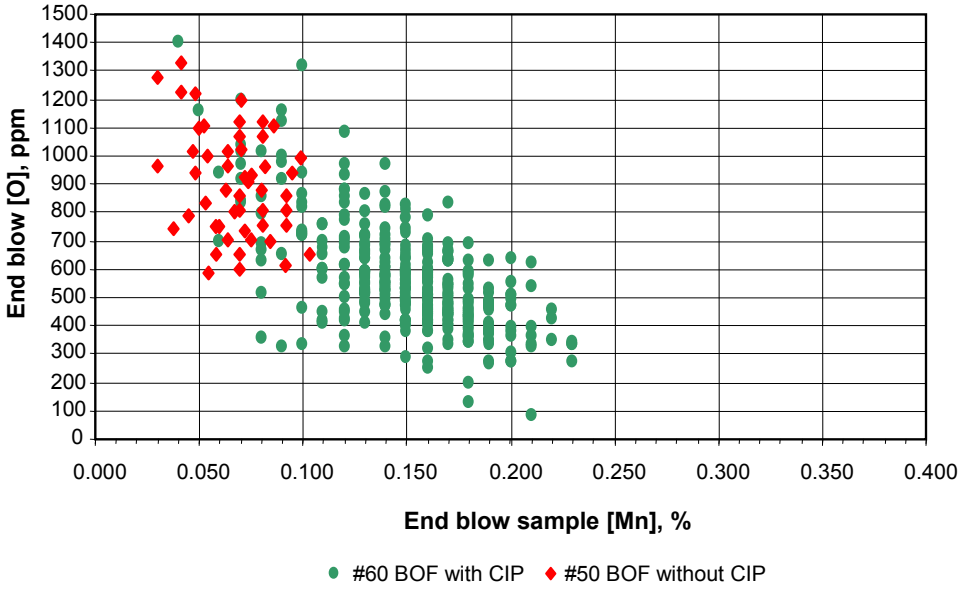

Figure 5-14: [O] and [Mn] level after end of blow.

Due to the end blow samples the [Mn] levels increase considerably up to a range between 0.1 and 0.23% with significantly lower [O] levels in liquid steel bath. The manganese specification of the LCAK steel grades normally are between 0.18 and 0.25%. The recovery of 0.1 kg manganese per tone liquid steel is equivalent to a direct saving of 0.133 kg FeMn75 per tone liquid steel at the secondary metallurgy. Depending on the Ferro-Manganese quality which is used, the savings deviate between 0.28 U$/kg for HC-Manganese and 1.17 U$/kg for MC-Manganese. Since the process without bottom purging is normally operated at higher carbon contents, the use of MC-Manganese is mandatory to meet the specification.

The manganese oxidation is also influenced by the total oxygen consumption and the reblow rate, which means higher (MnO) levels in slag at increased [O] contents after end of blow. The (MnO) levels can be reduced in average from 6 to 4.5 % (**Figure 5-15**).

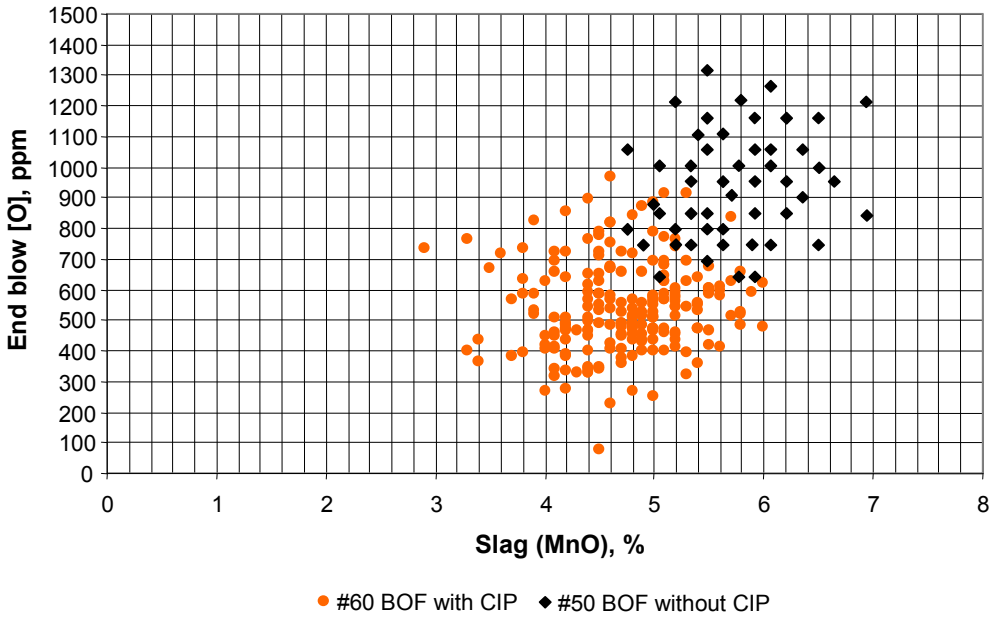

Figure 5-15: (MnO) due to [O] level after end of blow.

The installation of the CIP system is connected with an improvement in the bath kinetics and an enhancement of the mixing energy. Based on the calculated manganese distribution between slag and liquid steel bath, the values of the average mixing energy go up from 6 to about 24 J/min in comparison to #50 BOF (**Figure 5-16**). As a result the [Mn] level in the liquid steel bath increases by simultaneous dropping of the (MnO) content in slag (FeMn saving potential at secondary metallurgy treatments). Furthermore the deviation of the manganese values can be minimized additionally reasoned by the better process control.

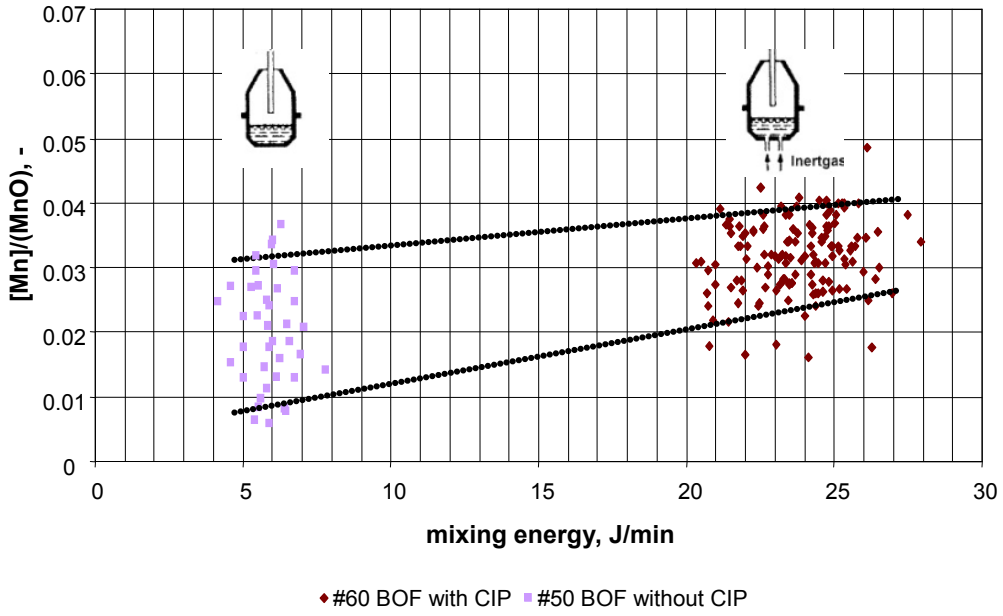

Figure 5-16: Manganese distribution dependent on the mixing energy.

Dependent on the total flows per heat and unchanged oxygen lance practises, the average achieved [Mn] level in liquid steel bath after end of blow was also estimated. The obtained results are given at **Figure 5-17**.

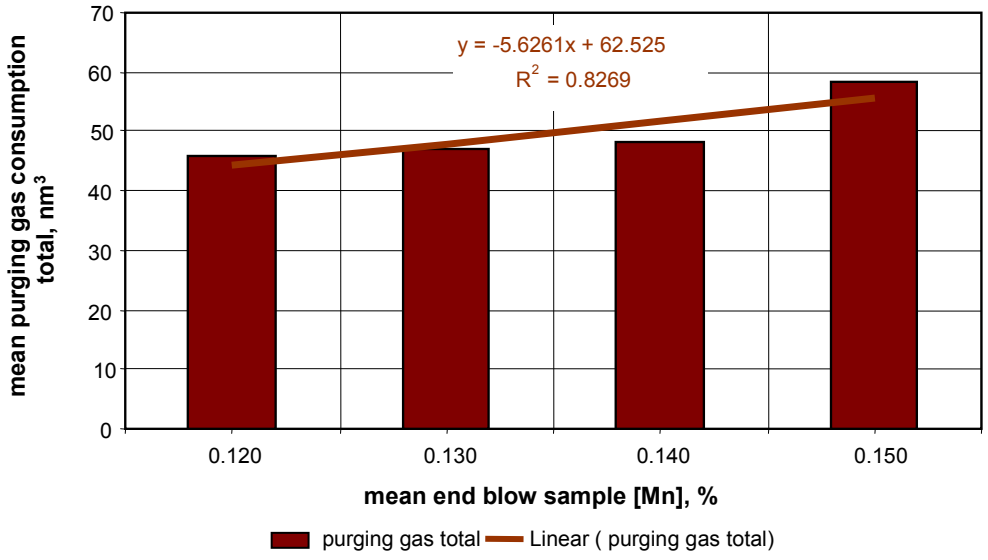

Figure 5-17: Mean [Mn] level according to mean purging gas consumption.

The results are summarized in **Table 5-5**.

Table 5-5: Manganese summary.

Parameter	Adjustment / Setting	[Mn] content after end blow	(MnO) in slag	[O] after end blow	Correlation between theory and evaluation
Purging intensity	↑	↑	↓	↓	YES
Mixing energy	↑	↑	↓	↓	YES
Results					
Difference to # 50 BOF (without bottom purging), mean values		**+ 0.8 [%]**	**- 1.5 [%]**	**- 200 to 300 [ppm]**	

5.2.4 Phosphorus

Regarding to the very low [P] levels in HM of 350 ppm (in Europe commonly between 750 and 1000 ppm), the effect of bottom purging does not show any differences in [P] values compared to the top blowing mode at #50 BOF. **Figure 5-18** reflects in average the same [P] level ranges by lower [O] contents after end of blow but various BOF philosophies.

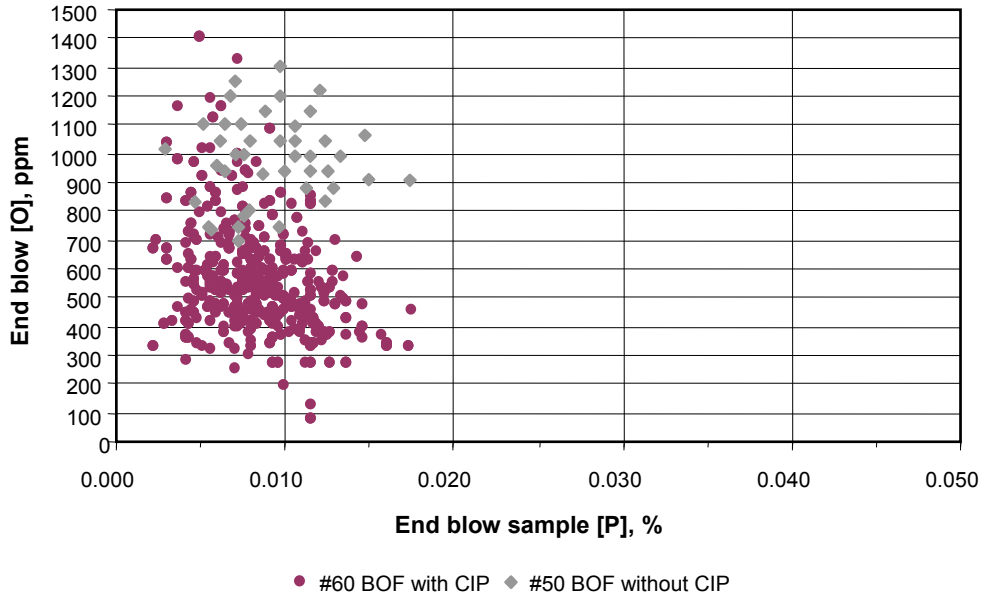

Figure 5-18: [O] and [P] level after end of blow.

Based on the changed slag practise, the higher sufficient (MgO) levels in slag for slag washing are reflected in increased [P] contents. An increase of the (MgO) levels in slag resulted in a higher slag viscosity with lower lime dissolution and less slag reactivity potential. These mentioned effects retard the dephosphorisation in the BOF. A considerable influence of the (MgO) level in slag on the [P] content after end of blow is noticeable when the (MgO) exceeds 6% (in good correlation with literature of Basu [45]) (**Figure 5-19**).

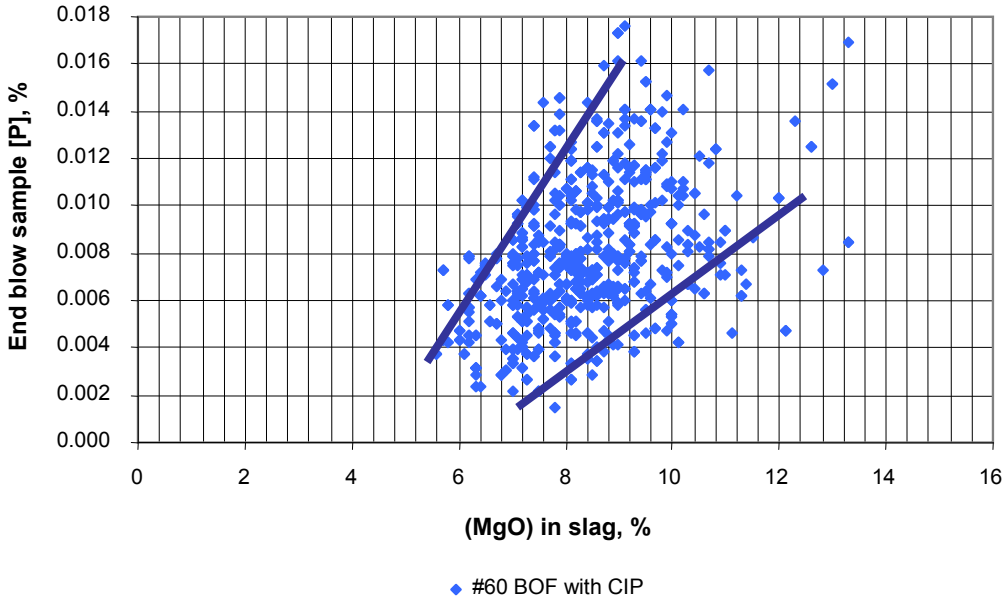

Figure 5-19: Inluence of the (MgO) on the [P] level after end of blow.

Bottom purging is connected on the one hand with lower slag volumes and on the other hand with less [Fe] losses and a better capacity for P_2O_5 in slag. Purged heats at #60 BOF achieve same [P] levels after end of blow by dropped $(Fe)_t$ contents in slag. For a [P] content after end of blow of approx. 0.010% , the $(Fe)_t$ level at #60 BOF is about 2% lower than #50 BOF (**Figure 5-20**).

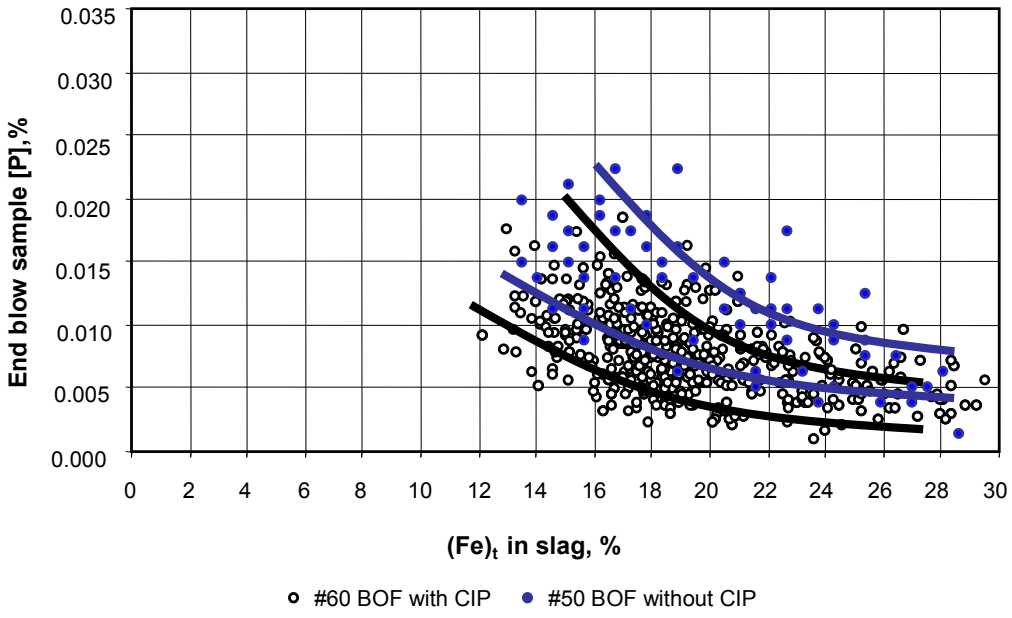

Figure 5-20: Influence of $(Fe)_t$ on the [P] level after end of blow.

Increased $(Fe)_t$ levels in slag enforce the dephosphorisation effect, because iron acts as primary flux in slag and support the quick lime dissolution, which is necessary for the phosphorus slag intake. However with CIP-system same [P] end levels can be achieved with lower $(Fe)_t$ in the slag, which means lower iron losses with the slag.

The calculated mixing energy based on the equation of Nakanishi (**Chapter 3.1.6**), expresses the effect of bath kinetics on the element distributions during the refining. Caused by the very low [P] level in the HM, the improved bath kinetics lead to identical [P] deviations after end of blow, in detail in the range between 0.005 and 0.015% (**Figure 5-21**). At this a mixing energy enhancement of about 20 J/min shows no effect.

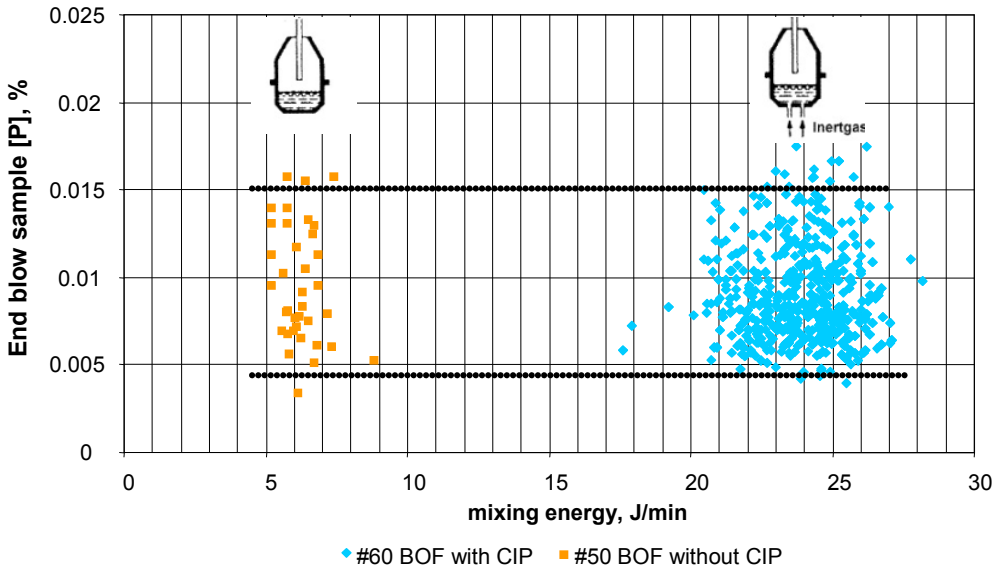

Figure 5-21: [P] level after end of blow dependent on the mixing energy.

In course of the phosphorus evaluation, a summary table with all results and their correlations with the published theory are created finally (**Table 5-6**).

Table 5-6: Phosphorus summary.

Parameter	Adjustment / Setting	[P] content after end blow	Correlation between theory and evaluation
Purging intensity	↑	=	NO
(MgO) in slag	↓	↓	YES
$(Fe)_t$ in slag	↑	↓	YES
Mixing energy	↑	=	NO
Results			
Difference to # 50 BOF (without bottom purging), mean values	**very low [P] levels in HM (~350 ppm)** **→ no influence visible !**		

5.2.5 Sulphur

The sulfur behavior of purged heats at #60 in comparison to non-purged at #50 BOF is shown in **Figure 5-22**. Bottom purging leads to lower oxygen levels but to identical [S] deviations after end of blow as well.

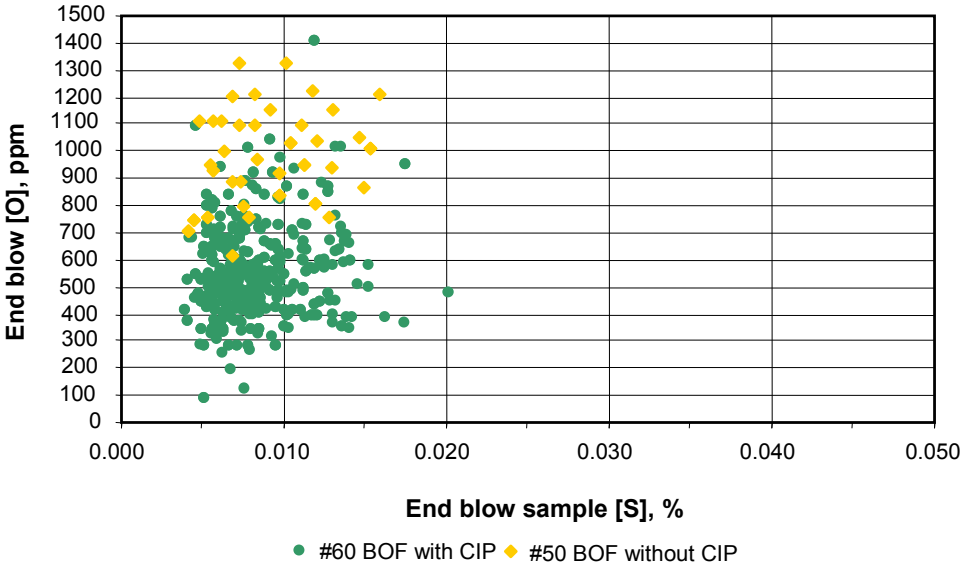

Figure 5-22: [O] due to the [S] level after end of blow.

That effect can be explained with the oxidizing atmosphere during the refining. A reducing atmosphere and high temperatures supports desulphurisation. The BOF process is generally known as a better decarburisation and dephosphorisation rather than a desulphurisation application. Connected with the changed slag practise, the influence of the higher (MgO) levels in slag is investigated as well. It is seen that against the theory no effects of different (MgO) values are visible (**Figure 5-23**) – lower (MgO) levels increase in common the effect of desulphurisation at the same time.

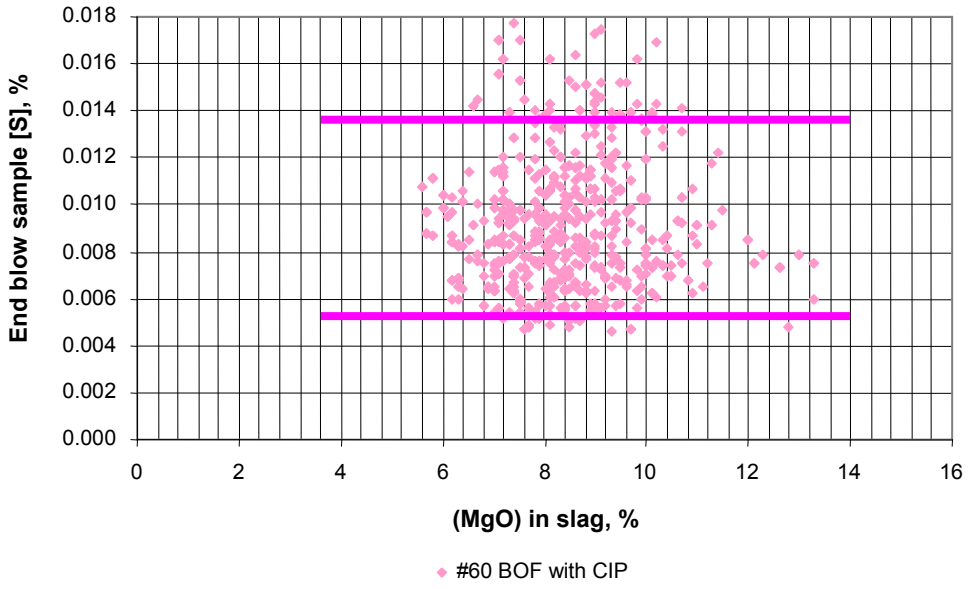

Figure 5-23: Influence of the (MgO) level on the [S] after end of blow.

A summary of the results is given in **Table 5-7**.

Table 5-7: Sulphur summary.

Parameter	Adjustment / Setting	[S] content after end blow	Correlation between theory and evaluation
Purging intensity	↑	=	NO
(MgO) in slag	↑	=	NO
Results			
Difference to # 50 BOF (without bottom purging), mean values	**no difference**		

5.2.6 Scrap / HM

A transition from top blowing to a top blowing mode with bottom purging is connected with a change in the HM / scrap ratio. More scrap can be charged caused by the better bath agitation and the quicker scrap melting. So it was necessary to balance the metallic charge agents like HM, scrap and WOBS to the new process. **Table 5-8** gives an overview about the amount of the metallic charge agents for #60 BOF with CIP and #50 BOF operated with top blowing mode.

Table 5-8: Metallic charge agents.

average metallic charge	#60 BOF,mt	#50 BOF, mt	Difference, mt
HM	213.5	216.1	-2.6
Scrap	35.8	32.3	+3.5
WOBS	2.0	2.9	-0.9
Sum	**251.3**	**251.3**	**0.0**

The sum of the charged metallic agents is in both cases identical (251.3 metric tons per heat) and limited by the BOF capacity. The essential difference is a decreasing of 2.6 metric tons HM and an increasing of 3.5 metric tons of scrap. At the BOF process WOBS are charged as cooling and especially for dropping the process temperature (special note to dephosphorisation conditions). Less WOBS total consumptions leads to higher scrap rates.

The scrap / HM ratio increases from 14.9 to 16.8% per heat (**Figure 5-24**).

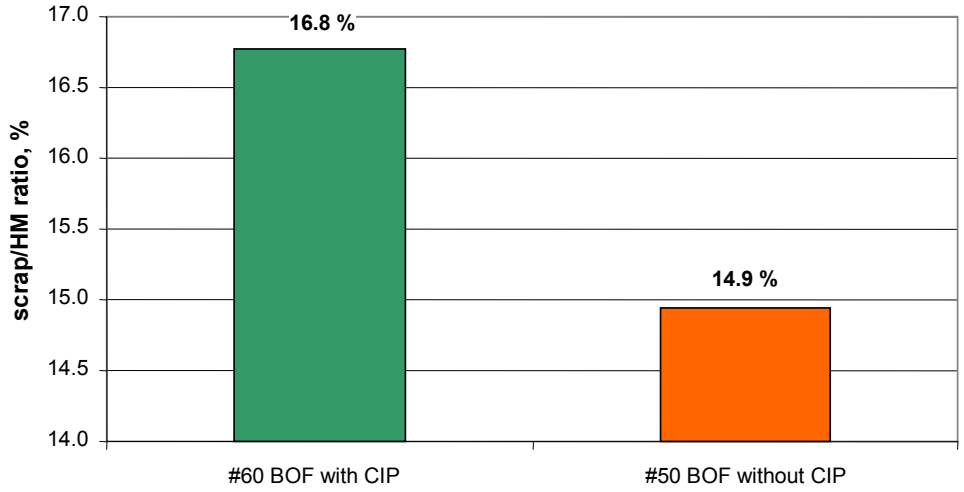

Figure 5-24: Scrap/HM ratio.

5.2.7 Reblow rate

The reasons for reblowing can be divided into three main groups:

- final [C] too high
- steel Temperature too low
- final [Mn], [P], or [S] not met

Compared to #50 BOF shows #60 BOF a total reblow rate of 19.5%, which means a reblow rate decrease of 3.5 % (**Figure 5-25**).

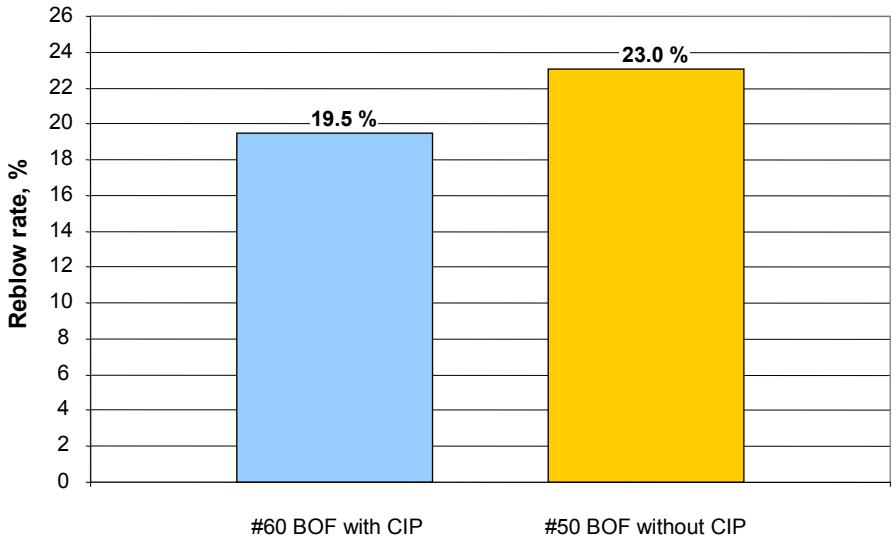

Figure 5-25: Reblow rate.

The share of the different reblow reasons are calculated and listed in **Table 5-9**.

Table 5-9: Reblow reasons.

Reblow reasons	#60 BOF,%	#50 BOF, %	Difference, %
Temperature	96.4	86.4	+10
Carbon	2.6	11.3	-8.7
[Mn], [P], [S]	1	2.3	-1.3
Sum	**100**	**100**	**0**

The biggest part is caused by temperatures failure at both BOF's. A significant change is reflected in the [C] reblow reason with a saving of 8.7%. Furthermore, the reblow factor for [Mn], [P], [S] is also reduced.

5.2.8 Tap to Tap

Bottom purging accelerates refining of the heat and ensures an economical BOF process. In course of the evaluation between #50 and #60 BOF in parallel operation a minimization of the average tap to tap time from 44 to 33.7 minutes was realized (**Table 5-10**). That equals a process acceleration of 23.4% in comparison to the top blowing mode.

Table 5-10: Tap to Tap Times.

# BOF	Average tap to tap time [min]
#50 BOF without CIP	44.0
#60 BOF with CIP	33.7
difference =	**10.3 [min]**

This process acceleration is connected with an enhancement of the productivity. After five heats, #60 BOF produces one heat more in comparison to #50 BOF (**Figure 5-26**) based on the same production period (one block stands for one average tap to tap time).

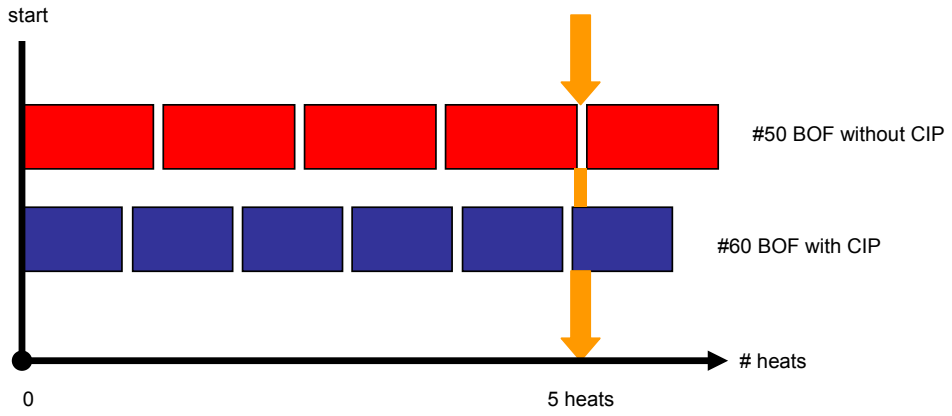

Figure 5-26: Production.

Figure 5-27 gives a detailed overview about the current process steps of #60 BOF during the refining.

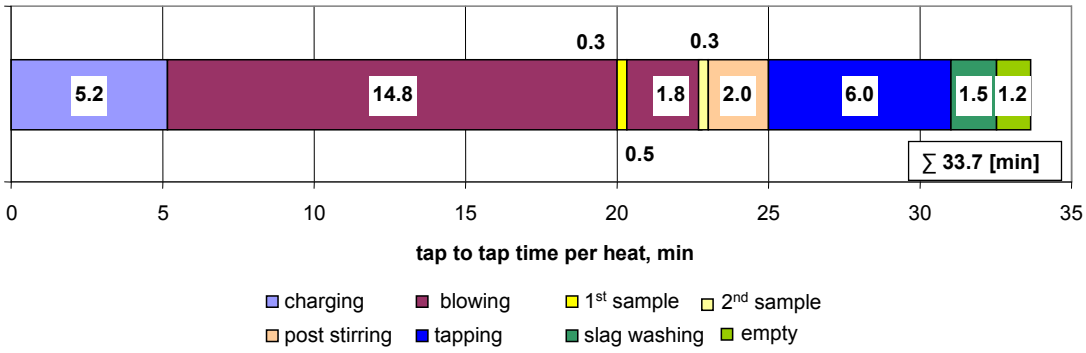

Figure 5-27: Process steps of #60 BOF with CIP.

After charging of scrap and HM, blowing is started in soft mode leading to a quick and reactive slag formation (charging of fluxes). Close to the hard blowing process step the first sample is taken (temperature and [C]). Based on the [C] level in liquid steel bath the quantity of oxygen for the aimed [C] level at tapping is estimated by a software program. Afterwards, the hard blowing mode leads to the main decarburisation effect in the liquid steel bath and at the end a second sample is taken. This sample contains a steel and a slag analysis. At this the duration of the post stirring is adjusted to meet the chemical analysis at tapping (in the worst case with reblowing), which is dependent on the produced steel grades. Finally, the liquid melt is tapped into a ladle and two to three tons of slag are left in the BOF for the slag washing practise. After the converter maintenance is finished the rest of un-sticky slag is dumped into the slag ladle and the BOF is ready for recharging. A detailed explanation is given in **Chapter 2.1**.

The total produced heat amount at steel plant is limited by the twin strand, vertical caster capacity and the HM availability. So the maximum of heats is defined by 30 to 40 heats per day. Due to the process acceleration at #60 BOF, a single BOF operation is definitely possible. **Figure 5-28** reflects the production situation of both vessels and the potential of #60 BOF in July 2009, where at 19th and 20th a single operation was carried out. At this 30 and 34 heats per day have been produced without any problems.

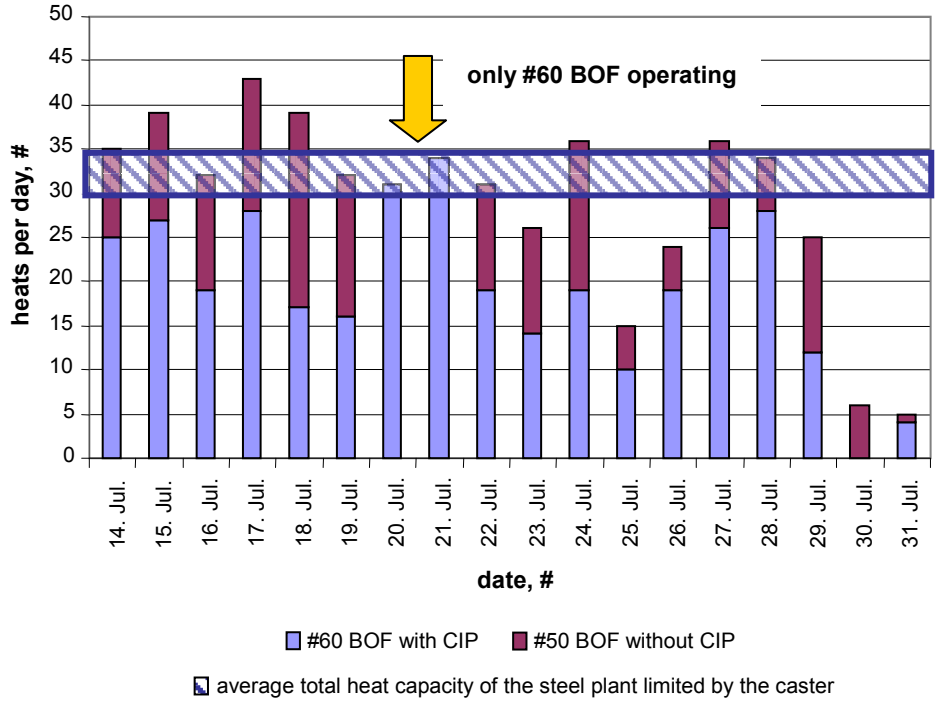

Figure 5-28: Production overview / July 2009.

5.3 Influence of different purging gas consumptions on the metallurgical results

In this chapter, the influence of various total flow rates on the metallurgical results is investigated. During the first purged campaign at #60 BOF, set flow rates have been changed caused by take out of plugs (water penetration in the pipe system trough the cooling system of the trunnion ring). The dimension of the flow rate effect is demonstrated in following with special focus on two different total gas consumptions at #60 and the non purging mode (in parallel operation) at #50 BOF (**Table 5-11**).

Table 5-11: Purging gas $_{total}$ overview.

Purging gas$_{total}$, nm³/ heat	#BOF
58.4	#60
47.1	#60
0.0	#50

5.3.1 [C]x[O] Product

Figure 5-29 demonstrates the influence of various total purging gas consumptions on the [C]x[O] products and the p_{CO} levels. Purged heats with a total gas consumption of 58.4 nm^3 are showing p_{CO} levels in average of 1.0 bar, which equates a [C]x[O] product of 25. A decreasing of the total purging gas consumption leads to an increasing of the p_{CO} levels at tapping and thereby to a worse purging performance and unchanged metallurgical results in comparison to a conventional LD process (#50 BOF). A reduction of the total gas consumption of approximately 11 nm^3 drifts the p_{CO} level up to 1.2 bar in average. Furthermore, the system gets closer to the non purging mode (red area) at #50 BOF with p_{CO} values in the range of 1.5 bar.

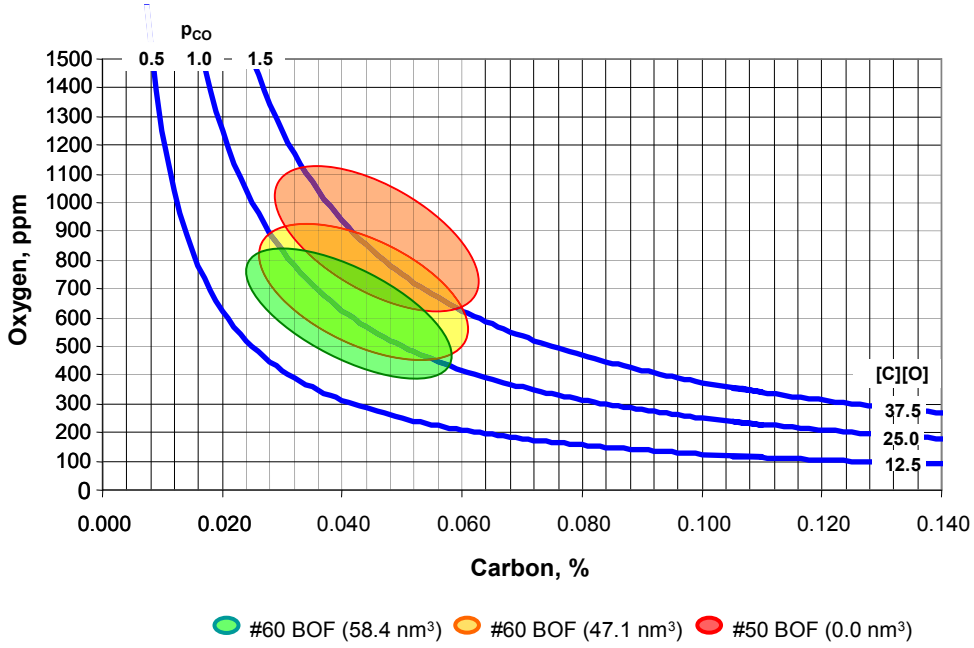

Figure 5-29: Influence of different purging gas consumptions on [C] and [O] levels.

5.3.2 Manganese

The influence of various total bottom purging gas consumptions is investigated according to the obtained [Mn] and their [O] levels after end of blow. The results are summarized in **Figure 5-30**. It shows the areas of the two analyzed set total flows – 58.4 and 47.1 nm^3 at #60 BOF in comparison to the non purging mode (flow = 0.0 nm^3) at #50 BOF.

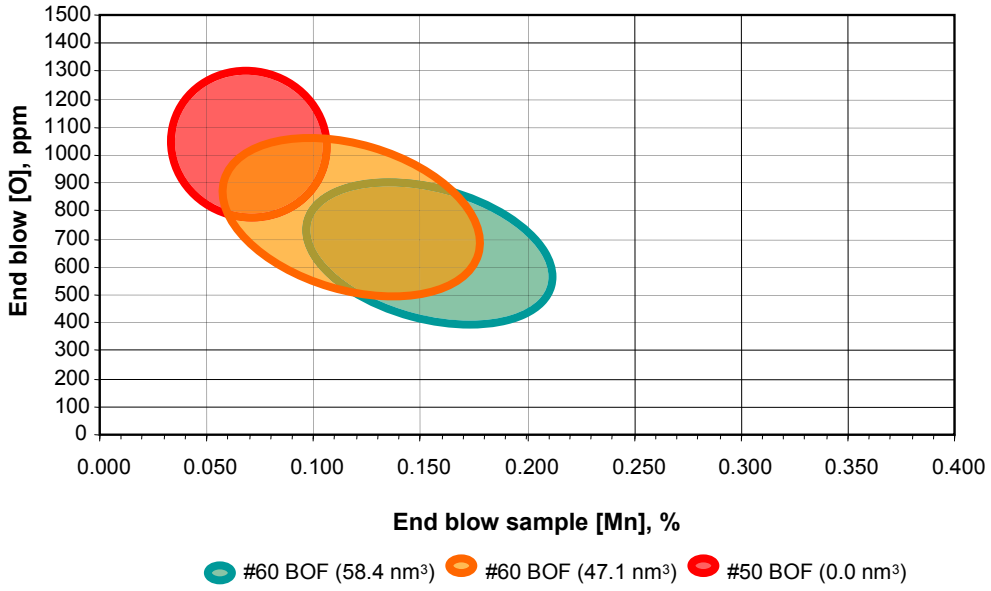

Figure 5-30: Influence of different purging gas consumptions on [Mn] and [O] levels after end of blow.

An effective purging with a total gas consumption of 58.4 nm^3 per heat leads to [Mn] levels in range between 0.1 and 0.23%. At this a reduction of 10 nm^3 drifts the values up to the area between 0.07 and 0.18%. The non-purging mode at #50 BOF (red area) contains [Mn] levels ranging from 0.04 to 0.1% with characteristic higher [O] contents over 700 ppm.

5.3.3 Phosphorus

The very low [P] levels of 350 ppm in the HM (in Europe commonly between 750 and 1000 ppm) lead to approximately equal [P] levels at the end of blow. This effect is demonstrated in **Figure 5-31**, where the [P] deviations range between 0.04 and 0.012% but various total set flow rates and [O] contents.

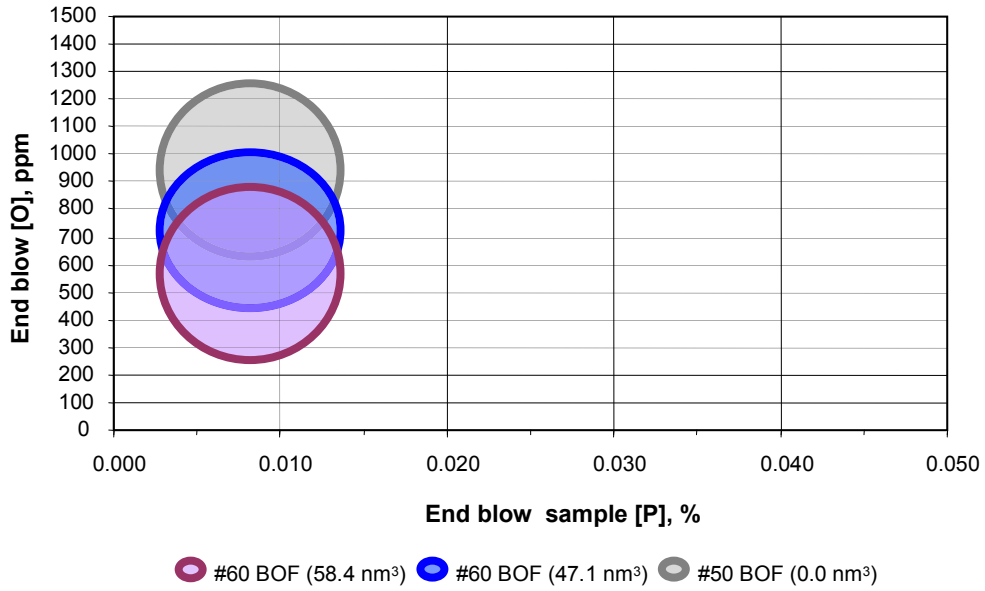

Figure 5-31: Influence of different purging gas consumptions on [P] and [O] levels after end of blow.

5.3.4 Reblow rates

Figure 5-32 shows that, there is a correlation between different total purging gas consumptions and the reblow rates. In detail, an increase of the total purging gas equals a minimization of the reblow factor.

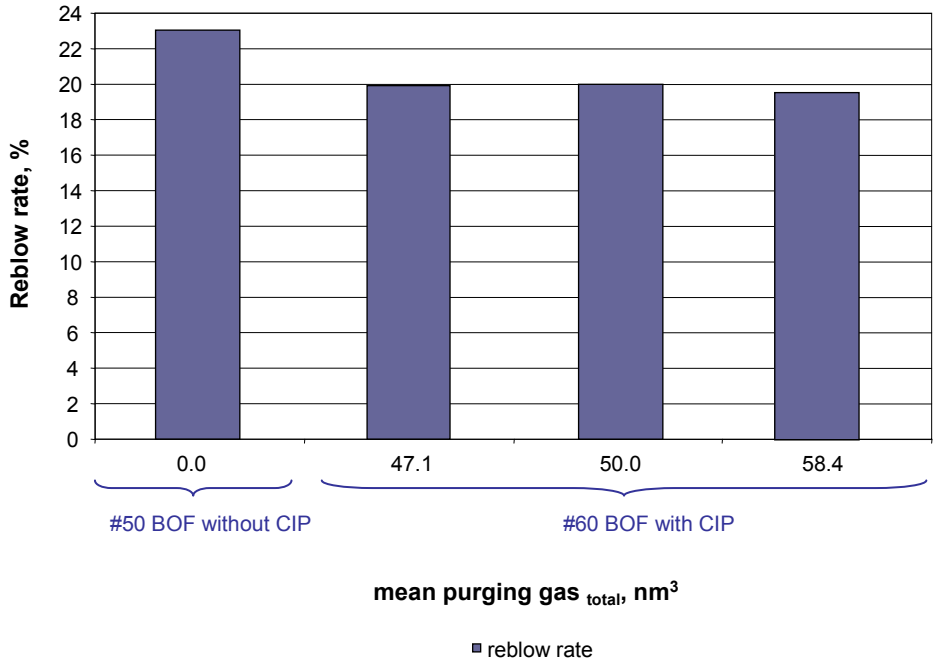

Figure 5-32: Influence of different purging gas consumptions on reblow rates.

The effect can be explained with the better BOF process control and liquid steel bath conditions closer to the equilibrium in relation to the non-purging mode at #50 BOF. As mentioned in **Chapter 5.2.7** there are three kinds of reblow reasons - temperature, [C] and wrong element levels ([Mn], [P], [S]). Due to different total gas consumptions the influence on the reblow reasons is investigated and documented as follows:

5.3.4.1 Temperature

Temperature reblows are more dependent on the converter model quality than on bottom purging.

5.3.4.2 Carbon

Due to closer conditions to the equilibrium an increase of the purging intensity leads to a reduction of the [C] reblow reason frequency down to the area of less percent compared to the non-bottom purging mode (**Figure 5-33**). Plugged bottom purging elements caused by too excessively slag washing and discontinuous production are parameters which have to be considered additionally. That is why a reduction to zero percent is unrealistic.

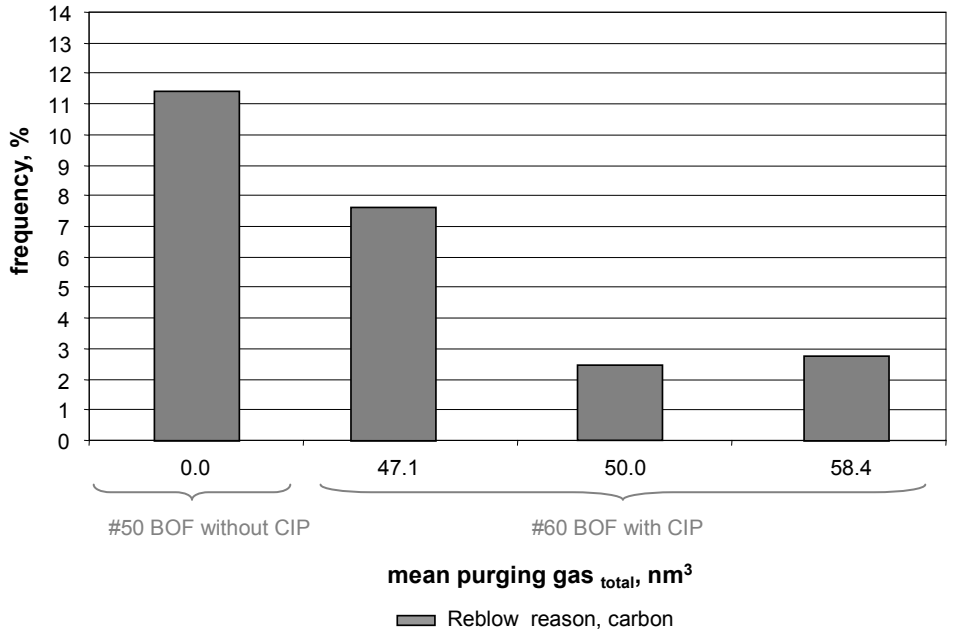

Figure 5-33: Influence of different purging gas consumptions on [C] reblow rates.

5.3.4.3 [Mn], [P], [S]

Wrong [Mn], [P], [S] levels have the lowest share in reblowing reasons (in the area of 2%). In **Figure 5-34** it is visible that a higher purging intensity causes decreased reblow frequencies by trend.

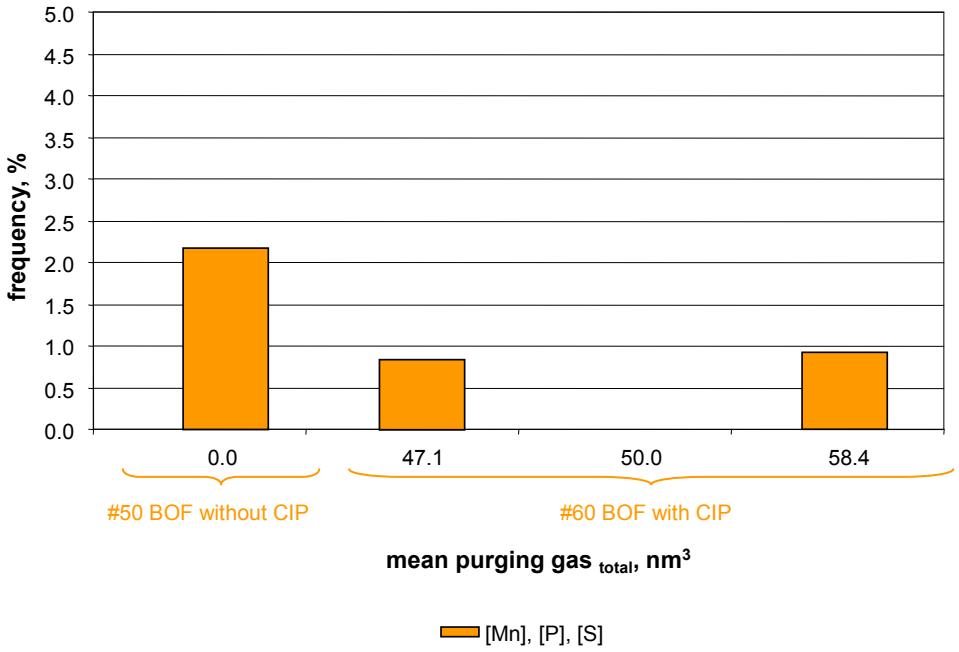

Figure 5-34: Influence of different purging gas consumptions on [Mn], [P], [S] reblow rates.

The results are summarized in **Table 5-12** and compared with the theory as well.

Table 5-12: Influence of purging gas increase on metallurgical results.

Parameter	Purging intensity increase	Correlation between theory and evaluation
[C]x[O]	↓	YES
[P] after end of blow	=	NO
[Mn] after end of blow	↑	YES
Reblow rate	↓	YES

5.4 Comparison between actual and set flow

For the reliability and the quality check of the purging gas automation, a comparison between actual and set flow was carried out. Heats with a total purging gas consumption of 58.4 nm^3 were analysed and individual process steps were investigated with the help of the measured flow rates which are transformed and stored in a excel data sheet. The measurement includes values of actual flow rates every two seconds. These values are compared with the set flow rate pattern. Finally the average deviation is calculated based on 100 heats. **Figure 5-35** shows the results during the refining at #60 BOF.

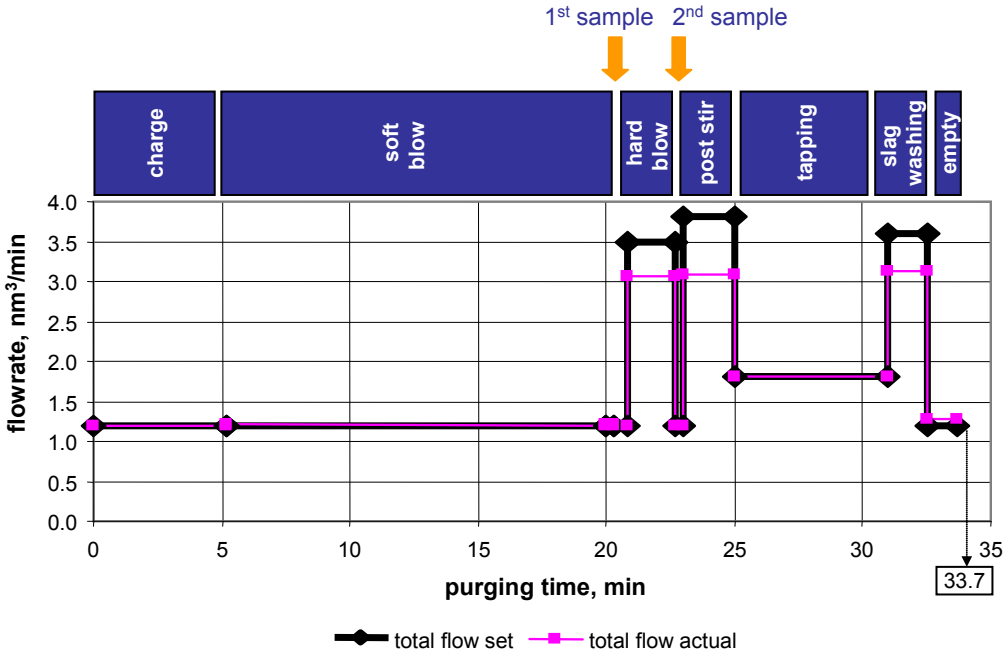

Figure 5-35: Comparison between set and actual flow.

In the area of low set flow rates, especially during charging, soft blowing, tapping and empty mode there is no difference between actual and set flow rate visible. The purging system works as it should.

An adjustment from a low to a high level is connected with a deviation of approximately 20%. In detail by the transition from the sublance measurements to the hard blowing and post

stirring mode and furthermore by the transition from the tapping to the slag washing process step.

Table 5-13 reflects the issues in the hard blowing, post stirring and tapping mode with values in detail.

Table 5-13: Flow rate comparison in different process steps.

process step	set flow [nm³]	actual flow [nm³]	check
charging	6.2	6.2	
soft blowing	18.1	18.1	
sublance measurement	0.4	0.4	
hard blowing	7.0	5.6	
sublance measurement	0.4	0.4	
post stirring	8.1	6.5	
tapping	11.0	11.0	
slag washing	5.6	5.0	
empty	1.6	1.6	
total	**58.4**	**54.8**	

o.k. not o.k.

A loss of 3.6 nm^3 per heat is the consequence of this effect. The reason is that the gas supply system was at the capacity limit with high flow rates. The consequence is an increased risk for plug blocking during the slag washing mode and worse metallurgical results.

5.5 Influence on slag practise, (MgO) level

Due to the BOF process transition to the top blowing mode with bottom purging system at #60 BOF the slag splashing practise is disabled and a new efficient philosophy (slag washing) especially for bottom wear stabilization activated. Slag washing is done after every three to five heat and it requires a (MgO) over saturated slag for adherence of the slag on the lining. The slag samples are taken after end of blow simultaneously with the steel samples. Based on the very low [P] content of the HM a realisation of the aimed [P] levels in liquid steel bath at tapping is ensured even with increased (MgO) values in the slag. **Figure 5-36** reflects the position of the slag analysis dependent on the (MgO) and the slag basicity according to the saturation line of Schürmann and Kolm (**Chapter 2.3.2.1**).

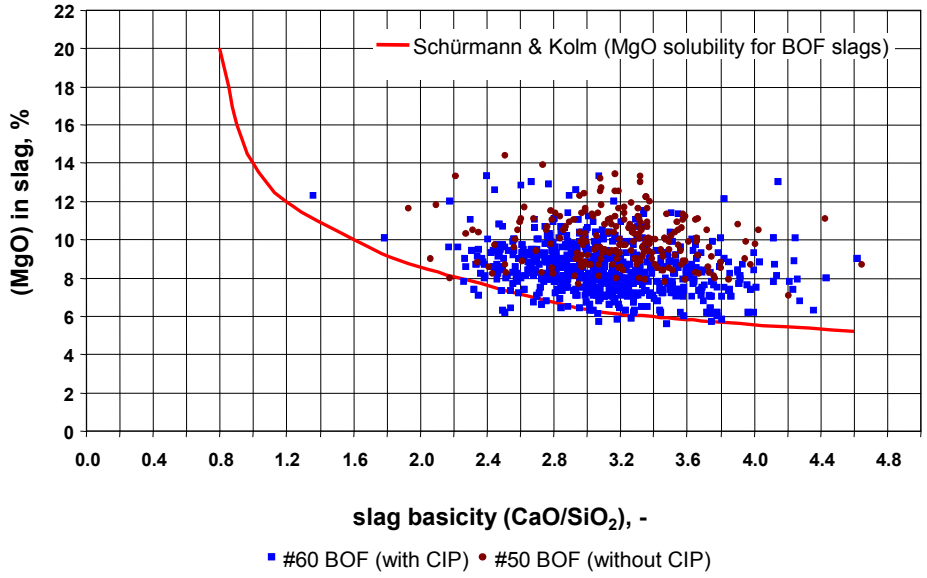

Figure 5-36: (MgO) solubility in BOF slags due to the slag basicity.

The values of #60 and #50 BOF as well are in the over saturated area and the average slag basicity at 60 BOF ranges between 3.0 and 3.5. At this for an over saturated slag a (MgO) level between 6 and 7% is necessary and aimed by the customer. A too high (MgO) level in slag is connected with a too sticky slag consistence with the risk of plug blocking during the slag washing practice. For aiming a slag with a defined (MgO) level of 7% the influence of

gunning preparation, lining and lime/dololime sequence on the (MgO) levels in slag are investigated in the following.

5.5.1 Gunning

Due to the very high pre wear of the charge pad, maintenance with slag washing, gunning and self flow mixes had to be started after 432 heats. **Figure 5-37** demonstrates the average gunning material per heat dependent on the average (MgO) level in slag for different heats on lining. It is seen that the maintenance until 700 heats on lining was quite unsuccessful with the effect of an increase of the average gunning material consumption from 1.0 up to 1.9 kg/mt steel. As a further consequence the average (MgO) level in slag raises up to 8.8%.

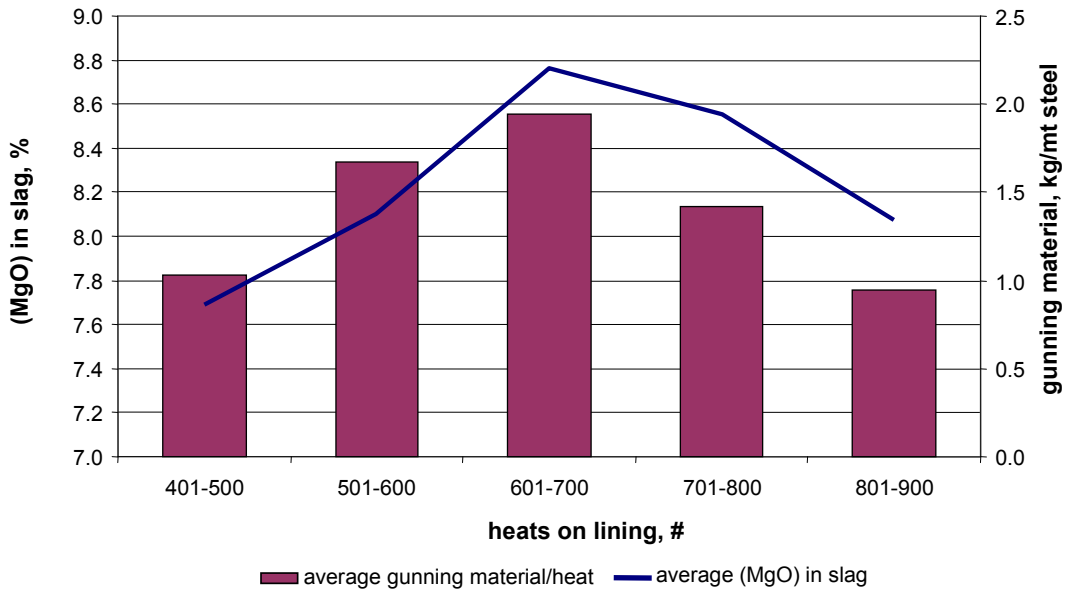

Figure 5-37: Course of the (MgO) level due to the used gunning material.

After 700 heats the most suitable monolithic mixes have been determined leading to a drop of total consumption down to 0.9 kg/mt steel. This effect is also related with a reduction of the (MgO) level back to 7.9%. **Figure 5-38** reflects the correlation between the gunning interval and material consumption in average dependent on the produced heats on lining. Due to the

advanced wear of the charge pad explained by the used gunning mixes at the beginning the gunning interval decreased until 700 heats (from seven to four heats).

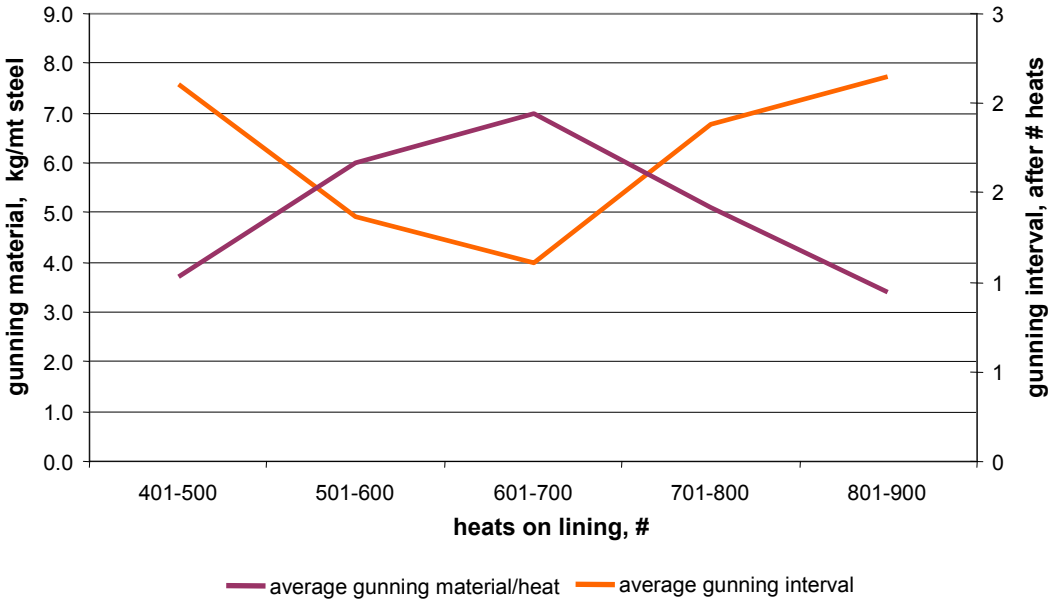

Figure 5-38: Course of the used gunning material due to the gunning interval.

Based on the slag analysis between 400 and 700 heats, the course of the (MgO) level in slag after gunning (constant lime and dololime additions) is investigated (**Figure 5-39**). In the second heat a rise of the (MgO) content in slag is visible which is a potential indication for the mix loss.

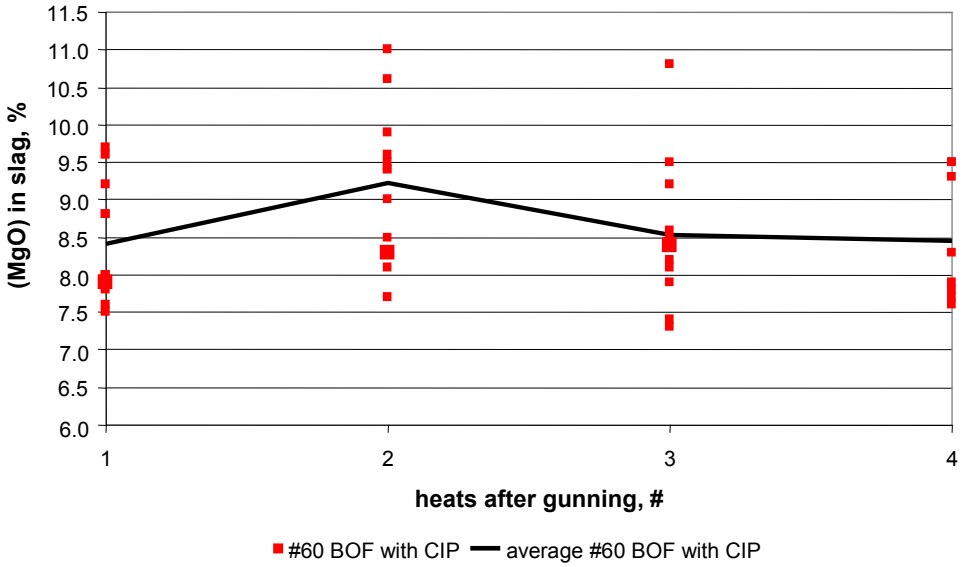

Figure 5-39: Course of the (MgO) level in slag after maintenance.

Due to the gunning reports and slag analysis with the main focus on the (MgO) levels in slag the frequency are calculated. **Figure 5-40** reflects a gunning mix loss from the charge pad area after two heats with over 60%.

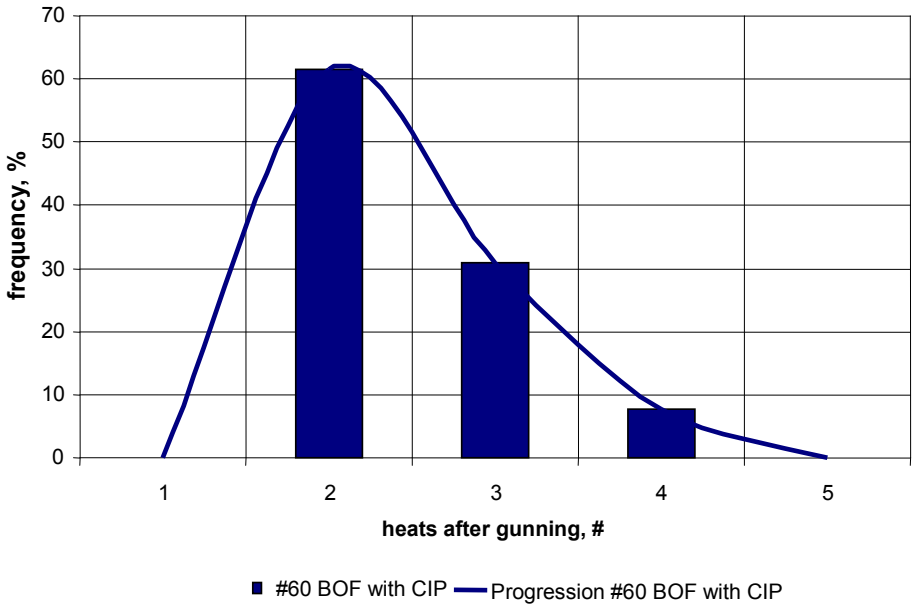

Figure 5-40: Frequency of gunning loss after # heats.

5.5.2 Lining

For the calculation of the <MgO> supply from the lining a slag balance was done. Values of the first 600 heats at #60 BOF have been used. The calculation is based on MgO sources (in- and output) with defined operation parameters (**Attachment D**). Finally, a comparison between calculated and residual slag volume is done for a plausibility check.

5.5.2.1 Slag balance calculation

Figure 5-41 demonstrates the results of the slag balance calculation. It is seen that in the area of the first 200 and after 400 heats on the lining the difference between actual and calculated slag volume is quite enormous. At the beginning no flux balance calibration was carried out. Caused by a power failure after 400 heats, the flux balance system has been displaced and recalibrated after 600 heats.

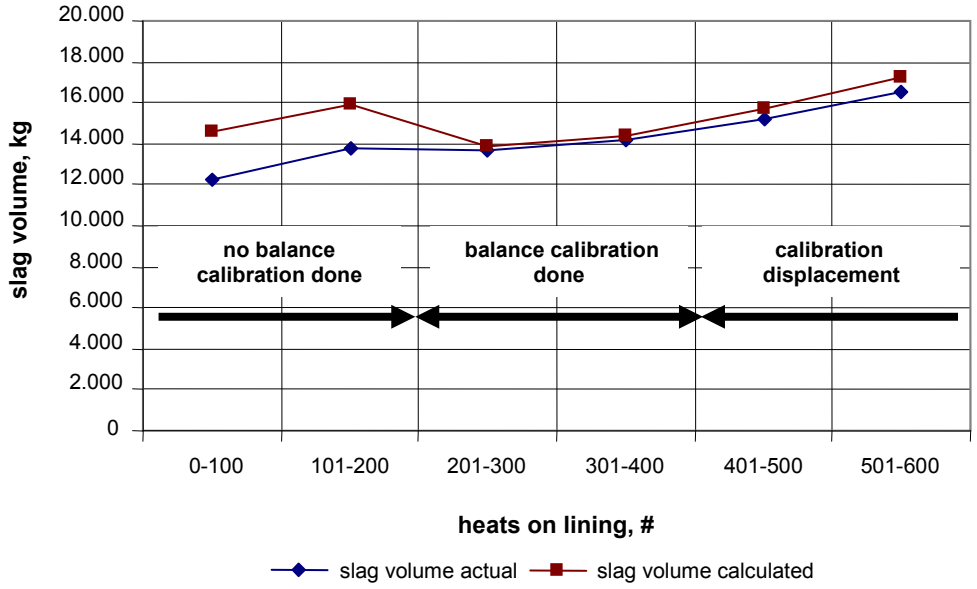

Figure 5-41: Comparison between actual and calculated slag volume.

The following investigation is focusing on the heat areas between 200 and 400.

Figure 5-42 shows the average course of the MgO sources, lining and gunning material according to the (MgO) level in slag for the heat interval between 200 and 400 heats.

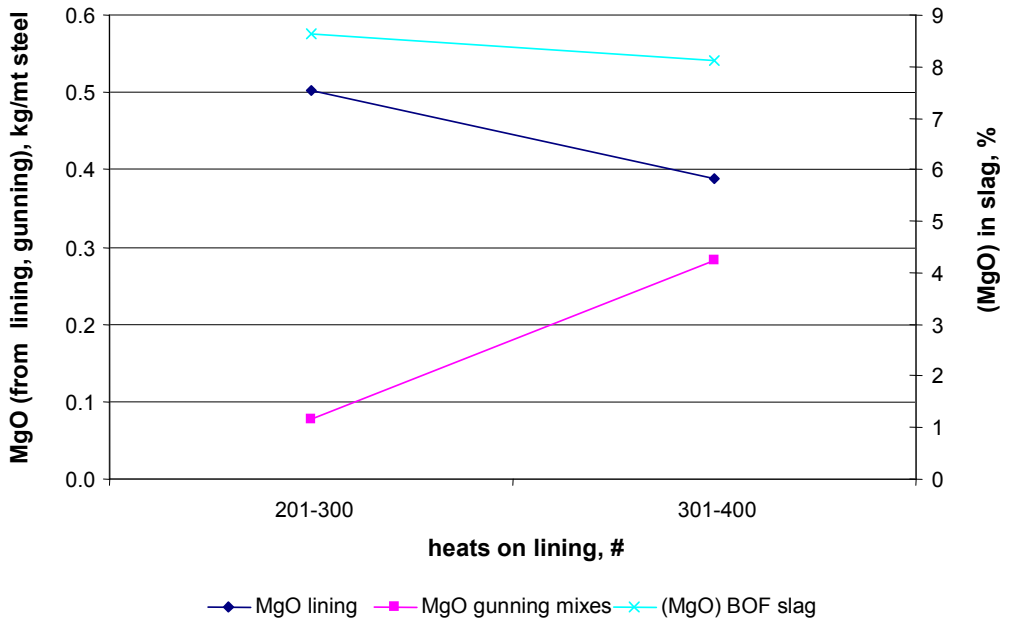

Figure 5-42: MgO from lining and gunning due to (MgO) in slag.

It is visible that there is correlation between lining and gunning material. Due to an approximately identically (MgO) level in slag, the behaviour or rather the (MgO) support of both sources are oppositely. Caused by increasing gunning material consumption the <MgO> coming of the lining is reduced.

5.5.3 Addition of lime / dololime

The influence of different addition time steps of lime and dololime (both MgO carrier are charged at the same time) on the (MgO) levels in slag after end of blow is investigated. **Figure 5-43** reflects the results at which one point stands for an average value including 100 heats.

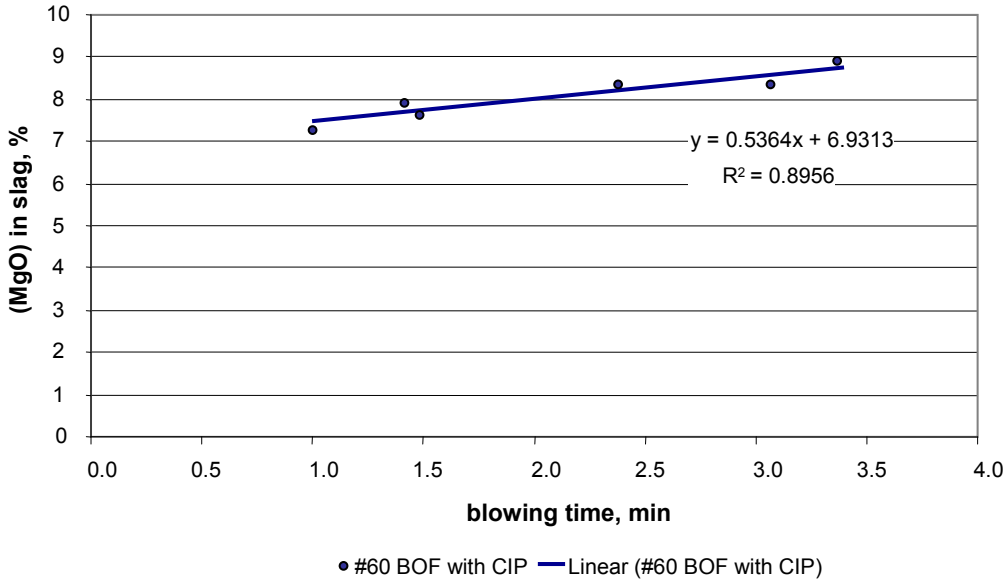

Figure 5-43: Influence of different lime/dololime additions on (MgO) in slag.

Figure 5-43 shows clearly the effect of a later charging of lime and dololime. It is combined with a an increase of the (MgO) level in slag. Due to constant lime and dololime addition it can be explained by the higher potential of <MgO> dissolution from the lining at the initial stage of the slag formation. Furthermore the wear rate is increasing simultaneously, especially at the slag area. For aimed (MgO) levels in slag in the area of 7% it is necessary to charge lime and dololime in the first two minutes of blowing.

5.6 Bottom wear profile

Beginning from an initial lining thickness in the area of 750 to 800 mm, the wear zones are investigated based on the data of the laser scans (**Attachment A**) - in detail the charge-, bottom-, trunnion- and tap pad area (**Figure 5-44**). The blue line represents the charge pad wear and it turns out that the wear had be en slowed down caused by gunning (after 432 heats) slag wash and hot repair mixes. After 1000 heats a residual brick length of 250 mm remained. In comparison the wear of the trunnions was much slower and seems to be almost linear. In this area a wear of 300 mm at 1000 heats also leads to an estimated campaign life of only 2167 heats for a zero-maintenance vessel. The tap pad and the bottom are with 700 mm and 580 mm residual thickness rather wear resistant and would have reached the target of 3000 heats easily. The bottom with the purging elements was not a critical issue at all.

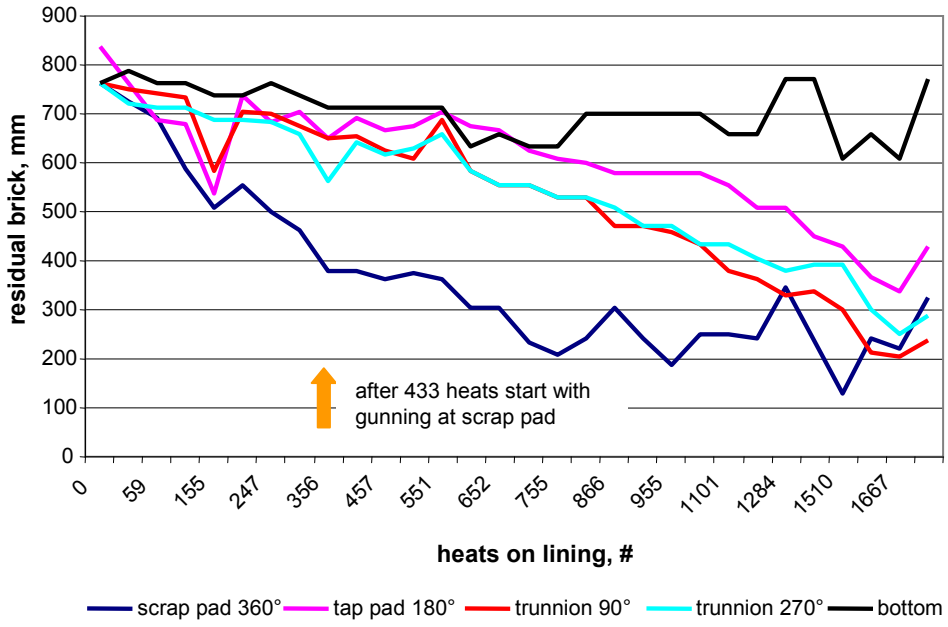

Figure 5-44: Wear profiles.

Furthermore the bottom wear profile is analysed in detail comparing with the plug areas (**Figure 5-45**). Besides plug 9, which was the first one to be closed caused by water leakage none of the multihole purging elements showed a pre-wear in the first 1000 heats of the campaign. Even the bottom area around line 9 was stabilized by gunning after disconnection.

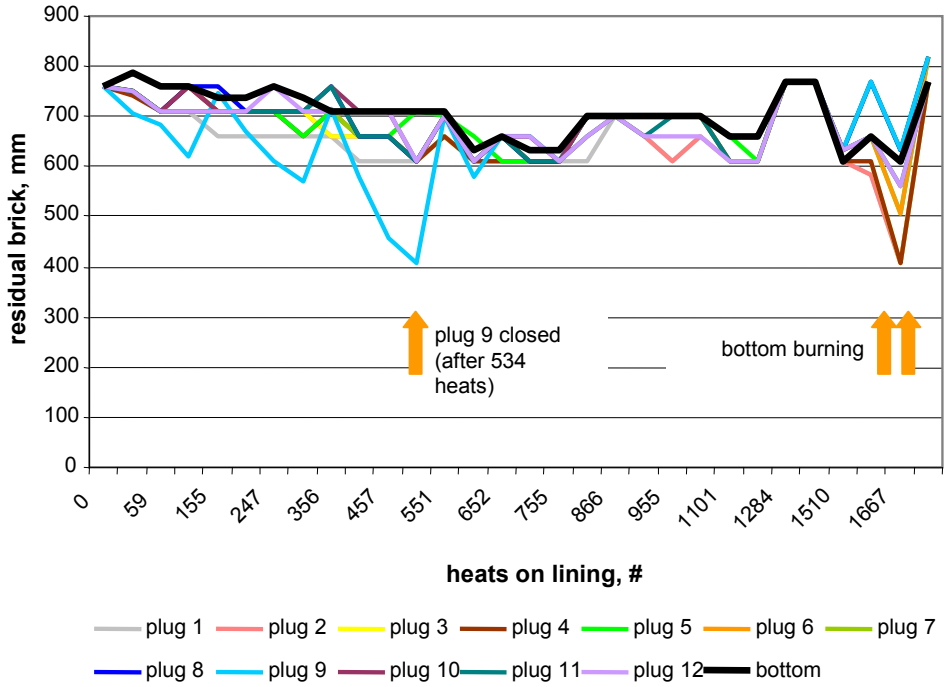

Figure 5-45: Plug area wear profile

5.7 Operational problems

During the first campaign at #60 BOF with bottom purging metallurgical results with the main focus on the [C]x[O] products are influenced by:

- The production situation (HM supply and financial crisis)
- Excessive slag washing practise (no plugs are visible, bottom build up)
- The removal of plugs (water penetration in the pipe system through the cooling system of the trunnion ring)
- Unsuccessfully gunning maintenance at the charge pad, especially at the beginning

As a result a solid slag layer at the bottom was created caused by the discontinuous production situation (**Attachment C**). At this the solid coating was frequently reduced using bottom burning.

5.7.1 Production

During the first campaign the influence of the worldwide financial crisis on the steel production became stronger and a production turndown was the logical consequence. **Figure 5-46** shows the trail of the p_{CO} values dependent on the production situation in detail.

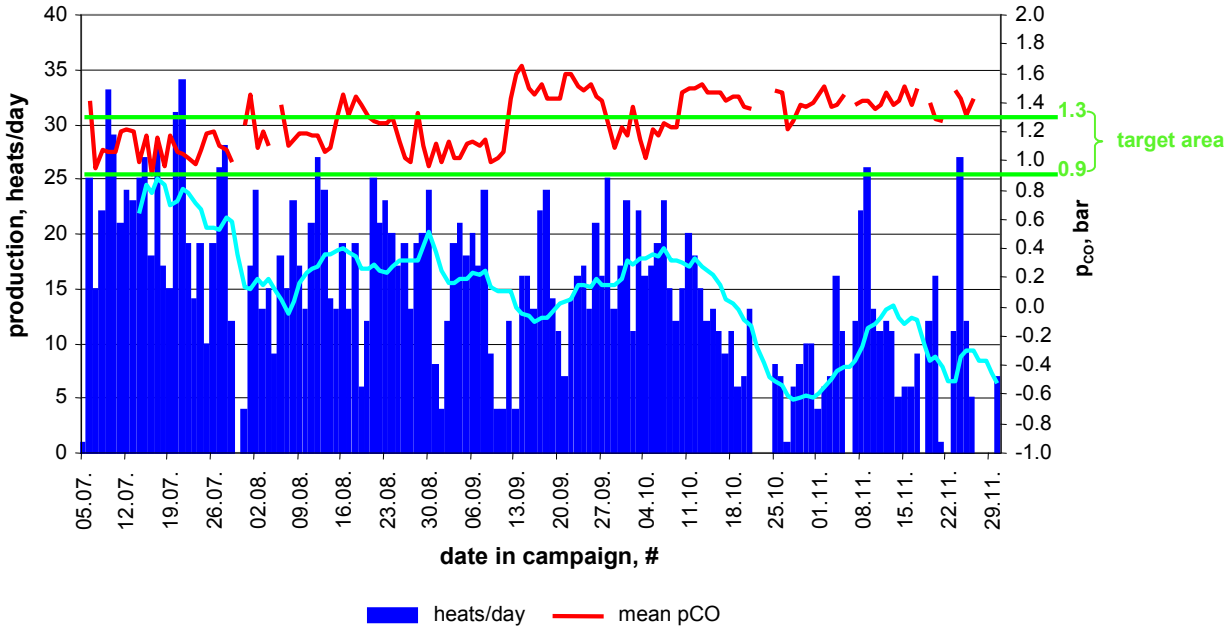

Figure 5-46: Course of the production and p_{CO} values.

The production of #60 BOF declined from a reasonable level of 25 heats/day in July to 15 heats/day in August and September and further down to 7 heats/day in November. The amount of down days at #60 BOF moves up to 4 in October and even to 7 in November. Due to the discontinuous production situation at the steel plant the bottom at #60 BOF had built up a solid layer of more than 130 mm (caused by the cooling of the vessel and the continued slag washing). In this connection the main target at middle of September was besides the charge pad stabilization, the bottom burning to remove the solid slag coating. On the 5th of October the steel plant decided to return to slag splashing mode and disable the bottom purging.

5.7.2 Bottom purging gas consumption

Figure 5-47 shows the p_{CO} values compared to the theoretical calculated total purging gas consumption per heat. The total gas consumption can be estimated by using the target flow rates from the purging pattern together with the cycle time reported in the database. The figure indicates anticipated p_{CO} values at a purging gas consumption of 60 nm^3/heat. When at the end of July the first two plugs had to be disconnected due to water leakage, the flow

rates have not been adjusted to compensate the flow. Therefore, the purging gas consumption was lowered below 50 nm^3/heat which immediately caused an increase in the p_{CO} over the upper control line. Afterward the values have been stabilized within the control, but on a higher level as achieved before. The same effect happened when the third plug had to be disconnected and again the situation came back under control within the following two weeks. In the middle of September a planned maintenance stop of the furnace over a few days was used to carry out a pressure check at the remaining lines.

The dramatic increase in the p_{CO} indicates that the purging gas was not longer going into the BOF. After a few days the system was brought back to operation by blowing the bottom build up several times. The production level at the beginning of October was at 15 heats/day and more. When the production went further down starting from the second half of October, the plugs were blocked again by bottom build up and the flow rates were finally reduced to the minimum to avoid steel infiltration (**Figure 5-47, Figure 5-48**).

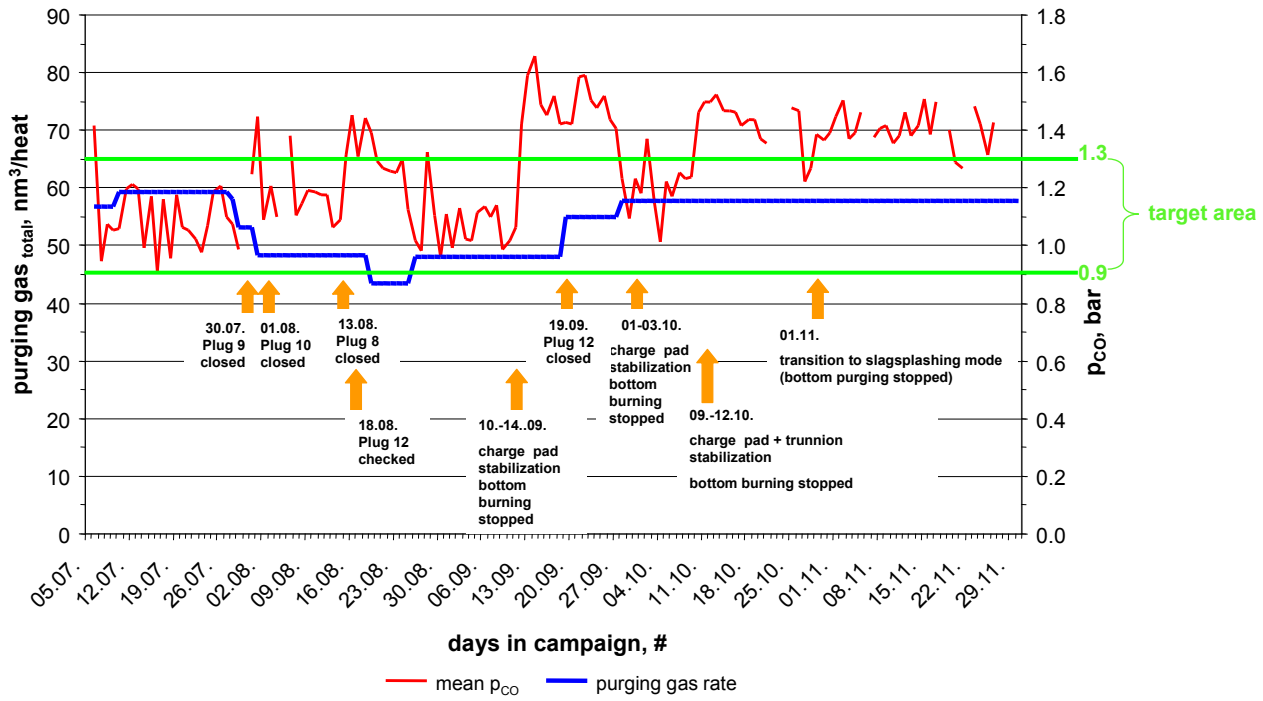

Figure 5-47: Course of the total purging gas consumption and p_{CO} values.

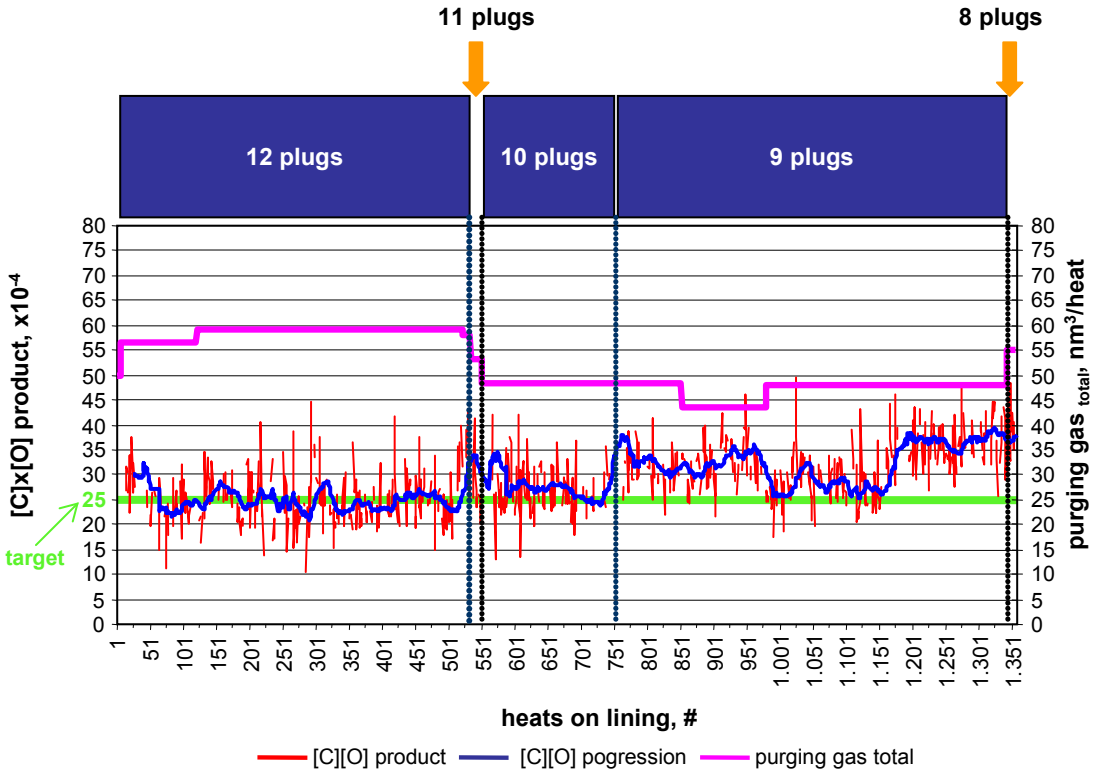

Figure 5-48: Influence of removal of plugs on the [C]x[O] product.

5.7.3 Wear stabilization at charge pad

After less than 400 heats the charge pad showed a severe large-area wear (**Figure 5-49**), caused by the scrap charging practice. That means a wrong distribution of scrap pieces. In detail very heavy pieces are in the front of the scrap box followed by lighter scrap pieces. This philosophy is connected with a very high mechanical impact in the charge pad during charging, because no damping effect trough the light pieces is available. Another reason is the lining concept which has been designed for a high degree of slag splashing. The initial concept is also connected with a brick quality change at the charge pad.

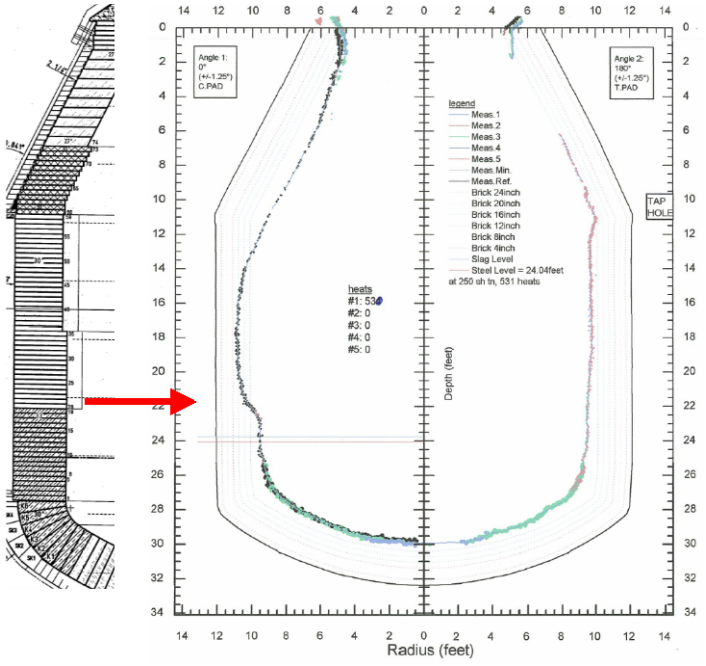

Figure 5-49: Wear at charge pad after 400 heats.

Figure 5-50 demonstrates the wear course during the first campaign at the charge pad. It reflects the unsuccessful gunning maintenance at the beginning and the transition to slag splashing after 1501 heats caused by the turndown of the production.

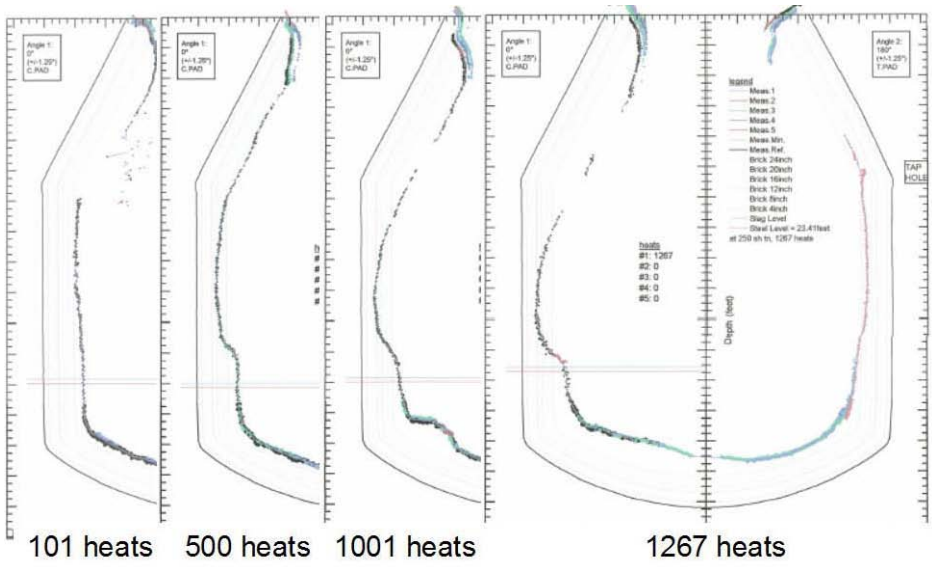

Figure 5-50: Course of the wear at the charge pad.

6 Summary

The investigated steel plant made a decision for a bottom purging system implementation at #60 BOF. The system was supplied by the VRA/RHI using FC-Technik and TBR components and installed by Middough in June 2008. After the commissioning on July 6th, 2008 the system showed the metallurgical benefits of the top blowing process with bottom purging system in comparison to a top blowing converter (#50 BOF) in simultaneous operation. The implementation was connected with a change in the refining (charging-, lance- and slag practise) and in the converter maintenance philosophy (stop of slag splashing). As a consequence the target lifetime of the lining decreased from 50.000 to 3.000 heats.

For bottom maintenance slag washing is done. At this the customer aimed for a (MgO) level in slag of 6 to 7%. Higher values lead to a too sticky consistence of the slag with the risk of plug blocking during the slag washing practice. For these (MgO) levels it is necessary to charge lime and dolime in the first three minutes of blowing, otherwise the < MgO> dissolution from the lining at the initial stage of slag formation is increased considerable.

Based on laser measurements the bottom with the stirring elements was not a critical pre-wear zone at all.

Due to the provided data base with the main focus on the first 534 purged heats at #60 BOF the effects or rather the benefits of bottom purging are clearly visible as given in the theory (**Table 6-1**). The indicators for bottom purging efficiency, the [C]x[O] product and the p_{CO} level have been lower in comparison to the top blowing mode at #50 BOF. In detail a [C]x[O] reduction from 34 to approximately $24*10^{-4}$ (p_{CO} level of 0.9 bar) was achieved.

Dependent on the better bath agitation and the improved bath kinetics caused by the increased mixing energy, a flux addition saving of 8.3 kg/mt was realized. The improved yield was also connected with a minimization of the slag volume of two tons. Furthermore the $(Fe)_t$ level in slag droped from 19 down to 17%.

The [Mn] recovery is also demonstrated in course of the evaluation. An enhancement of the [Mn] levels in average from 0.75% up to 1.55% was achieved after end of blow. That equals FeMn savings in the secondary metallurgy.

Regarding the final phosphorus content, there seems to be no difference between the purged and the non purged heats. An explanation can be that the [P] in both BOFs' was below 100 ppm (coming from initially 350 ppm of the HM), which is an excellent result for deep drawing qualities at all. Due to this very low [P] content the mixing energy even in the first 534 heats was too low to show an effect.

Caused by the better bath mixing and the quicker scrap melting more scrap can be charged. The scrap / HM ratio increased from 14.9 to 16.8% per heat.

In comparison to #50, #60 BOF showed a total reblow rate of 19.5%, which means a decrease of 3.5 %. Reblows caused by [C] were lowered at 8.7%.

Furthermore, a minimization of the average tap to tap time from 44 to 33.7 minutes was realized. That equals a process acceleration of 23.4% in comparison to the top blowing mode at #50 BOF. The maximum production capacity of the steel plant is limited to 30 to 40 heats per day (caused by CC). Due to the process acceleration it is possible to operate with #60 BOF in single operation.

During the first purged campaign at #60 BOF metallurgical results are influenced by the unsuccessful gunning maintenance at the charge pad at the beginning and by take out of plugs (leaky pipe welding in the water cooled trunnion). Later the reduced production due to the arising financial crisis resulted in too few heats/day for an economic operation of the CIP system. As a result bottom build-up was created that had to be reduced frequently by bottom blowing using FeSi and $\{O_2\}$.

Table 6-1: Summary of the metallurgical results.

Parameter	#50 BOF without CIP	#60 BOF with CIP	Difference/ Saving	Correlation between theory and evaluation
[C]x[O], *10⁻⁴	32-35	22-25	-10	YES
p_{CO}, bar	1.3	0.9	-0.4	YES
[C] after end of blow, %	0.05	0.045	-0.003	YES
[O] after end of blow, ppm	700	500	-200	YES
flux addition, kg/mt	69.9	61.6	- 8.3	YES
slag volume, kg	14000	12000	-2000	YES
$(Fe)_t$, %	19	17	-2	YES
(MnO), %	6	4.5	-1.5	YES
[Mn] after end of blow, %	0.75	1.55	+0.8	YES
[P] after end of blow, %	0.009	0.009	-+0	NO
[S] after end of blow, %	0.008	0.008	+-0	NO
scrap/HM ratio, %	14.9	16.8	+1.9	YES
Reblow rate, %	23.0	19.5	-3.5	YES
tap to tap, min	44.0	33.7	-10.3	YES

7 Discussion

By paying only minor attention to the metallurgical benefits of the bottom purging, a minimum target campaign lining life of 3.000 heats was the main focus of the operation in this first campaign. All control parameters of the “purging mode” were adjusted to minimize potential wear of the purging elements and the bottom refractories. The comparison of the metallurgical data of the #60 and the #50 BOF in the provided database shows that during the start of the campaign significantly positive metallurgical results were obtained even with much lower flow rates than recommended by RHI. The bottom is no critical pre wear zone at all. At this an operation with higher total gas consumptions over 70 nm^3 per heat should be aimed for the future resulting in even higher benefits.

The (MgO) content in slag almost never reached the desired minimum target level of 6%. A level over 8% was established during the campaign. Caused by the too sticky slag consistence the bottom builds up. In this connection a stop of the slag washing mode must be done until the plugs are visible again (look into the BOF after tapping). Furthermore, lime and dololime should be charged in the first two minutes of blowing to keep the <MgO> dissolution from the lining low and to achieve the aimed level of 6 to 7% (MgO) in slag.

The end blow samples do not show the effect of post stirring. Additionally post stirring enhances the dephosphorisation and decarburisation effect. So the influence of post stirring should be analysed at the next purged campaign in detail.

The purging gas automation shows weaknesses by the regulation from low to high flow rate levels ($\rightarrow$ installation of pressure manometers next to plug and rotary union).

References

[1] Wallner, F. und E. Fritz, Fifty years of Oxygen-Converter Steelmaking, Steel Gets Together, NO 1, 2002, pp 1-8.

[2] Krieger, W., 50 Jahre LD-Prozess – 50 Jahre Innovation, BHM 148, 2003, pp 247-253.

[3] Lachmund, H., Der Sauerstoffaufblasprozess – Metallurgie und Wechselwirkung mit ff-Material, Workshop Dillinger Hütte, Bad Neuenahr, 2004.

[4] Wiemer, H., H. Delhey and H. Sperl, Verfahrenstechniken und metallurgische Ergebnisse der Blasstahlerzugung in der Bundesrepublik Deutschland, Stahl und Eisen 105, 1985, pp 1142-1150.

[5] Selines, R., Selection of Stirring and Shrouding Gases for Steelmaking Applications, Union Carbide Cooperation, New York, 1988.

[6] Wünnenberg, K. and J. Cappel, Cost saving operation and optimisation of metallurgical reactions in BOF practise, Stahleisen 9, 2008, pp 55-66.

[7] Kreulitsch, H., W. Krieger and A. Jungreithmeier, Der LD-Prozesse - ein ökologisch optimiertes Verfahren, Neue Hütte 37, 1992, pp 313-321.

[8] VoestAlpine, Stahlerzeugung, www.expeditionvoestalpine.com, abgerufen am 10. Dezember 2008.

[9] Hiebler, H. and W. Krieger, Metallurgie des LD-Prozesses, BHM 137, 1992, pp 256-262.

[10] Gudenau, H., Praktikum zur Metallurgie, RWTH Aachen, 2002.

[11] Verein Deutscher Eisenhüttenleute, Stahlfibel, Verlag Stahleisen, Düsseldorf, 2002.

[12] Kootz, T., K. Behrens and P. Baumgarten, Zur Metallurgie des Sauerstoffaufblas-Verfahren, Stahl und Eisen 14, 1985, pp 857-865.

[13] Krieger, W. und F. Plaul, Reduktions- und Schmelzmetallurgie, Vorlesungsskriptum, Lehrstuhl für Metallurgie, Montanuniversität Leoben, 2006.

[14] Trentini, B., Scrap consumption in the oxygen converter, Steel Times, 1985, 609.

[15] Dimitrov, D., H. Pirker and A. Moser, Metallurgieseminar zur Stahlerzeugungstechnik, Linz, 1996.

[16] Antlinger, K., H. Preßlinger and H. Hiebler, Untersuchungen zur Verschlackung von Phosphor und Schwefel im LD-.Prozess, BHM 133, 1988, pp 401-407.

[17] Kothani, T., On the metallurgical and blowing characteristicsof the LD-Prozess I&SM 33, 1982, pp 28-33 .

[18] Chukwulebe, B., A. Klimushkin and G. Kuznetsov, The utilization of high Phosphorus HM in BOF steelmaking, Iron and Steel Technology Conference (AISTech), Ohio, 2006.

[19] Jandl, C., BOF prea wear zones, interne RHI Schulungsunterlagen, Wien, 2008.

[20] Verein Deutscher Eisenhüttenleute, Schlackenatlas, Verlag Stahleisen, Düsseldorf, 1985.

[21] Verein Deutscher Eisenhüttenleute, Schlacken in der Metallurgie, Verlag Stahleisen, Düsseldorf 1981.

[22] Koch, K., Metallurgie des Eisens, VDEh-Weiterbildung, Glosar, 1996.

[23] Schürmann, E. and I. Kolm, Auflösungsverhalten von Dolomit in Stahlwerksschlacken sowie Grenzen der Löslichkeit und Folgen für den Feuerfestverschleiß, steel research 57, 1986, pp 51-57.

[24] Obst, K., E. Schürmann, D. Nolle, Auflösungsvehalten und Sättigungsgehalte des Magnesiaoxids in Anfangsschlacken des LD-Verfahrens, Arch. Eisenhüttenwes. 51, 1980, pp 407-412.

[25] Schürmann, E. and I. Kolm, Mathematische Beschreibung der MgO Sättigung in komplexen Stahlwerksschlacken beim Gleichgewicht mit flüssigem Eisen,steel research 57, 1986, pp 7-12. 2006.

[26] Reisinger, P., H. Preßlinger, H. Hiebler, MgO Löslichkeiten in Stahlwerksschlacken, BHM 144, 1999, pp 196-203 .

[27] Obst, K., E. Schürmann, D. Nolle , Über das Auflösungsverhalten des Magnesiumoxids in der Schlacke beim LD-Verfahren, Stahl und Eisen 100, 1980, pp 1194-1200.

[28] Krieger, W., F. Hubner, A. Patuzzi, LD-Prozess mit Bodenspülung – Maßnahmen, Möglichkeiten, Ergebnisse, Stahl und Eisen 105, 1985, pp 673-678.

[29] Fliege, L., V. Schiel, H. Schröer, Einfluss des Bodenspülens auf die metallurgischen Ergebnisse in den LD-Stahlwerken der Krupp Stahl AG, Stahl und Eisen 103, 1983, pp 159-164.

[30] Krieger, W., G. Poferl, Metallurgische und betriebliche Vorteile des LD-Prozesses mit Bodenspülung, Weiterbildungsunterlagen VOEST, Linz, 1982.

[31] Berger, M., W. Ebner, A. Wagner, Implementation of Basic Oxygen Furnace Bottom Purging at Mittal Steel Newcastle, RHI Bulletin 2, 2006, pp 7-11.

[32] Marsh, R., B. Bliss, BOP bottom bubbling practise at National Steel, Steel Technology 12, 1999, pp 40-44.

[33] Schürmann, E., K. Obst, H. Schäfer, Einfluss des Bodenspülens und Nachspülens auf die Gleichgewichtseinstellung im System Eisen – Kohlenstoff – Sauerstoff, Stahl und Eisen 105, 1985, pp 459-464.

[34] Bruckhaus, R., H. Lachmund, Stirring strategies to meet the highest metallurgical requirements in the BOF process, Iron and Steel Technology Conference and Exposition (AISTech), Indianapolis, 2007.

[35] Nakanishi, K., T. Nozaki, Y. Kato, K. Suzuki, Physical and Metallurgical Charakteristics of Combined Blowing Processes, Proceedings of the 65th Steelmaking Conference of AIME, Earrendale, 1982, pp 101-108.

[36] Krieger, W., G. Poferl, R. Apfolterer, Erzeugung von Stählen mit niedrigen Kohlenstoffgehalten in einem bodenspülenden LD-Tiegel, BHM 129, 1984, pp 188-195.

[37] Choudhary, S., A. Ghosh, Assessment and application of the equlibrium slag-metal phosphorus partition for basic oxygen steelmaking, Ironmaking and Steelmaking, Volume 34, 2007, pp 343-350.

[38] Choudhary, S , S. Ajmani, Evaluation of Bottom Stirring System in BOF Steelmaking Vessel using cold model study and thermodynamic analysis, Research and Development Division, Tata Steel, 2006, pp 1171-1176.

[39] Schrott, R., P. Hausen, H. Peterson, Das kombinierte Blasen mit Argon und Stickstoff beim LD-Verfahren der Hoesch Hüttenwerke AG, Stahl und Eisen 103, 1983, pp 163-166.

[40] Majcenovic, C., Feuerfeste Baustoffe im Hüttenwesen, Vorlesungsskriptum, Institut für Gesteinshüttenwesen, Montanuniversität Leoben, 2006.

[41] Mörtl, G., W. Kraft, H. Barthel, Entwicklung und derzeitiger Stand der ff-Zustellung von Sauerstoffkonvertern, BHM 137, 1992, pp 196-203.

[42] Mills, K, Y. Su, A. Fox, A review of slag splashing, ISIJ International, Volume 45, 2005, pp 619-633.

[43] Messina, C. ,Salg splashing in the BOF- worldwide status, practise and results, Iron and Stell Engineer, Volume 6, 1996, pp 17-19.

[44] Jandl, C., K. Zettl, Interne RHI-Weiterbildungsunterlagen, Wien, 2009.

[45] Basu, S., Studies on dephosphorisation during steelmaking, doctoral thesis, Sweden, 2007.

Attachements

A Laser measurement of the #60 BOF

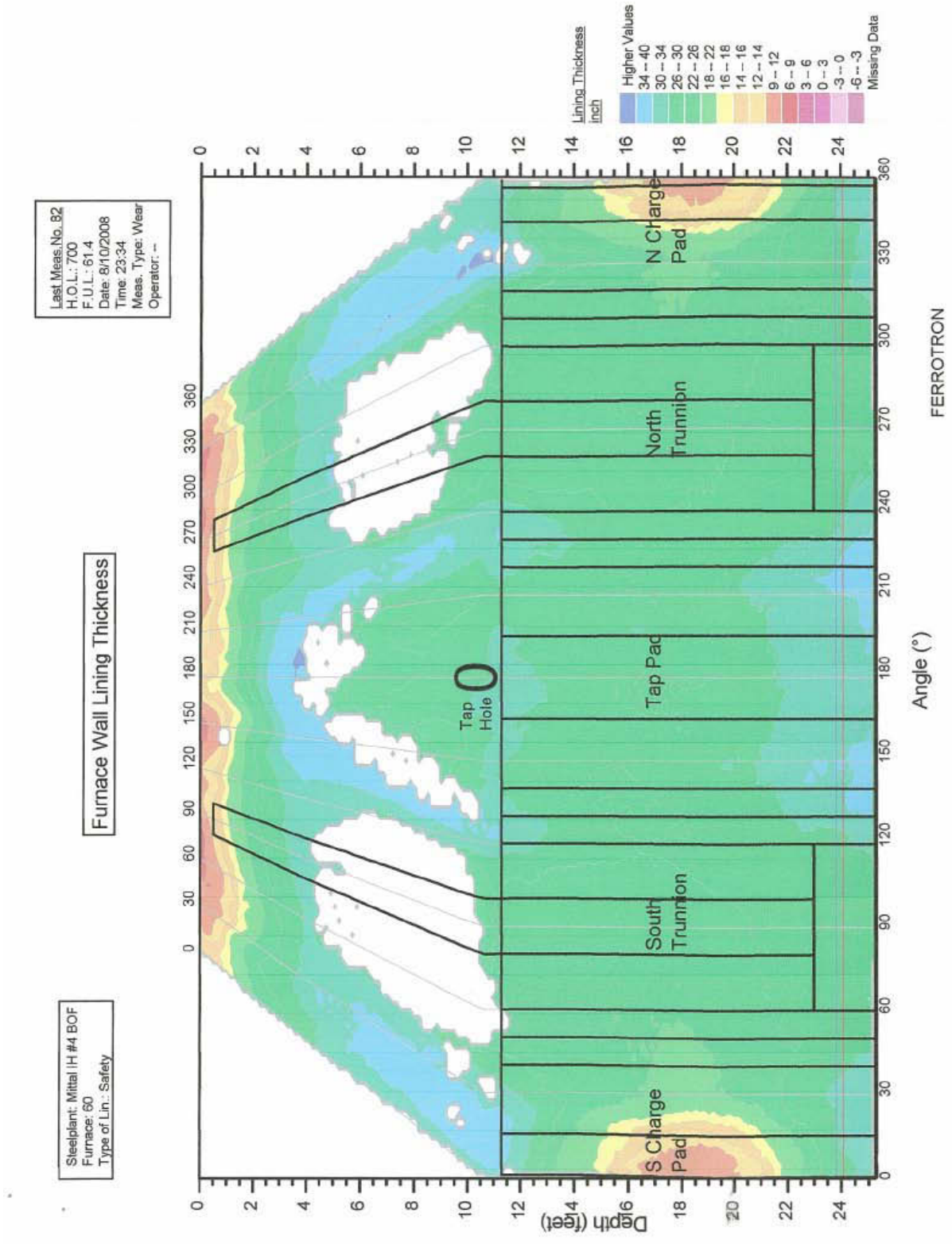

Attachment 1: Wear of the wall lining.

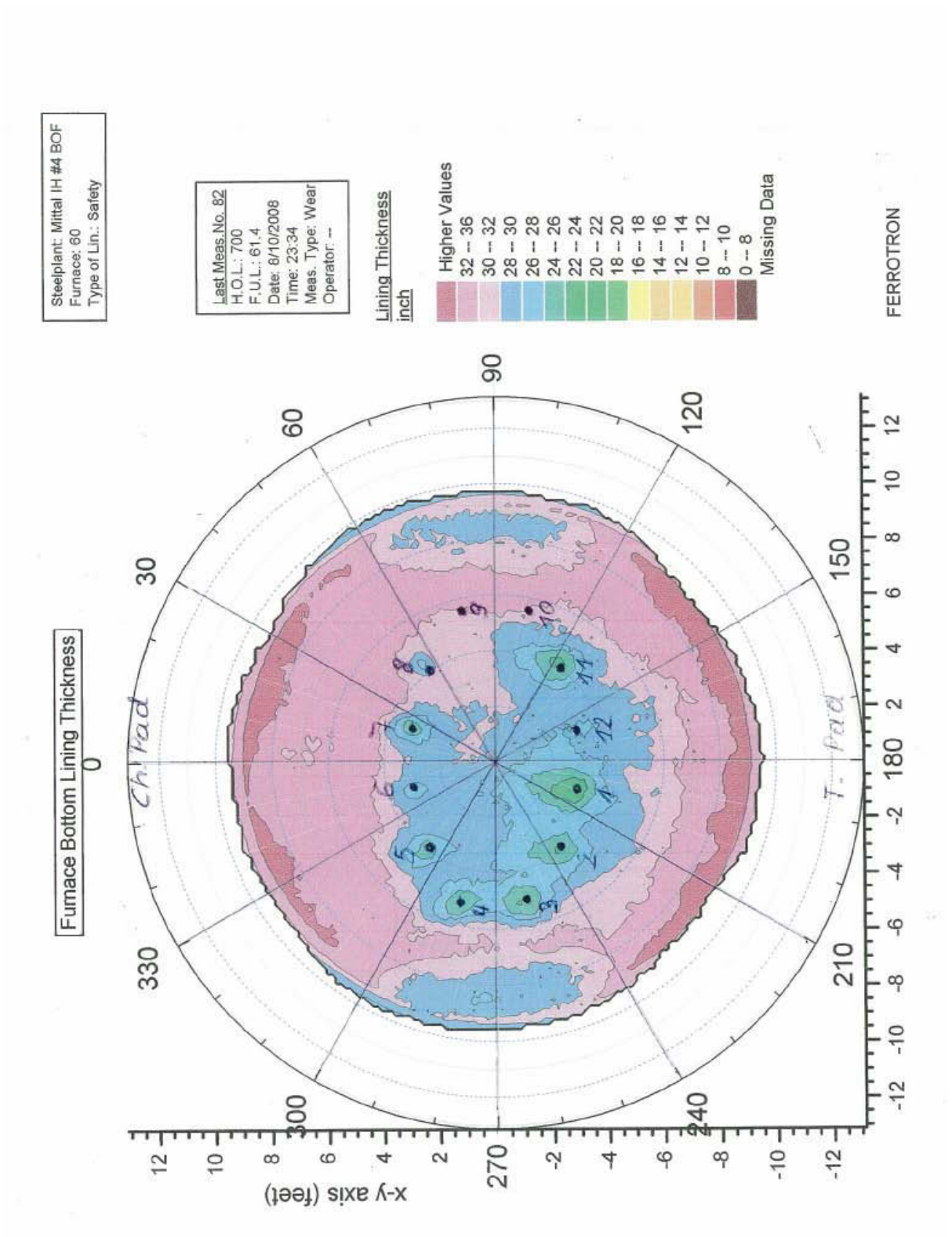

Attachment 2: Wear of the bottom.

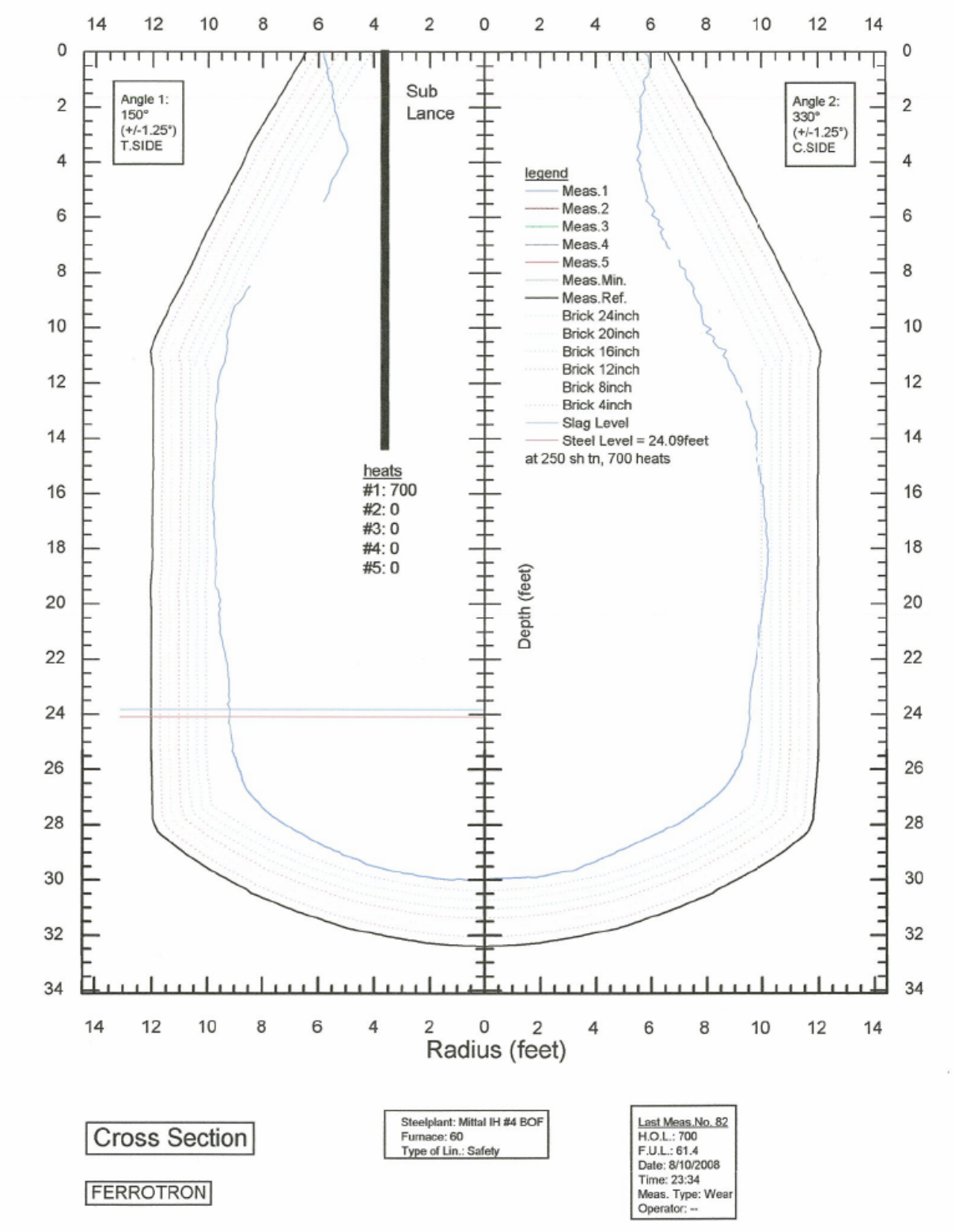

Attachment 3: Wear profile (cross section).

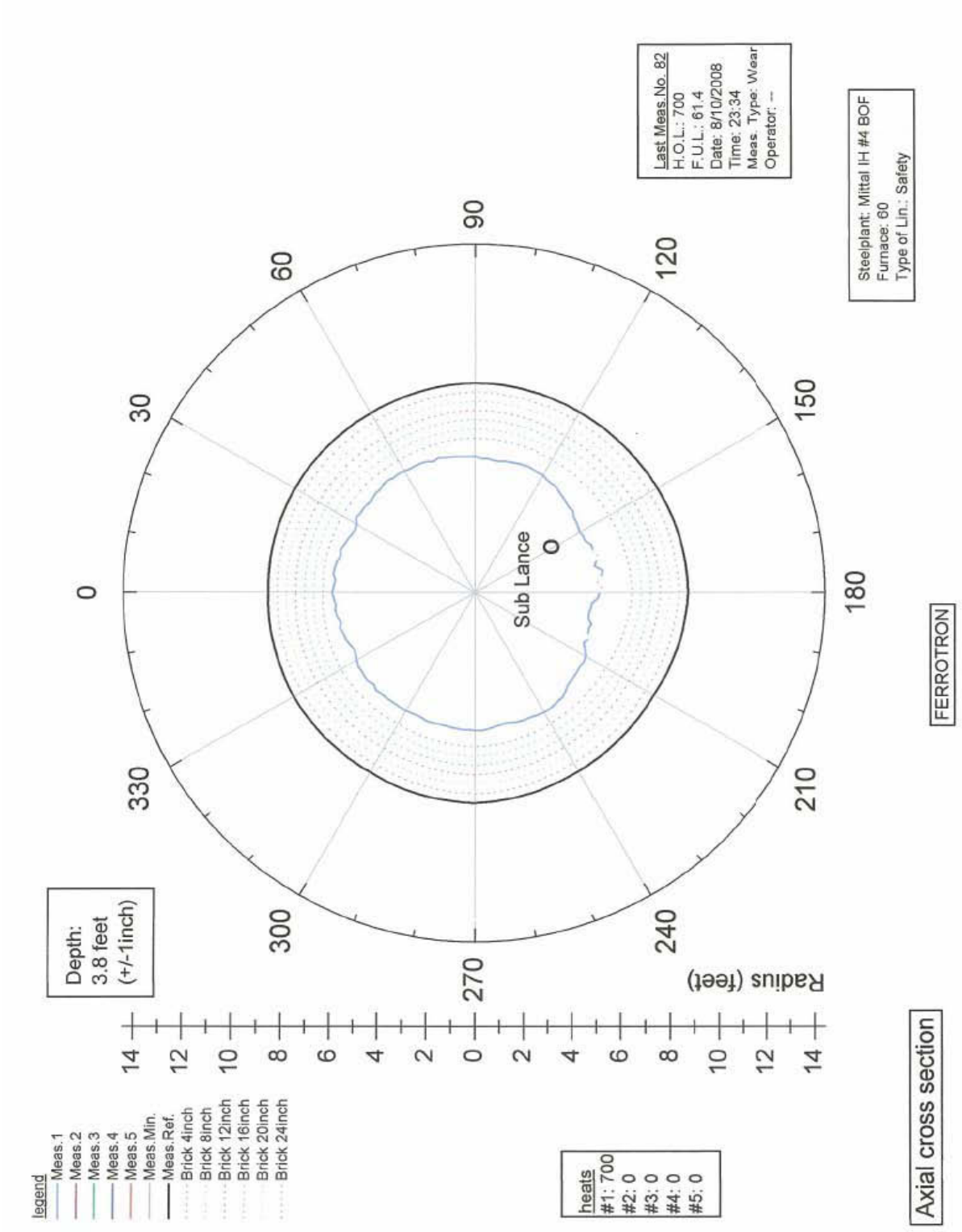

Attachment 4: Wear profile (axial cross section).

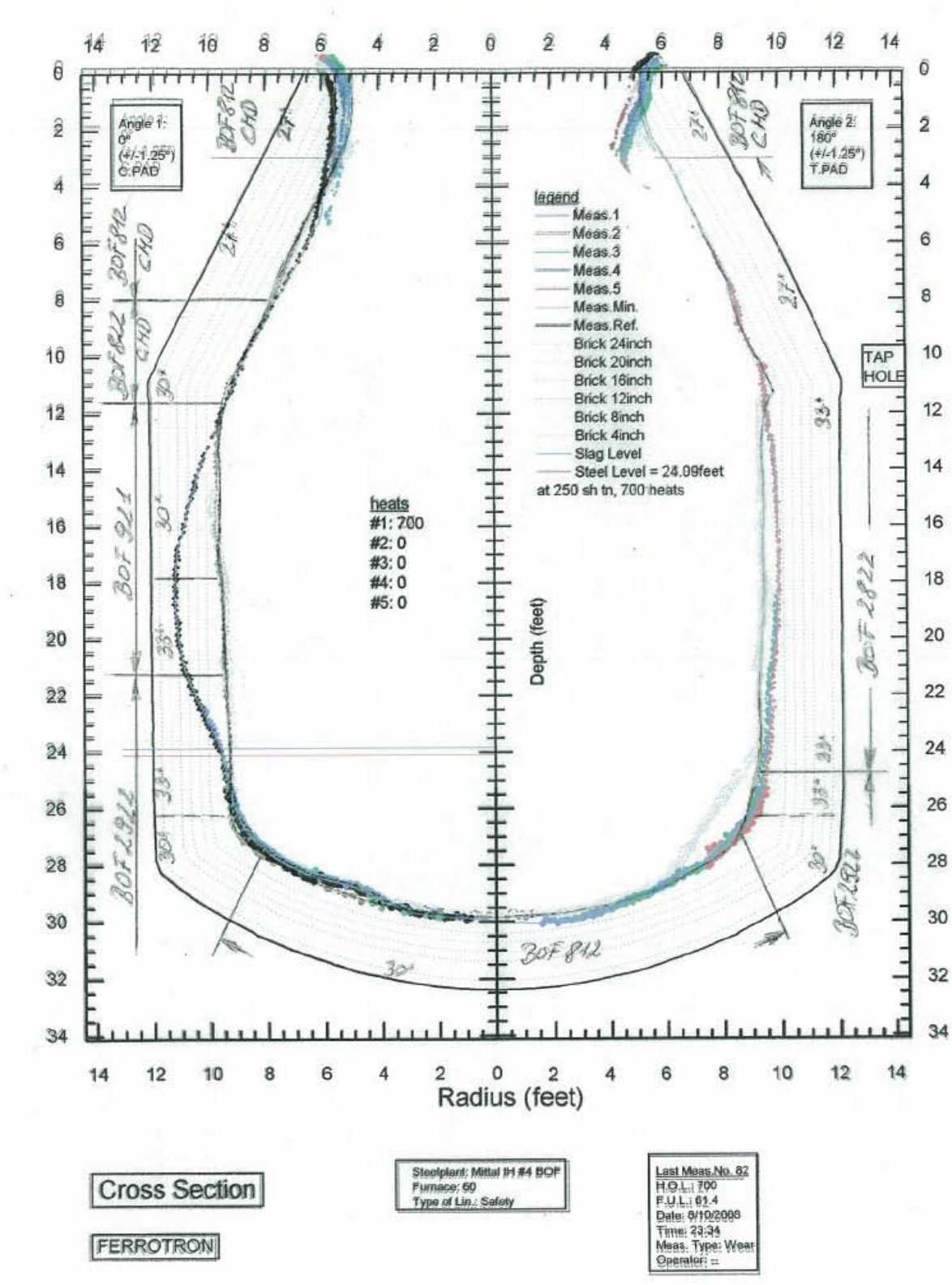

Attachment 5: Wear profile (cross section_bricks).

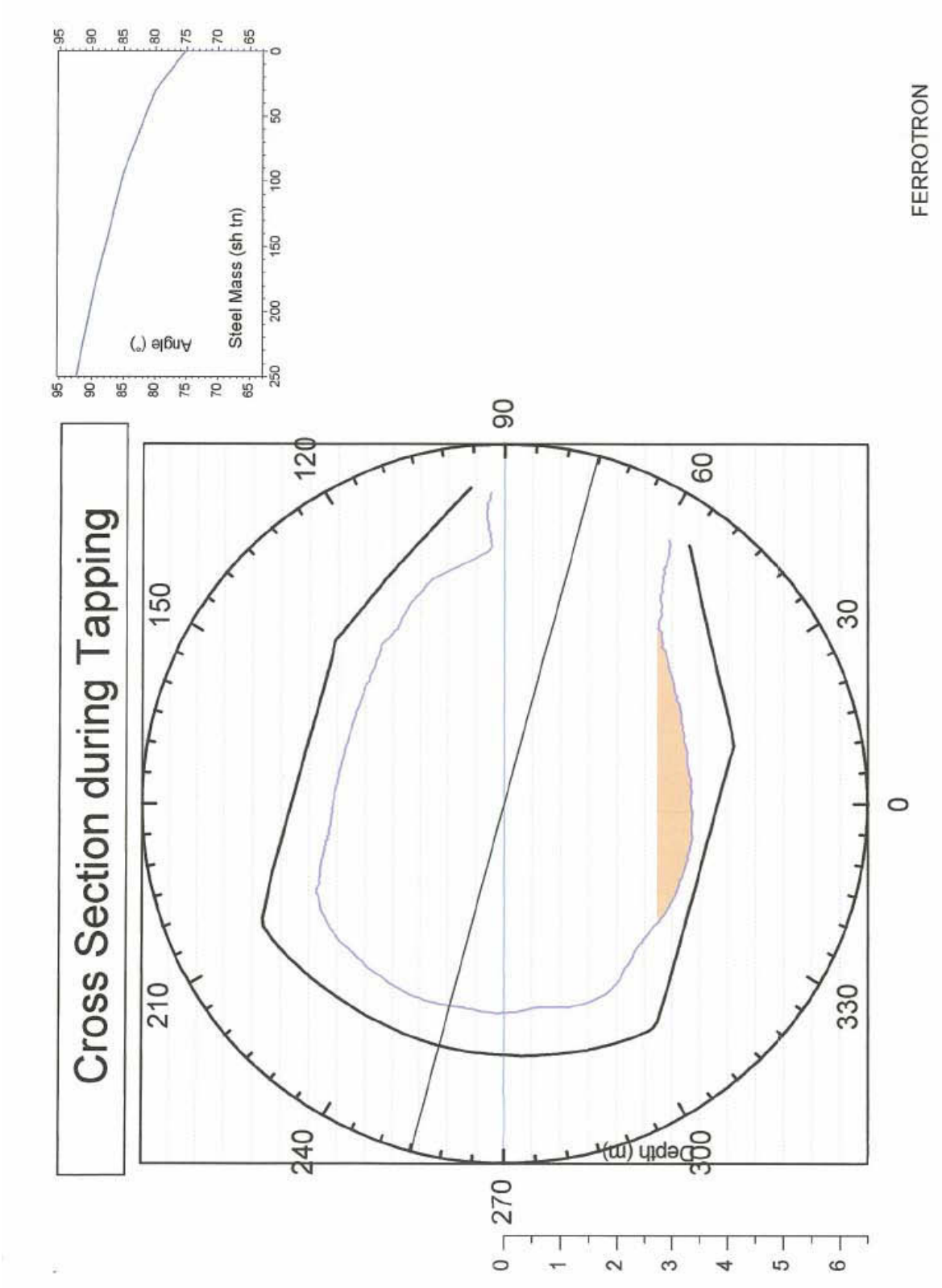

Attachment 6: Cross section during tapping.

Mittal Inland #4 BOF LASER Report

FURNACE	60
MEAS. NUMBER	82
DATE	8/10/2008
TIME	23:34
H.O.L.	700
F.U.L.	61.4

Tilt Angles (degrees):
C Pos. Scan #1: 200
R Pos. Scan #2: 200
L Pos. Scan #3: 200
C Meas. Scan #1: 105
C Meas. Scan #2: 72
R Meas. Scan #3: 90
L Meas. Scan #4: 90

Volume Calculation

Total Vessel Length	400"
Bath Level from Top	289.06"
Bath Level from Bottom	110.94"
Vessel Volume:	6855 ft³
Cone Volume	619 ft³
Percent Cone Closed	94.6%
Full Up Lance Height:	61.52'

Narrowest Cone Cross Section

Section 1:	167.5° @ 3.3' depth
Section 2:	347.5° @ 2.6' depth
Distance:	121"

Area Name	Area Angles	Area Depths	Minimum	Min. Location	Average	Maximum
South Cone	80° to 100°	0.5' to 11.3'	12.6	80° and 0.5'	25.2	
S Trunn - High	60° to 80°	11.3' to 23.0'	21.7	67.5° and 16.2'	24.4	28.3
S Trunn - Mid	80° to 100°	11.3' to 23.0'	21.9	85° and 17.2'	24.8	29.1
S Trunn - Low	100° to 120°	11.3' to 23.0'	23.1	100° and 15.9'	26.7	33.6
S Stadium	60° to 120°	23.0' to 25.3'	26.2	67.5° and 23.1'	28.2	30.7
S TD Slag - High	120° to 130°	11.3' to 25.3'	25.0	125° and 16.9'	28.4	34.6
S TD Slag - Low	130° to 140°	11.3' to 25.3'	25.3	132.5° and 17.1'	28.8	37.0
North Cone	260° to 280°	0.5' to 11.3'	11.8	280° and 0.5'	25.9	34.4
N Trunn - High	280° to 300°	11.3' to 23.0'	22.0	287.5° and 16.7'	24.5	28.1
N Trunn - Mid	260° to 280°	11.3' to 23.0'	21.9	275° and 16.4'	24.7	29.3
N Trunn Low	240° to 260°	11.3' to 23.0'	22.7	260° and 15.8'	26.2	32.4
N Stadium	240° to 300°	23.0' to 25.3'	25.6	300° and 23.1'	28.1	32.3
N TD Slag - High	230° to 240°	11.3' to 25.3'	25.3	240° and 16.2'	28.8	35.7
N TD Slag - Low	220° to 230°	11.3' to 25.3'	25.8	227.5° and 16.4'	29.6	37.7
S Tap Pad	140° to 165°	11.3' to 25.3'	25.4	140° and 15.9'	29.2	37.0
Tap Pad	165° to 195°	11.3' to 25.3'	25.4	172.5° and 16.7'	28.8	34.9
N Tap Pad	195° to 220°	11.3' to 25.3'	25.7	210° and 16.4'	29.4	38.1
S Low Chg Slag	40° to 50°	11.3' to 25.3'	19.9	42.5° and 17.7'	24.1	31.1
S High Chg Slag	50° to 60°	11.3' to 25.3'	20.8	50° and 17.7'	24.2	28.6
S Chg Pad	15° to 40°	11.3' to 25.3'	12.7	15° and 17.7'	24.1	36.1
Chg Pad	345° to 15°	11.3' to 25.3'	9.4	2.5° and 18.4'	19.9	36.3
N Chg Pad	320° to 345°	11.3' to 25.3'	14.2	345° and 18.4'	24.7	39.7
N High Chg Slag	300° to 310°	11.3' to 25.3'	21.5	310° and 17.2'	24.5	28.0
N Low Chg Slag	310° to 320°	11.3' to 25.3'	20.7	320° and 17.6'	24.5	30.9

BOTTOM	Area Angles	Area Radii	Minimum	Pnt. Radius	Average	Maximum
North Charge	292.5° to 337.5°	0.0' to 5.5'	25.3	4.1'	29.1	33.8
Charge	337.5° to 22.5°	0.0' to 5.5'	25.0	3.3'	30.2	34.3
South Charge	22.5° to 67.5°	0.0' to 5.5'	25.0	3.3'	30.5	34.5
South	67.5° to 112.5°	0.0' to 5.5'	25.7	3.9'	30.0	33.0
South Tap	112.5° to 157.5°	0.0' to 5.5'	23.7	4.3'	28.6	31.0
Tap	157.5° to 202.5°	0.0' to 5.5'	22.3	3.0'	27.9	31.2
North Tap	202.5° to 247.5°	0.0' to 5.5'	22.6	3.0'	27.2	31.5
North	247.5° to 292.5°	0.0' to 5.5'	24.3	5.3'	27.8	29.6

B Technical report

Customer:

Project: CIP-System / BOF

Daily-Report

Name of the service technician:

Date of inspection: / /

day / month / year

Production

Heats on lining last insp.: date & time :

Heats on lining today: date & time :

produced heats: **time since last visit [h]:**

Values p_{CO}, Flowrates

p_{CO} values are achieved:

☐ yes (in the tolerance)

☐ no (out of tolerance)

comment:

flowrates are achieved:

(compare set and real flow)

☐ yes

☐ no

comment:

flowrate changes:

☐ yes

☐ no

step [ ]	set flow $_{old}$ [l/min]	set flow $_{new}$ [l/min]
charging		
soft blowing		
hard blowing		
sample 1		
sample 2		
tapping		
slag washing		
empty		

Optical survey at #BOF

all plugs are viewable:

☐ yes

☐ no

(**X**.. mark the blocked plugs at the drawing and insert the appropriated back pressures additionally)

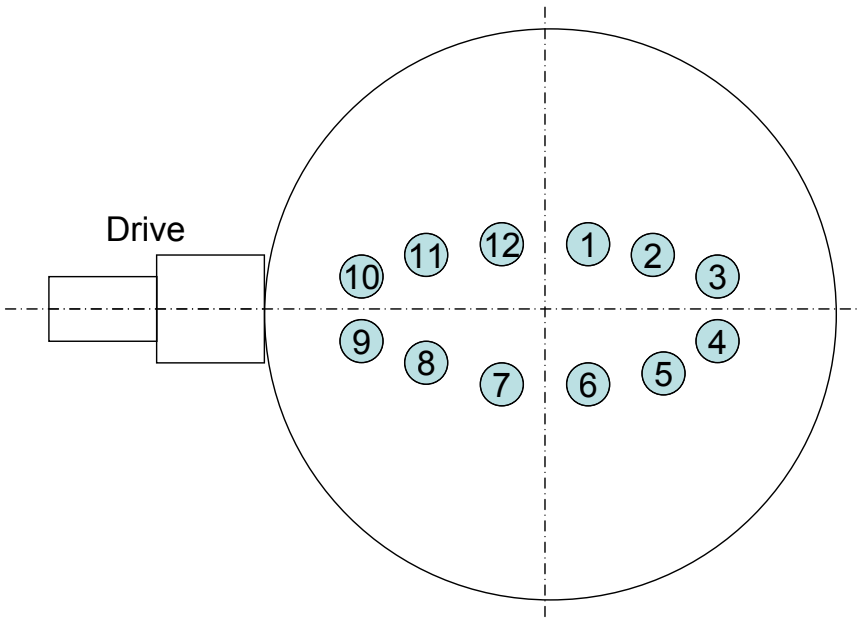

plug 1
plug 2
plug 3
plug 4
plug 5
plug 6
plug 7
plug 8
plug 9
plug 10
plug 11
plug 12

View: Charge side look into the BOF

amount of working plugs:

amount of take out plugs (**X**):

amount of blocked plugs (**X**):

water outside of the pipes:

☐ yes

☐ no

comment:

Maintenance

gunning:

☐ yes

☐ no

gunning mix (quality)	amount [kg]	BOF zone	duration [min]

bottom blowing:

☐ yes

☐ no

other interruption times:

- bear removing from the converter mouth duration: [min]
- problems with HM duration: [min]
- disconnecting of plugs duration: [min]

---

interruption total: [min]

C Operation Problems

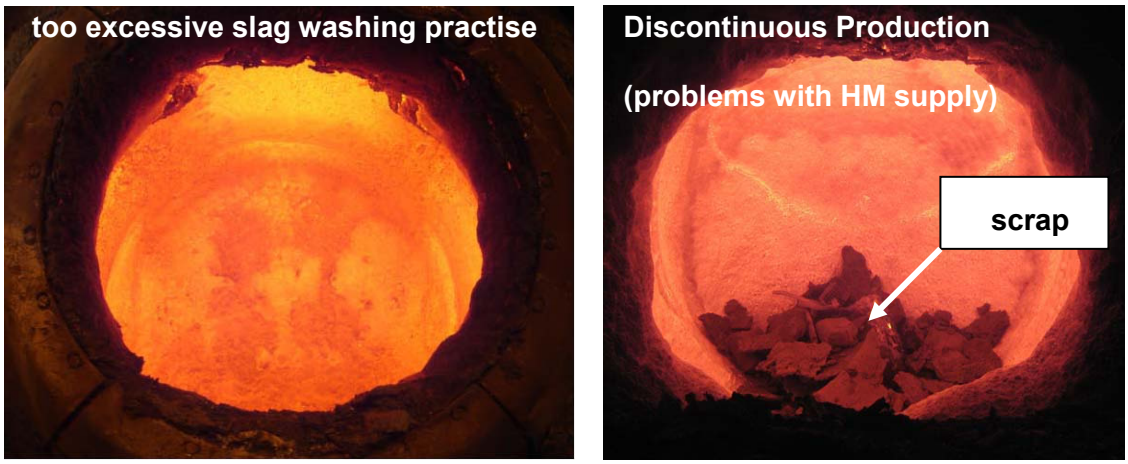

Attachment 7: Creation of a solid slag layer (look into the BOF; charge side).

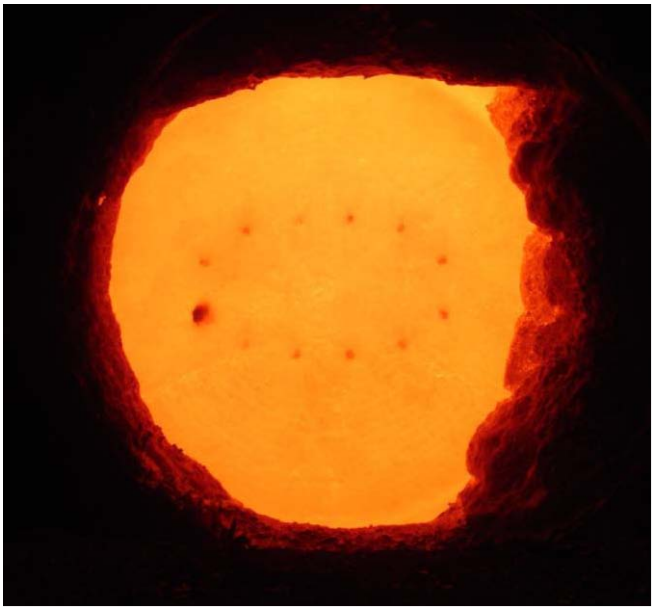

Attachment 8: Thin slag layer (all plugs are visible).

D Slag balance

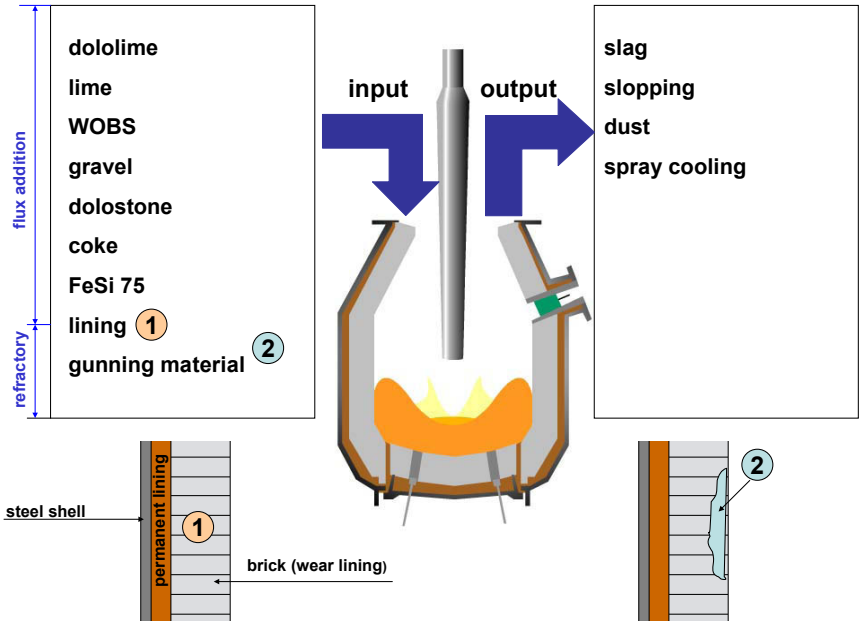

Attachment 9: MgO sources.

	MgO sources / heats on lining	0-100	101-200	201-300	301-400	401-500	501-600	601-700
INPUT	MgO Dololime, kg	527.4	655.3	513.6	599.7	672.8	423.3	344.9
	MgO Coke, kg	0.0	0.0	0.0	0.0	0.0	0.0	0.0
	MgO WOBS, kg	56.9	36.8	33.4	20.9	3.5	52.4	60.0
	MgO FeSi75, kg	0.3	0.2	0.3	0.4	0.4	0.3	0.3
	MgO Silicon gravel, kg	0.3	0.1	0.3	0.5	0.1	0.1	0.4
	MgO Dolostone, kg	357.4	364.5	375.2	281.1	442.8	435.4	530.5
	MgO Burnt lime, kg	95.7	108.3	92.3	90.3	94.3	114.9	115.5
	MgO gunning mixes, kg	14.4	28.8	18.0	65.6	190.8	309.6	360.0
	MgO lime/dololime transition, kg	250.0	250.0	150.0	130.0	-150.0	50.0	-215.0
	MgO brick lining wear, kg	200.0	116.7	116.7	90.0	80.0	50.0	0.0
OUTPUT	MgO dust, kg	51.4	51.1	51.3	51.3	51.2	51.3	51.4
	MgO slopping material, kg	34.4	32.4	31.0	29.2	36.8	27.9	31.6
	MgO soluted in water (Dololime), kg	3.1	16.2	2.1	10.8	18.9	-6.3	-51.4
	MgO soluted in water (Lime), kg	18.2	20.6	17.6	17.2	17.9	21.8	21.9
	MgO slag, kg	1.395.3	1.440.4	1.197.7	1.170.0	1.209.9	1.341.2	1.143.1
RESULTS	Slag volume calculated, kg	14.594.6	15.917.4	13.870.3	14.403.2	15.732.6	17.285.4	13.040.6
	Slag volume actual, kg	12.268.0	13.806.8	13.689.7	14.138.6	15.222.6	16.483.6	16.500.4
	Difference	**2.326.6**	**2.110.6**	**180.6**	**264.6**	**510.0**	**801.8**	**-3.459.8**

PARAMETERS	volume of dust, kg/mt	10.0	10.0	10.0	10.0	10.0	10.0	10.0
	volume of slopping material, kg/mt	1.5	1.5	1.5	1.5	2.0	1.5	1.5
	Dololime losses during feeding, %	10.0	10.0	10.0	10.0	10.0	10.0	0.0
	Burned lime losses during feeding, %	19.0	19.0	19.0	19.0	19.0	19.0	19.0

Attachment 10: Table of MgO balance calculation.